

Implementation of Quantum Search Algorithms in Cavity QED

Michael N. Kalogerakis

Chania, 2013

Implementation of Quantum Search Algorithms in Cavity QED

**Master thesis for the MSc. of Applied and Technological
Physics and Laser Technology, Science Department,
Technical University of Crete**

Chania, Crete 2013

Examining Committee:

Prof. D. Ellinas	Science Department, Technical University of Crete
Assistant Prof. I. Kominis	Physics Department, University of Crete
Assistant Prof. D.G. Angelakis	Science Department, Technical University of Crete (Supervisor)

Copyright ©2013 by Michael N. Kalogerakis

Author email: neo24483 [at] gmail . com

To teachers and students who never lost their persistence

Abstract

Cavity QED systems have been proved to be excellent platforms for the implementation of quantum information processing algorithms. In this thesis we review the major results in this field and conclude by proposing how to implement the Deutch-Jozsa in a system of two evanescently coupled cavities. In the first part we review the physics of both the ideal and dissipative cases of a two-level-atom coupled to an optical cavity mode. We analyze in detail the corresponding Jaynes-Cummings model and derive the dynamics of the system in the presence of dissipation using both the Master Equation and the Quantum Trajectories approach. We then proceed with a presentation of the Deutsch-Jozsa, Grover and Shor search algorithms and review in detail some early results regarding their implementation using flying Rydberg atoms in open microwave cavities. We extend our study to novel systems by analyzing the quantum dynamics of a system of two evanescently coupled optical cavities, each interacting with atomic emitters. This is done for different regimes of interactions (dispersive, resonant and strongly coupled) using both the Schrödinger and the Master equation approach. We conclude with a proposal for the implementation of Deutsch-Jozsa algorithm in the presence of significant cavity losses and analyze the robustness for different regimes by calculating the fidelity of the basic entangling gate of the algorithm.

Περίληψη

Έχει γινεί αποδεκτό ότι τα συστήματα κοιλότητων Κβαντικής Ηλεκτροδυναμικής αποτελούν πολύ καλές πλατφόρμες για την υλοποίηση αλγορίθμων κβαντικής πληροφορίας. Σε αυτή τη διπλωματική διατριβή κάνουμε ανασκόπηση των σημαντικότερων αποτελεσμάτων σε αυτό το ερευνητικό πεδίο και καταλήγουμε προτείνοντας μια μέθοδο υλοποίησης του αλγορίθμου Deutsch-Jozsa σε ένα σύστημα δύο συζευγμένων κοιλοτήτων. Στο πρώτο μέρος κάνουμε ανασκόπηση της ιδανικής περίπτωσης καθώς και της περίπτωσης με απώλειες για ένα σύστημα ενός ατόμου δύο επιπέδων συζευγμένου με έναν τρόπο ταλάντωσης της οπτικής κοιλότητας. Αναλύουμε λεπτομερώς το μοντέλο Jaynes-Cummings και βρίσκουμε τις εξισώσεις της δυναμικής του συστήματος παρουσία απωλειών χρησιμοποιώντας την Master Equation, αλλά και τη Μέθοδο Κβαντικών Τροχιών. Συνεχίζουμε μετέπειτα με την παρουσίαση των κβαντικών αλγορίθμων αναζήτησης Deutsch-Jozsa, Grover και Shor και παρουσιάζουμε αναλυτικά δύο από τις αρχικές προτάσεις που αφορούν την υλοποίησή τους χρησιμοποιώντας ιπτάμενα άτομα Rydberg σε ανοικτές κοιλότητες μικροκυμάτων. Επεκτείνουμε τη μελέτη μας αναλύοντας τη δυναμική συμπεριφορά ενός νέου συστήματος δύο συζευγμένων κοιλοτήτων, κάθε μία εκ των οποίων αλληλεπιδρά με άτομα ξεχωριστά. Αυτή η μελέτη γίνεται για διάφορες περιοχές αλληλεπίδρασης (περιοχή αποσυντονισμού, συντονισμού και ισχυρής σύζευξης), χρησιμοποιώντας και την εξίσωση Schrödinger και την Master Equation. Καταλήγουμε, παρουσιάζοντας μια καινούργια πρόταση υλοποίησης του αλγορίθμου Deutsch-Jozsa και αναλύουμε την αποτελεσματικότητα της υλοποίησής του, παρουσία σημαντικών απωλειών, υπολογίζοντας την πιστότητα (fidelity) της βασικής πύλης εναγκαλισμού του αλγορίθμου.

Contents

Contents	iii
Introduction - Motivation	v
1 Introduction to Cavity Q.E.D.	1
1.1 Quantization of the electromagnetic field	1
1.2 Quantum states of the electromagnetic Field	4
1.2.1 Fock States	5
1.2.2 Coherent States	7
1.2.3 Thermal states	9
1.3 The Jaynes-Cummings model	10
1.3.1 Photon-atom interaction	11
1.3.2 Dressed states approach	20
1.4 Cavity QED experiments	23
1.4.1 Tailoring spontaneous emission rates and atomic energies in confined space	24
1.4.2 Microwave cavities and the strong coupling regime	24
1.5 Cavity QED with lossy cavities	27
1.5.1 The empty cavity case	27
1.5.2 Monte Carlo - Quantum Trajectory method	28
2 Quantum Computation and Algorithms	35
2.1 Quantum Bits and Gates	36
2.1.1 One qubit operations	38
2.1.2 Two qubit operations	39
2.1.3 Three qubit operations	39
2.2 Deutsch-Jozsa algorithm	40
2.3 Grover's search algorithm	43
2.4 Shor's Algorithm	47
2.4.1 The Quantum Fourier Transform	49
2.4.2 Finding the period of a function using QFT	50

3 Implementation of quantum algorithms on cavity QED systems	53
3.1 Grover's search algorithm	54
3.1.1 An alternative realization of the quantum phase gate	58
3.2 Implementation of the quantum Fourier transform	61
4 Implementing quantum gates in coupled cavity arrays	67
4.1 Quantum dynamics in the two coupled cavities model	68
4.2 Analytical treatment	70
4.2.1 Case A: Large intercavity hopping regime	72
4.2.2 Case B: Large Detuning regime	75
4.2.3 Case C: Resonant interaction regime	77
4.3 Quantum Dynamics in a two cavity system with dissipation	79
4.4 A proposal for Deutsch-Jozsa algorithm in a two cavity system . .	81
5 Conclusions and Future work	85
Appendix A	87
1 Usefull packages for Quantum Optics	87
2 Details on Mathematica code	87
3 Python code used for plots.	89
Appendix B. Theoretical tools for cavity QED	95
1 Review of the harmonic oscillator	95
2 Schrödinger picture	103
3 Heisenberg picture	104
4 Interaction Picture	106
5 Dissipative processes in cavity QED	108
References - Bibliography	113
Acknowledgements	127
List of Figures	129
List of Tables	133

Introduction - Motivation

Indisputably, one of the most important scientific fields developed during the 20th century, was the field of Quantum Mechanics [1, 2, 3, 4, 5]. We are endowed with a set of the basic rules that govern our Universe and we have actually managed to teach ourselves how to use these rules in different fields of Science and Technology to construct many of the modern devices of our everyday life; these include the electronical systems of our cars and our mobile phones, to the state-of-the-art super-clusters of computers.

In the early days of Quantum Mechanics, the term "*Gedankenexperimenten*" (thought experiments) was established, in order to describe an idealised situation that could help us understand the problems that emerged. Probably the most famous case of this sort of examples, is the famous "**Schrödinger's cat**".¹ Another famous *Gedanken experiment* regarding the situation of having a **photon in a box**, was used in the famous public correspondence between Niels Bohr and Albert Einstein. In their correspondence, the main argument regards the violation of energy-time uncertainty principle, in the case when a photon that is trapped in a box with a shutter, is allowed to exit the shutter, at a specific time instant.

Interestingly, it was the idea of the photon in a box that gave rise to the modern *Cavity Quantum Electrodynamics (Cavity QED)* [6, 7], which in twist of fate later allowed the first experimental realization of the Schrödinger's cat. It all started by Purcell in 1946[8], in the study of one of the most mysterious effects that came along with the photoelectric effect. The study of the factors that affect the spontaneous emission rate and the quantization of the electromagnetic field [9], opened the road for lasers, masers and a whole new era in Modern Physics, enriching the field of Quantum Optics [10, 11, 12, 13, 14, 15] and offering a solid testbed for the emerging field of Quantum Information and Quantum Computation [16, 17, 18, 19, 20, 21, 22, 23, 24].

The primary objective of the current thesis is to give a short introduction on

¹Actually Schrödinger being "shocked" about the possibility of a system being in a superposition of states, trying to reject this scenario, used the example of the cat as "reductio ad absurdum" ie. stating that it is ridiculous to suppose a physical system could be in such a state.

aspects of Cavity QED and demonstrate how those systems can be used in order to implement certain Quantum Algorithms.

In Chapter 1 , we describe the quantization of the electromagnetic field and the Jaynes-Cummings model [25, 26], that describes the simplest, ideal, case of light-matter interaction when both the atom and the field are fully quantized. We continue by giving a short description of cavity QED systems following mainly [7] and discussing the primary features of lossy cavity QED system as laid out in [27], [28, 29]. In Chapter 2 we will give the outline of the notion of *Quantum Computation* and describe the class of *search algorithms*, namely Deutsch-Jozsa algorithm [22, 30, 23], Grover's search algorithm [31, 32, 33, 34] and Shor's factoring algorthm[35]. In Chapter 3, we present in detail the implementation of Grover's search algorithm and Shor's factoring algorithm, following the approach of two early papers from M.O. Scully [36] and the Haroche group[37].

In Chapter 4, we briefly touch the novel field of *Coupled Cavity Arrays for quantum information and simulation applications* [21, 38, 39]. After briefly introducing the field, we propose a new protocol on implementing quantum computation in small scale arrays comprised of pairs of coupled resonators. We specifically discuss a case to implement the Deutch-Josza algortihm and study the robustness of the implementation against experimental errors due to the finite lifetime of the photonic excitations in the arrays. This is done using both numerical and analytical techniques.

The present thesis primarily focuses on aspects of microwave QED and its applications on Quantum Information Processing as explored by the Haroche group in ENS in Paris. Equivalently important and thorough work has been performed by other experimental groups working on optical QED, among which, the groups of J. Kimble [40],[41],[42, 43] and D. Meschede [44],[45],[46]. Apart from optical and cavity QED, there have been great advancements regarding the implementation of Quantum Computation in other experimental platforms supplied by ion traps [47, 48, 49], Nuclear Magnetic Resonance [50] and last but not least, from the superconducting circuit community and the Yale and E.T.H. groups, regarding a new kind of experimental demonstration of Jaynes Cummings model, which has led to the establishment of the field of circuit QED [51], [52], [53]. In future work we would like to explore this novel direction.

We would like to add that, during the writing of this thesis, which took place in the period between August 2012 - December 2012, it was announced that "*The Nobel Prize in Physics 2012 is awarded jointly to Serge Haroche and David J. Wineland "for ground-breaking experimental methods that enable measuring and manipulation of individual quantum systems".*

Chapter 1

Introduction to Cavity Q.E.D.

1.1 Quantization of the electromagnetic field

1

In the simple case of the harmonic oscillator, we describe ideally the case of a particle of mass m moving under action of an harmonic potential in a 1D confined space. Starting from the notion of electromagnetic fields as waves, we will derive the equivalent expression that includes the correspondent quantities in their quantum mechanical form, which is the reason that we refer to this process as the *quantization of the electromagnetic field*. The equations of electromagnetism in free space, read:

$$\begin{aligned}\vec{\nabla} \cdot \vec{B} &= 0 \\ \vec{\nabla} \times \vec{E} &= -\frac{\partial \vec{B}}{\partial t} \\ \vec{\nabla} \cdot \vec{D} &= 0 \\ \vec{\nabla} \times \vec{H} &= -\frac{\partial \vec{D}}{\partial t}\end{aligned}\tag{1.1}$$

where $\vec{B} = \mu_0 \vec{H}$, $\vec{D} = \epsilon_0 \vec{E}$, μ_0 and ϵ_0 are the magnetic permeability and electric permittivity of free space and $\mu_0 \epsilon_0 = \frac{1}{c^2}$.

Maxwell's equation have the characteristic of *gauge invariance* when no sources are present. This actually enables us to choose a suitable gauge which depends on the field we wish to study. A convenient choice of gauge for problems in quantum optics is the *Coulomb gauge*, in which we substitute both the electric

¹The derivation for the quantization of the EM field, is virtually described in any textbook of quantum mechanics, though we consider the treatments described in [2] , [4] and [12] to be quite extensive and didactic.

\vec{E} and magnetic \vec{B} fields by expressions derived from a new vector potential $\vec{A}(\vec{r}, t)$ as follows:

$$\vec{E} = -\frac{\partial \vec{A}}{\partial t} \quad (1.2)$$

$$\vec{B} = \vec{\nabla} \times \vec{A} \quad (1.3)$$

with the Coulomb gauge condition

$$\vec{\nabla} \cdot \vec{A} = 0 \quad (1.4)$$

Substituting the expression for \vec{B} from 1.2 into the set of equations 1.1 we find that $\vec{A}(\vec{r}, t)$ satisfies the wave equation :

$$\vec{\nabla}^2 \vec{A}(\vec{r}, t) = \frac{1}{c^2} \frac{\partial^2 \vec{A}(\vec{r}, t)}{\partial t^2} \quad (1.5)$$

Since wave-equation holds, we are able to separate the vector potential into two complex terms:

$$\vec{A}(\vec{r}, t) = \vec{A}^{(+)}(\vec{r}, t) + \vec{A}^{(-)}(\vec{r}, t) \quad (1.6)$$

where $\vec{A}^{(+)}(\vec{r}, t)$ contains all amplitudes which vary as $e^{-i\omega t}$ for $\omega > 0$, $\vec{A}^{(-)}(\vec{r}, t)$ contains all amplitudes which vary as $e^{i\omega t}$ and $\vec{A}^{(-)} = (\vec{A}^{(+)})^*$

Now, we choose to restrict our discussion to a discrete set of variables rather than the whole continuum, namely, describe the electromagnetic field restricted to a certain definite volume of space and expand the vector potential in terms of a discrete set of orthogonal mode functions:

$$\vec{A}^{(+)}(\vec{r}, t) = \sum_k c_k \vec{u}_k(\vec{r}) e^{-i\omega_k t} \quad (1.7)$$

where the Fourier coefficients c_k are constant for a free field. The set of vector mode functions $\vec{u}_k(\vec{r})$ which correspond to the frequency ω_k will satisfy the equation

$$\left(\vec{\nabla}^2 + \frac{\omega_k^2}{c^2} \right) \vec{u}_k(\vec{r}) = 0 \quad (1.8)$$

provided the volume contains no refracting material. The mode functions are also required to satisfy the transversality condition

$$\vec{\nabla} \cdot \vec{u}_k(\vec{r}) = 0 \quad (1.9)$$

The mode functions form a complete orthonormal set, which is stated by the expression

$$\int_V \vec{u}_k^*(\vec{r}) \vec{u}_{k'}(\vec{r}) d\vec{r} = \delta_{kk'} \quad (1.10)$$

Those mode functions are defined by the boundary conditions of the physical volume under consideration, which will prove to be of crucial importance in what follows. If we consider the plane wave mode functions appropriate to a cubical volume of side L , we may write them us:

$$\vec{u}_k(\vec{r}) = L^{-\frac{3}{2}} \hat{e}^{(\lambda)} \exp [i \vec{k} \cdot \vec{r}] \quad (1.11)$$

where $\hat{e}^{(\lambda)}$ is the unit polarization vector. The mode index k describes several discrete variables, the polarization index ($\lambda = 1, 2$) and the three Cartesian components of the propagation vector \vec{k} take the values

$$k_x = \frac{2\pi n_x}{L}, \quad k_y = \frac{2\pi n_y}{L}, \quad k_z = \frac{2\pi n_z}{L}, \quad n_x, n_y, n_z = 0, \pm 1, \pm 2, \dots \quad (1.12)$$

Regarding the transversality condition 1.9, the polarization vector $\hat{e}^{(\lambda)}$ is required to be perpendicular to \vec{k} , so we may rewrite the vector potential in the form:

$$\vec{A}(\vec{r}, t) = \sum_k \sqrt{\frac{\hbar}{2\omega_k \epsilon_0}} [a_k \vec{u}_k(\vec{r}) e^{-i\omega_k t} + a_k^\dagger \vec{u}_k^*(\vec{r}) e^{i\omega_k t}] \quad (1.13)$$

The corresponding form for the electric field now becomes:

$$\vec{E}(\vec{r}, t) = i \sum_k \sqrt{\frac{\hbar\omega_k}{2\epsilon_0}} [a_k \vec{u}_k(\vec{r}) e^{-i\omega_k t} + a_k^\dagger \vec{u}_k^*(\vec{r}) e^{i\omega_k t}] \quad (1.14)$$

In classical electromagnetic theory these Fourier amplitudes are complex numbers. Since photons are bosons, i.e. they are ruled by the commutator relations that are described in the 1D harmonic oscillator, it is easy to choose \hat{a}_k and \hat{a}_k^\dagger to be mutually adjoint operators.

The dynamical behaviour of the electric-field amplitudes may then be described by an ensemble of independent harmonic oscillators obeying the boson commutation relations:

$$[\hat{a}_k, \hat{a}_{k'}] = [\hat{a}_k^\dagger, \hat{a}_{k'}^\dagger] = 0, \quad [\hat{a}_k, \hat{a}_{k'}^\dagger] = \delta_{kk'} \quad (1.15)$$

The quantum states of each mode may now be discussed independently of one another. The state in each mode may be described by a state vector $|\Psi\rangle_k$ of the Hilbert state appropriate to that mode. The states of the entire field are then defined as the tensor product space of the Hilbert spaces for all the modes.

The Hamiltonian for the electromagnetic field is given by [15]

$$H = \frac{1}{2} \int (\varepsilon_0 \vec{E}^2 + \mu_0 \vec{H}^2) d\vec{r} \quad (1.16)$$

Using the expression 1.14 for \vec{E} and the equivalent expression for \vec{H} and making use of the transversality and orthonormality conditions, the Hamiltonian can be reduced to the form

$$H = \sum_k \hbar \omega_k \left(\hat{a}_k \hat{a}_k^\dagger + \frac{1}{2} \right) \quad (1.17)$$

Therefore we have argued that the energy of the electromagnetic field is nothing more than the sum of the number of photons in each mode, plus $\frac{1}{2}\hbar\omega_k$, representing the energy of the vacuum fluctuations in each mode.

Before getting an insight into the applications of the above procedure, it is useful to give the relations for the so-called field *field quadratures*. As it is quite easy to show, the canonical variables \hat{X}_1 and \hat{X}_2 represent the canonical position and momentum respectively.

$$\begin{aligned} \hat{X}_1 &= \sqrt{\frac{\hbar}{2\omega}} (\hat{a} + \hat{a}^\dagger) \\ \hat{X}_2 &= i\sqrt{2\hbar\omega} (\hat{a} - \hat{a}^\dagger) \end{aligned} \quad (1.18)$$

Using the quadratures and considering a single mode plane wave we may write the expression for the electric field as:

$$\hat{E}(\vec{r}, t) = \frac{1}{L^{\frac{3}{2}}} \left(\frac{\hbar\omega}{2\varepsilon_0} \right)^{1/2} \varepsilon_k \left[\hat{X}_1 \sin(\vec{k}\vec{r} - \omega t) - \hat{X}_2 \cos(\vec{k}\vec{r} - \omega t) \right] \quad (1.19)$$

The canonical variables \hat{X}_1 and \hat{X}_2 are the amplitudes of the quadratures into which the EM field can be decomposed.

1.2 Quantum states of the electromagnetic Field

The quantization of the electromagnetic field, namely the explicit expression of the Hamiltonian of the field in terms of operators, gives rise to the exploration of the eigenvalues of the Hamiltonian, regarding the energy levels and the respective wave functions.

1.2.1 Fock States

The Hamiltonian 1.17 has the eigenvalues $\hbar\omega_k (n_k + \frac{1}{2})$ where n_k is a natural number. The eigenstates are written as $|n_k\rangle$ and are known as *number or Fock states*. They are eigenstates of the number operator $\hat{N}_k = \hat{a}_k \hat{a}_k^\dagger$

$$\hat{a}^\dagger \hat{a}_k |n_k\rangle = n_k \hat{n}_k \quad (1.20)$$

The ground state of the harmonic oscillator in which we usually refer to as *vacuum state* is defined by

$$\hat{a}_k |0\rangle = 0 = |0\rangle \hat{a}_k^\dagger \quad (1.21)$$

which means that the expectation values of creation and annihilation operators vanish at this state.

Acting the Hamiltonian that we previously derived on the vacuum state, we obtain the relation:

$$\langle 0 | H | 0 \rangle = \frac{1}{2} \sum_k \hbar\omega_k \quad (1.22)$$

The above equation is quite intriguing. There is no explicit upper bound to the frequencies in the sum over the electromagnetic field modes, therefore the energy of the ground state is infinite. This infinite value of the zero-point energy (ZPE) is not the only case of "*peculiar*" infinities in quantum electrodynamics. The renormalization procedure manages to deal with most of these cases. In fact, the vacuum energy and fluctuations is responsible for a big variety of observable effects, like *Cassimir effect* and *Lamb shift*. In modern gauge field theory, the notion of "*Fermi-sea*", describing the vacuum as an entity which is everything than empty, with millions of particles being created and annihilated at the same time, describes exactly the point made out by equation 1.22. Another important detail that should be noted is the fact that the vacuum state, like all stationary states of the field, is an eigenstate of the Hamiltonian but not the electric and magnetic field operators. In the vacuum state therefore the electric and magnetic fields do not have definite values. We may easily calculate the mean value for electric and magnetic field for the vacuum state to be zero, but they do not have a definite value. Actually, they fluctuate about their mean values of zero for the case of a single mode of the field. Extensive discussion on the issues arising from the strange properties of the vacuum state may be found in the books [13] and [10]. Regarding the names we used for operators \hat{a} and \hat{a}^\dagger now it is clear that given a Fock state $|n\rangle$ with n photons, creation operator "adds" a photon leading to the state $|n+1\rangle$, while annihilation operator "removes" a photon, leading to

the state $|n - 1\rangle$, with the respective normalization constants:

$$\hat{a}_k |n_k\rangle = \sqrt{n_k} |n_k - 1\rangle, \quad \hat{a}_k^\dagger |n_k\rangle = \sqrt{n_k + 1} |n_k + 1\rangle \quad (1.23)$$

Starting from the vacuum state, it is obvious that in order to get the system into the state $|n_k\rangle$, we should act the creation operator n times, therefore:

$$|n_k\rangle = \frac{(\hat{a}_k^\dagger)^{n_k}}{\sqrt{n_k!}} |0\rangle, \quad n_k = 0, 1, 2, \dots$$

(1.24)

The Fock states are orthonormal and complete, which is stated by the relations:

$$\langle n_k | m_k \rangle = \delta_{nm} \quad (1.25)$$

$$\sum_{n_k=0}^{\infty} |n_k\rangle \langle n_k| = 1 \quad (1.26)$$

While the number states form a useful representation for high-energy photons, e.g. γ -rays where the number of photons is very small, they are not the most suitable representation for optical fields where the total number of photons is large. Moreover, though they can be produced experimentally, e.g. when an atom interacts with an electromagnetic field in a high quality optical resonator (cavity) and emits a single photon, it is not possible to create many photons in the very same cavity. We usually say that *Fock states are the states in which the quantum character manifests more than in every other representation of light*.

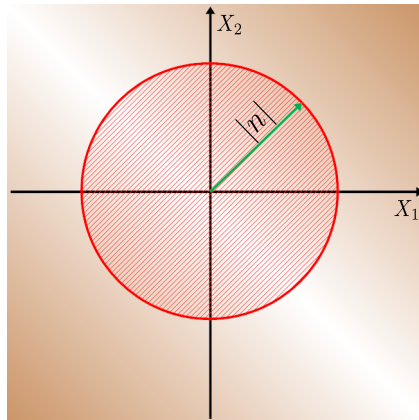


Figure 1.1: Optical phase space representation for a Fock state.

In the optical phase space representation, using as axes the canonical coordinates in natural units, we are able to visualize the properties of the Fock

states. Since canonical coordinates, as they were defined in equations 1.18 do not commute, we say that the system *is not well localized in optical phase space*. Moreover, one is possible to verify that the Fock states maximize the phase uncertainty, so that $\Delta\phi = 2\pi$.

1.2.2 Coherent States

Coherent states are superpositions of Fock states $|n\rangle$. They are denoted by $|\alpha\rangle$ and we need to be careful when dealing with the action of creation and annihilation operators on them. One could consider different possible superpositions but the coherent state is of particular importance in practical applications. Coherent states describe with great accuracy, states of CW monochromatic lasers above threshold and wave packets formed by coherent states describe very well states of pulsed lasers.

Probably the most practical way of introducing coherent states is the one deduced by Glauber in [54] and Sudarshan in [55] which also justifies the fact that they are also called *Glauber-Sudarshan states*. We will consider a single mode, so that we will get rid of index k . First of all, we need to define the *displacement operator*:

$$\hat{D}(\alpha) = e^{(\alpha\hat{a}^\dagger - \alpha^*\hat{a})} \quad (1.27)$$

The *Baker-Haussdorff formula* for two operators \hat{A} and \hat{B} such that $[A, [A, B]] = [B, [A, B]] = 0$, reads:

$$e^{\hat{A}+\hat{B}} = e^{\hat{A}} e^{\hat{B}} e^{-[\hat{A}, \hat{B}]/2} \quad (1.28)$$

Using the above formula for the expression we introduced for the displacement operator, we obtain:

$$\hat{D}(\alpha) = e^{-|a|^2/2} e^{\alpha\hat{a}^\dagger} e^{-\alpha^*\hat{a}} \quad (1.29)$$

The proof of the Baker-Haussdorff formula employs the following identity, valid for arbitrary operators:

$$e^{\hat{A}} \hat{B} e^{-\hat{A}} = B + \frac{[A, B]}{1!} + \frac{[A, [A, B]]}{2!} + \dots \quad (1.30)$$

Using the above identity we derive:

$$\begin{aligned} \hat{D}^\dagger(\alpha) \hat{a} \hat{D}(\alpha) &= \hat{a} + \alpha \\ \hat{D}^\dagger(\alpha) \hat{a}^\dagger \hat{D}(\alpha) &= \hat{a}^\dagger + \alpha^* \end{aligned} \quad (1.31)$$

The above expressions explain why $\hat{D}(\alpha)$ is called displacement operator. We are now in position to define *coherent state* $|\alpha\rangle$, as displaced vacuum state $|0\rangle$.

$$|\alpha\rangle = \hat{D}(\alpha) |0\rangle \quad (1.32)$$

Another approach on defining the coherent states relies on the following property:

$$\begin{aligned}
 \hat{D}^\dagger(\alpha) \hat{a} |\alpha\rangle &= \hat{D}^\dagger(\alpha) \hat{a} \hat{D}(\alpha) |0\rangle \\
 &= \alpha |0\rangle \\
 &= \alpha \hat{D}^\dagger(\alpha) \hat{D}(\alpha) |0\rangle \\
 &= \alpha \hat{D}^\dagger(\alpha) |\alpha\rangle
 \end{aligned} \tag{1.33}$$

We thus, conclude the equations:

$$\hat{a} |\alpha\rangle = \alpha |\alpha\rangle \tag{1.34}$$

$$\langle \alpha | \hat{a}^\dagger = \alpha^* \langle \alpha | \tag{1.35}$$

The above equations mean that coherent states are eigenstates of the annihilation operator. Since operator \hat{a} is not hermitian, its *eigenvalues are complex*. Contrary to the Fock states that contain finite and fixed number of photons, coherent states are superpositions of Fock states with arbitrary photon numbers. To prove this property, we will make use of the fact that $|n\rangle \hat{a} = \sqrt{n+1} \langle n+1|\alpha\rangle = \alpha \langle n|\alpha\rangle$ and equation 1.34, which leads us to:

$$\begin{aligned}
 \langle n | \hat{a} | \alpha \rangle &= \sqrt{n+1} \langle n+1 | \alpha \rangle = \alpha \langle n | \alpha \rangle \Rightarrow \\
 \langle n | \alpha \rangle &= \frac{\alpha}{\sqrt{n}} \langle n-1 | \alpha \rangle \Rightarrow \\
 \langle n | \alpha \rangle &= \frac{\alpha^n}{\sqrt{n!}} \langle 0 | \alpha \rangle
 \end{aligned} \tag{1.36}$$

Using the equation 1.29, the expansion of the exponential and the property $\hat{a}|0\rangle = 0$, we get the relation:

$$\langle 0 | \alpha \rangle = \langle 0 | \hat{D}(\alpha) | 0 \rangle = \exp(-|\alpha|^2/2) \tag{1.37}$$

Therefore the coherent states have the following Fock-states representation:

$$\boxed{|\alpha\rangle = \sum_{n=0}^{\infty} |n\rangle \langle n | \alpha \rangle = e^{-\alpha^2/2} \sum_{n=0}^{\infty} \frac{\alpha^n}{\sqrt{n!}} |n\rangle} \tag{1.38}$$

Supposing we want to calculate the probability of having n photons, it is easy to show that this probability follows the poissonian distribution:

$$p_n = |\langle n | \alpha \rangle|^2 = \frac{|\alpha|^{2n}}{n!} \exp[-|\alpha|^2] \tag{1.39}$$

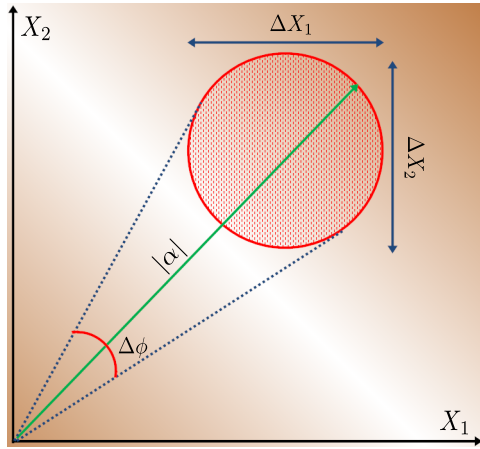


Figure 1.2: Optical phase space representation for a coherent state.

In order to obtain the mean number of photons we may use the number operator, therefore we obtain:

$$\bar{n} = \langle \alpha | \hat{n} | \alpha \rangle = \langle \alpha | \hat{a}^\dagger \hat{a} | \alpha \rangle = \alpha^* \langle \alpha | \alpha | \alpha \rangle = \alpha^* \alpha \langle \alpha | \alpha \rangle = |\alpha|^2 \quad (1.40)$$

Regarding the orthogonality of coherent states, let's suppose we have two coherent states, namely α and β . Their scalar product is

$$\langle \beta | \alpha \rangle = \langle 0 | \hat{D}^\dagger(\beta) \hat{D}(\alpha) | 0 \rangle = \exp \left[-\frac{|\alpha|^2}{2} - \frac{|\beta|^2}{2} + \alpha \beta^* \right] \quad (1.41)$$

This means that coherent states are not orthogonal, therefore we may calculate that the state overlap is:

$$|\langle \beta | \alpha \rangle|^2 = \exp [-|\alpha - \beta|^2] \quad (1.42)$$

1.2.3 Thermal states

Fock states and coherent states are pure states, in the sense that they are adequately described by their state vectors and their density matrix ρ which is defined by the equation:

$$\rho = \sum_i p_i |\psi_i\rangle \langle \psi_i|, \quad (1.43)$$

has the property that $\rho^2 = 1$, which denotes that they are indeed pure states. A statistical mixture can be represented only by its *density matrix*. The typical example of a *mixed state* is the case of the so-called *thermal states*. Introducing the notion of thermal states, which correspond very well to the states of radiating

black body, one is able to describe adequately thermal light, i.e. the light that is unavoidably present due to the black-body radiation. Recalling the partition function Z from statistical physics and defining $\beta = \frac{1}{k_B T}$, we may write:

$$\rho \equiv \frac{e^{-\beta \hat{a}^\dagger \hat{a}}}{Z} = (1 - e^{-\beta \hbar \omega}) e^{-\beta \hat{a}^\dagger \hat{a}} \quad (1.44)$$

The mean number of photons in such state is defined by

$$\bar{n} = (1 - e^{-\beta \hbar \omega}) \sum_{n=0}^{\infty} n e^{-\beta \hbar \omega n} = \frac{e^{-\beta \hbar \omega}}{1 - e^{-\beta \hbar \omega}} \quad (1.45)$$

therefore, we are able to rewrite ρ as:

$$\rho = \frac{1}{\bar{n}} \left(\frac{\bar{n}}{\bar{n} + 1} \right)^{\hat{a}^\dagger \hat{a}} \quad (1.46)$$

The photon number distribution for a thermal state is given by the relation

$$p_n = \frac{1}{\bar{n}} \left(\frac{\bar{n}}{\bar{n} + 1} \right)^n \quad (1.47)$$

which means that their distribution is geometric. Another important characteristic of thermal states, that makes clear the fact that they are chaotic, is the the order of the variance of the number of photons, which signifies the fluctuation of the number of photons in a thermal state.

$$(\Delta n)^2 = \overline{n^2} - \bar{n}^2 \quad (1.48)$$

The calculation for $\overline{n^2}$ gives us:

$$\overline{n^2} = \sum_{n=0}^{\infty} \left(\frac{n^2 \bar{n}^2}{\bar{n} + 1} \right)^{n+1} = \frac{1}{(\bar{n} + 1)} x \frac{d}{dx} x \frac{d}{dx} \sum_{n=0}^{\infty} x^n \Big|_{x=\frac{\bar{n}}{\bar{n}+1}} = 2\bar{n}^2 + \bar{n} \quad (1.49)$$

Therefore we find that indeed the variance of the number of photons in a thermal state is of the order of the mean value, which signifies very strong fluctuations, since

$$(\Delta n) = \bar{n}^2 + \bar{n} \quad (1.50)$$

1.3 The Jaynes-Cummings model

The simplest case of light-matter interaction is the case of a two-level atom interacting with a single mode of the quantized field. In the following, we discuss the basic mathematical techniques that are used to derive the fully quantized version of the field-matter interaction model, the Jaynes-Cummings model.

1.3.1 Photon-atom interaction

The fully quantized version of the Rabi model, which may be found analytically presented in [11], considers a two-level atom with states $|g\rangle$ for the ground state and $|e\rangle$ for the excited state, interacting with a single mode field of the form:

$$\hat{E} = \vec{e} \sqrt{\frac{\hbar\omega}{\varepsilon_0 V}} \cdot (\hat{a} + \hat{a}^\dagger) \sin(kz) \quad (1.51)$$

With \vec{e} we denote the arbitrary directioned polarization vector. Denoting with \hat{d} the dipole moment operator, the atom-field Hamiltonian may be written as:

$$\hat{H} = -\hat{d} \cdot \hat{E} \quad (1.52)$$

Setting $g = -\sqrt{\frac{\hbar\omega}{\varepsilon_0 V}} \cdot \sin(kz)$, then the Hamiltonian may be written in the form:

$$\hat{H}^{(I)} = \hat{d}g(\hat{a} + \hat{a}^\dagger) \quad (1.53)$$

It should be pointed out that g is a number, while $|g\rangle$ is a state of the system! It will prove useful for what follows to define at this point the operators describing the atomic transitions. Since we are talking for a two-level atom there should be an operator describing the transition of the atom from state $|g\rangle$ to state $|e\rangle$, which we denote as $\hat{\sigma}_+$ and from state $|e\rangle$ to $|g\rangle$, which will be denoted as $\hat{\sigma}_-$. Therefore we set:

$$\begin{aligned} \hat{\sigma}_+ &= |e\rangle \langle g| \\ \hat{\sigma}_- &= |g\rangle \langle e| \\ \hat{\sigma}_3 &= |e\rangle \langle e| - |g\rangle \langle g| \end{aligned} \quad (1.54)$$

Operator $\hat{\sigma}_3$ is called *atomic inversion operator* and its average value measures the atomic population inversion $W(t)$ as its name implies. The operators described in 1.54 obey the rules of Pauli matrices algebra, therefore the following commutation relations hold and this can be easily verified setting $|g\rangle = \begin{pmatrix} 1 \\ 0 \end{pmatrix}$ and $|e\rangle = \begin{pmatrix} 0 \\ 1 \end{pmatrix}$ or by just using their definition as it is described in 1.54.

$$\begin{aligned} [\hat{\sigma}_+, \hat{\sigma}_-] &= \hat{\sigma}_3 \\ [\hat{\sigma}_3, \hat{\sigma}_\pm] &= 2\hat{\sigma}_\pm \end{aligned} \quad (1.55)$$

The only non-zero elements of the dipole moment operator are non-zero, since $\langle e | \hat{d} | e \rangle = \langle g | \hat{d} | g \rangle = 0$, therefore we can show that

$$\hat{d} = d |g\rangle \langle e| + d^* |e\rangle \langle g| = d\hat{\sigma}_- + d^*\hat{\sigma}_+ = d(\hat{\sigma}_- + \hat{\sigma}_+) \quad (1.56)$$

where we have set $\langle e | \hat{d} | g \rangle = d$ and we supposed that d is a real number. Thus, setting $\lambda = \frac{dg}{\hbar}$, the Hamiltonian may be written in the form:

$$\hat{H}^{(I)} = \hbar\lambda(\hat{\sigma}_+ + \hat{\sigma}_-)(\hat{a} + \hat{a}^\dagger) \quad (1.57)$$

If we define as a zero-energy level the middle between the energy levels as in figure 1.3 then the Hamiltonian of the free atom may be written as:

$$\hat{H}_A = \frac{1}{2}(E_e - E_g)\hat{\sigma}_3 = \frac{1}{2}\hbar\omega_0\hat{\sigma}_3 \quad (1.58)$$

where ω_0 denotes the atomic transition frequency (also denoted with ω_{eg} in many textbooks. The Hamiltonian of the free field after changing the energy zero point

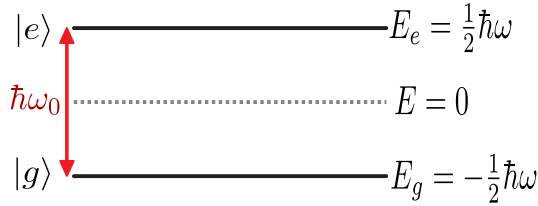


Figure 1.3: Atom energy levels after setting the zero energy level in the middle of the two levels E_g and E_e . The atomic transition frequency is denoted with ω_0

level, may be written as:

$$\hat{H}_F = \hbar\omega\hat{a}^\dagger\hat{a} \quad (1.59)$$

The total Hamiltonian that describes the interaction of the two-level atom with the single mode electromagnetic field, takes the form:

$$\hat{H} = \hat{H}_A + \hat{H}_F + \hat{H}^{(I)} = \frac{1}{2}\hbar\omega_0\hat{\sigma}_3 + \hbar\omega\hat{a}^\dagger\hat{a} + \hbar\lambda(\hat{\sigma}_+ + \hat{\sigma}_-)(\hat{a} + \hat{a}^\dagger) \quad (1.60)$$

In the case of the free field, as it is known, the time evolution of the creation and annihilation operators is described by the relations

$$\hat{a}(t) = \hat{a}(0)e^{-i\omega t} \quad (1.61)$$

$$\hat{a}^\dagger(t) = \hat{a}^\dagger(0)e^{i\omega t} \quad (1.62)$$

The time evolution for the raising and lowering operators of the atom are:

$$\hat{\sigma}_\pm(t) = \hat{\sigma}_\pm(0)e^{\pm i\omega_0 t} \quad (1.63)$$

Considering the time evolution of the total Hamiltonian 1.60 of the system, we need to take under consideration the following proportions:

$$\begin{aligned}\hat{\sigma}_+ \hat{a} &\sim e^{i(\omega_0 - \omega)t} \\ \hat{\sigma}_- \hat{a}^\dagger &\sim e^{-i(\omega_0 - \omega)t} \\ \hat{\sigma}_+ \hat{a}^\dagger &\sim e^{i(\omega_0 + \omega)t} \\ \hat{\sigma}_- \hat{a} &\sim e^{-i(\omega_0 + \omega)t}\end{aligned}\tag{1.64}$$

Supposing that $\omega_0 \simeq \omega$ which in fact means that the frequency of the single-mode field is almost equal to the eigen-frequency of the atom, the last two terms do not conserve energy! The term $\hat{\sigma}_+ \hat{a}^\dagger$ corresponds to the emission of a photon while an atom raises from its ground state to the excited, while the term $\hat{\sigma}_- \hat{a}$ describes the absorption of a photon while the atom transits from its excited state to the ground state. Taking under consideration the Rotating Wave Approximation, the quantities that are proportionate to the terms $\omega_0 + \omega$ are equal to 0 since they oscillate much faster than the terms with the quantity $\omega_0 - \omega$, therefore the Hamiltonian takes the form:

$$\hat{H} = \frac{1}{2} \hbar \omega_0 \hat{\sigma}_3 + \hbar \omega \hat{a}^\dagger \hat{a} + \hbar \lambda (\hat{\sigma}_+ \hat{a} + \hat{\sigma}_- \hat{a}^\dagger)\tag{1.65}$$

In literature, the equation 1.65 is referred to as *Jaynes-Cummings model*. The original paper was published in 1963 [25], while an exquisite topical review may be found in [26]. Having obtained the Hamiltonian, what remains to be done is to study the dynamics of the system. First of all, we will define two constants of motion, \hat{P}_e which in fact counts the electrons that are involved in the process of the interaction and \hat{N}_e which is the number of excitations. Those constants are defined by the relation:

$$\hat{P}_e = |e\rangle \langle e| + |g\rangle \langle g| = 1, \quad [\hat{H}, \hat{P}_e] = 0\tag{1.66}$$

$$\hat{N}_e = \hat{a}^\dagger \hat{a} + |e\rangle \langle e|, \quad [\hat{H}, \hat{N}_e] = 0\tag{1.67}$$

Looking into equation 1.65 we observe that we can split the Hamiltonian \hat{H} it into two commuting parts,

$$\hat{H}_I = \hbar \omega \hat{N}_e + \hbar \left(\frac{\omega_0}{2} - \omega \right) \hat{P}_e\tag{1.68}$$

$$\hat{H}_{II} = -\hbar \Delta + \hbar \lambda (\hat{\sigma}_+ \hat{a} + \hat{\sigma}_- \hat{a}^\dagger)\tag{1.69}$$

so that the for the two terms holds the relation $[\hat{H}_I, \hat{H}_{II}] = 0$. The first term contributes only some phase terms, while the second terms contains the dynamics of the problem. The quantity $\Delta = \omega_0 - \omega$ is called *detuning* and obviously signifies the difference between the frequency of the single mode field and the eigenfrequency of the two-level atom.

Jaynes Cummings model in the resonant case

Supposing we have a system having initially the atom in its excited state $|e\rangle$ and the field in the state $|n\rangle$, so this initial state may be written as $|i\rangle = |e\rangle|n\rangle$ and the initial energy is $E_i = \frac{1}{2}\hbar\omega + n\hbar\omega$. State $|i\rangle$ is coupled to the state $|f\rangle = |g\rangle|n+1\rangle$, since we supposed there are only two atomic levels. The final state $|f\rangle$ has energy $E_f = -\frac{1}{2}\hbar\omega + (n+1)\hbar\omega$ and it is obvious (as it was expected) that the two states have equal energies. We want to obtain an equation describing explicitly the time-dependence of this system, so we will write down the state vector and solve the Schrödinger equation. The state vector $|\psi(t)\rangle$ is

$$|\psi(t)\rangle = C_i(t)|i\rangle + C_f(t)|f\rangle \quad (1.70)$$

where $C_i(0) = 1$ since the atom at $t = 0$ is in the initial state and $C_f(0) = 0$. The use of the \hat{H}_{II} term of the Hamiltonian 1.69 in the Schrödinger equation reads:

$$i\hbar \frac{d|\psi(t)\rangle}{dt} = \hat{H}_{II}|\psi(t)\rangle \Leftrightarrow \quad (1.71)$$

Therefore we end up with the system of differential equations

$$\begin{aligned} \dot{C}_i &= -i\lambda\sqrt{n+1}C_f \\ \dot{C}_f &= -i\lambda\sqrt{n+1}C_i \end{aligned} \quad (1.72)$$

If we eliminate C_f we obtain the equation:

$$\ddot{C}_i + \lambda^2(n+1)C_i = 0 \quad (1.73)$$

and by substitution in the system of differential equations we find that

$$C_f(t) = -i \sin(\lambda t \sqrt{n+1}) \quad (1.74)$$

Therefore the solution of the problem is:

$$|\psi(t)\rangle = \cos(\lambda t \sqrt{n+1})|e\rangle|n\rangle - i \sin(\lambda t \sqrt{n+1})|g\rangle|n+1\rangle \quad (1.75)$$

Therefore, the probability of finding our system in state $|i\rangle$ is:

$$P_i(t) = |C_i(t)|^2 = \cos^2(\lambda t \sqrt{n+1}) \quad (1.76)$$

while the probability of finding the system in state $|f\rangle$ is:

$$P_f(t) = |C_f(t)|^2 = \sin^2(\lambda t \sqrt{n+1}) \quad (1.77)$$

The atomic inversion is calculated as

$$\begin{aligned} W(t) &= \langle \psi(t) | \hat{\sigma}_3 | \psi(t) \rangle \\ &= P_i(t) - P_f(t) \\ &= \cos(2\lambda t \sqrt{n+1}) \end{aligned} \quad (1.78)$$

We are in position to define the quantum electrodynamic analogue of Rabi frequency, as $\Omega(n) = 2\lambda\sqrt{n+1}$, thus the atomic inversion may be written in the form:

$$W(t) = \cos[\Omega(n)t] \quad (1.79)$$

As it is clear from both equation 1.79 and figure 1.4, the atomic inversion for a

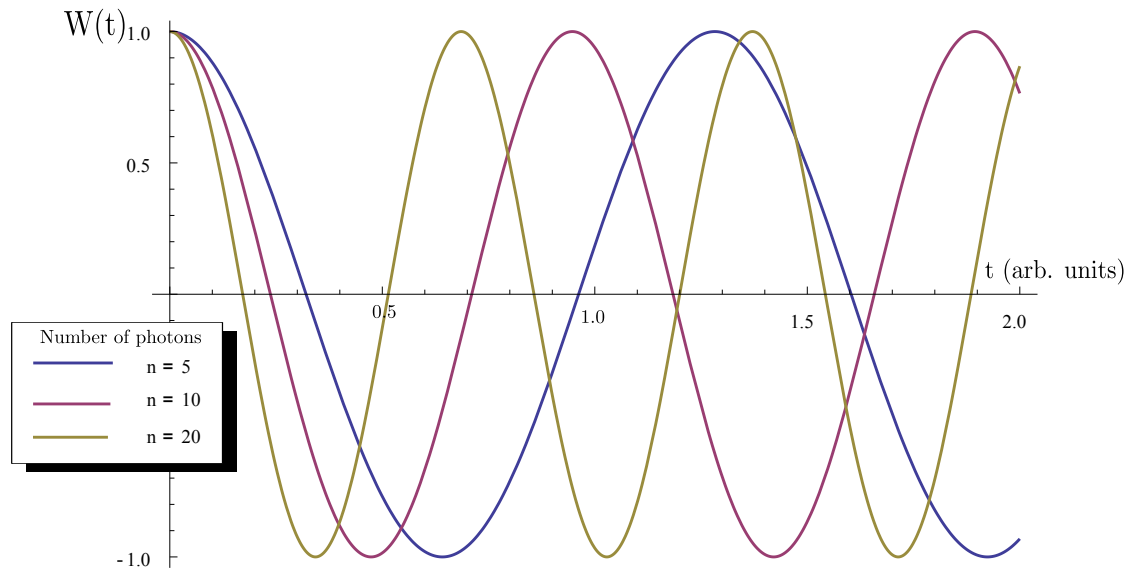


Figure 1.4: Atomic inversion for number states with different number of n

field that is initially in a number state is periodical, just like in the semiclassical case of Rabi model. Though, there are some striking differences. In the quantum electrodynamic case, there are Rabi oscillations even for the case when $n = 0$ ie the vacuum state. Those are called vaccum Rabi oscillations and do not have a classical analogue. They are arising from the spontaneous absorption and re-emission of a photon, an effect that originates from the Purcell effect [8] and may be observed in high Q cavities sustaining those fields as we will see later. It may be counter-intuitive the fact that number states, the more quantum states of light manifestate this almost classical behaviour. In fact we would expect this kind of periodicity to be present when having initially a coherent field. Examining this case, let's suppose that the atom is initially in a superposition of its ground

and excited state, thus:

$$|\psi(0)\rangle_{atom} = C_g |g\rangle + C_e |e\rangle \quad (1.80)$$

If the field is in a superposition of number states

$$|\psi(0)\rangle_{field} = \sum_{n=0}^{\infty} C_n |n\rangle \quad (1.81)$$

then we may write down the initial state of the system as:

$$|\psi(0)\rangle = |\psi(0)\rangle_{atom} \otimes |\psi(0)\rangle_{field} \quad (1.82)$$

The solution of Schrödinger equation in this case yields:

$$\begin{aligned} |\psi(t)\rangle = & \sum_{n=0}^{\infty} \{ [C_e C_n \cos(\lambda t \sqrt{n+1}) - i C_g C_{n+1} \sin(\lambda t \sqrt{n+1})] |e\rangle + \\ & + [-i C_e C_{n-1} \sin(\lambda t \sqrt{n}) + C_g C_n (\cos \lambda t \sqrt{n})] |g\rangle \} |n\rangle \end{aligned} \quad (1.83)$$

In general, this is an entangled state. For the case that the atom is initially in the excited state where $C_e = 1$ and $C_g = 0$ we may write down the solution as:

$$|\psi(t)\rangle = |\psi_g(t)\rangle |g\rangle + |\psi_e(t)\rangle |e\rangle \quad (1.84)$$

where $|\psi_g(t)\rangle$ and $|\psi_e(t)\rangle$ are the field components that are given by the relations:

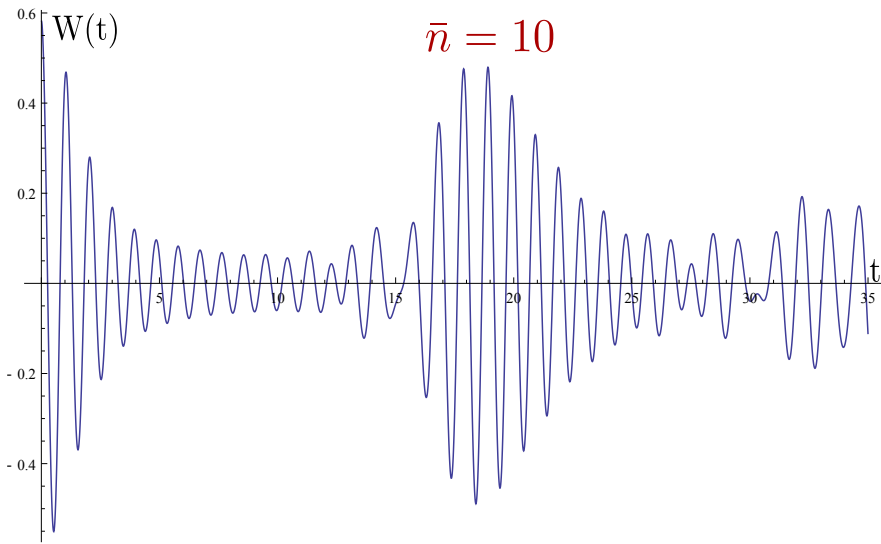
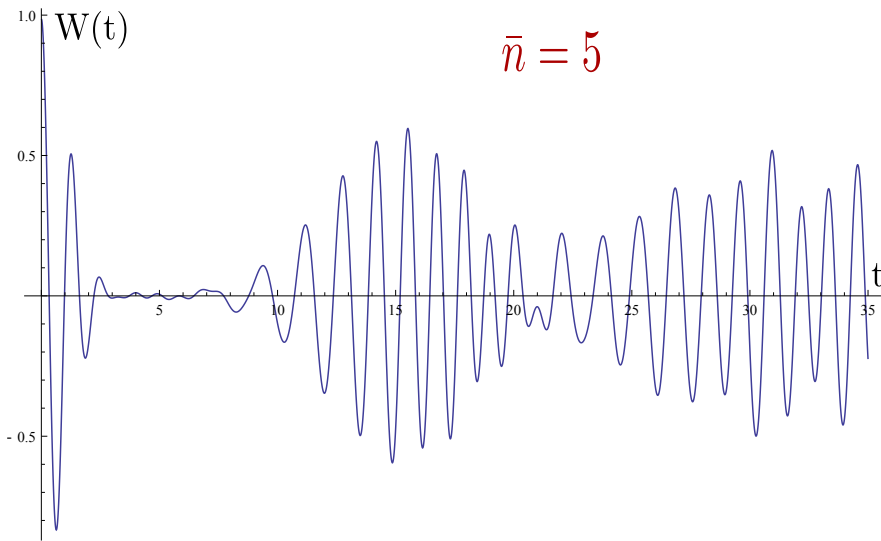
$$\begin{aligned} |\psi_g(t)\rangle &= -i \sum_{n=0}^{\infty} C_n \sin(\lambda t \sqrt{n+1}) |n+1\rangle, \\ |\psi_g(t)\rangle &= \sum_{n=0}^{\infty} C_n \cos(\lambda t \sqrt{n+1}) |n\rangle \end{aligned} \quad (1.85)$$

Now, the atomic inversion is

$$\begin{aligned} W(t) &= \langle \psi(t) | \hat{\sigma}_3 | \psi(t) \rangle \\ &= \langle \psi_e(t) | \psi_e(t) \rangle - \langle \psi_g(t) | \psi_g(t) \rangle \\ &= \sum_{n=0}^{\infty} |C_n|^2 \cos(2\lambda t \sqrt{n+1}) \end{aligned} \quad (1.86)$$

and supposing we have a *coherent state*, so that $C_n = e^{-\frac{|a|^2}{2}} \frac{a^n}{\sqrt{n!}}$, the inversion finally becomes

$$W(t) = e^{-\bar{n}} \sum_{n=0}^{\infty} \frac{\bar{n}^n}{n!} \cos(2\lambda t \sqrt{n+1}) \quad (1.87)$$

**Figure 1.5:** Atomic inversion for $\bar{n} = 10$ **Figure 1.6:** Atomic inversion for $\bar{n} = 5$

The difference from 1.79 becomes obvious if we plot 1.87, which is done in figures 1.5 and 1.6. First of all we observe that Rabi oscillations are collapsing and reviving, though they do not fully recover to the initial amplitude. Using bigger time intervals it is possible to observe this sequence of collapses and revivals, with the revivals becoming more and more indistinguishable as time increases. This is probably the main difference of the Jaynes-Cummings model with the semiclassical Rabi model. In order to explain this difference we should find an

expression for the collapse. The average number of photons is $\bar{n} = |\alpha|^2$, thus the dominant Rabi frequency is

$$\Omega(\bar{n}) = 2\lambda\sqrt{\bar{n} + 1} \approx 2\lambda\sqrt{\bar{n}}, \quad \bar{n} \gg 1 \quad (1.88)$$

Though, there will be a spectrum of secondary frequencies as a result of the width of probabilities $|C_n|^2$ around \bar{n} , in the region $\bar{n} + \Delta n$, for example the frequencies in the region from $\Omega(\bar{n} - \Delta n)$ to $\Omega(\bar{n} + \Delta n)$. The collapse time t_c may be approximated by the energy-time uncertainty relation:

$$t_c[\Omega(\bar{n} + \Delta n) - \Omega(\bar{n} - \Delta n)] \simeq 1 \quad (1.89)$$

where the width of frequencies is responsible for the phase difference in Rabi oscillations. For a coherent state we know that $\Delta n = \sqrt{\bar{n}}$, therefore:

$$\begin{aligned} \Omega(\bar{n} \pm \sqrt{\bar{n}}) &\simeq 2\lambda\sqrt{\bar{n} \pm \sqrt{\bar{n}}} \\ &= 2\lambda\sqrt{\bar{n}} \left(1 \pm \frac{1}{2\sqrt{\bar{n}}}\right) \\ &= 2\lambda\sqrt{\bar{n}} \pm \lambda \end{aligned} \quad (1.90)$$

So, we may obtain that $t_c = \frac{1}{2\lambda}$, which is a quantity that doesn't depend on the average photon number. A more rigorous estimation [11] of the collapse time gives us the expression

$$t_c = \frac{\sqrt{2}}{\lambda} \quad (1.91)$$

Regarding the revival time, with a similar procedure we find it to be

$$t_R \simeq k\sqrt{\frac{2\pi\bar{n}}{\lambda}} \quad (1.92)$$

How to create a Schrödinger cat: The dispersive regime.

We define the dispersive regime as the set of cavity frequencies that satisfy the requirement:

$$\Delta = (\omega - \omega_0), \quad \hbar|\Delta| \gg \lambda \quad (1.93)$$

When the detuning is very large compared to the coupling constant, the coupling between the atom and the field cannot induce transitions, but still the coupling will renormalize the energies of the system. Doing perturbation theory in the parameter λ/Δ we can verify that the effective dispersive Hamiltonian is:

$$\hat{H}_{disp} = -\frac{1}{2} \left(\hbar\omega_0 + \frac{\lambda^2}{\hbar\Delta} \right) \hat{\sigma}_z + \left(\hbar\omega - \frac{\lambda^2}{\hbar\Delta} \hat{\sigma}_z \right) \hat{a}^\dagger \hat{a} \quad (1.94)$$

This expression points out the fact that the effective cavity frequency now depends on the atom state and equivalently the atomic energy splitting depends on the number of photons inside the cavity. The term proportional to $(\hat{\sigma}_z \hat{a}^\dagger \hat{a})$ is referred to in literature as **ac Stark shift**, while the vacuum shift of the atomic energy splitting $(\hat{\sigma}_z \lambda^2 / \hbar \Delta)$ is called the Lamb shift.

Another approach on dealing with the dispersive regime, is returning to the term of relation 1.69 that contains the dynamics of the problem and take the effective Hamiltonian.

$$\hat{H}_{eff} = \hbar \chi (\hat{\sigma}_+ \hat{a} + \hat{\sigma}_- \hat{a}^\dagger) \quad (1.95)$$

where $\chi = \frac{\lambda^2}{\Delta}$. Supposing the initial state of the system is a Fock state,

$$|\psi(0)\rangle = |g\rangle |n\rangle \quad (1.96)$$

the time-evolution of the system leads us to the equation

$$|\psi(t)\rangle = e^{-\frac{iH_{eff}t}{\hbar}} |\psi(0)\rangle = e^{i\chi nt} |g\rangle |n\rangle \quad (1.97)$$

We therefore obtain a phase factor that cannot be measured or give us any more information. Supposing that instead of a Fock state we have a coherent state $|\alpha\rangle$, the time evolution of the system will lead to the equation

$$|\psi(t)\rangle = e^{-i\chi t} |e\rangle |\alpha e^{-i\chi t}\rangle \quad (1.98)$$

We see that in the case of the field being a coherent state, we have the amplitude of the system state rotated in the phase space by the angle χt , while the direction of the state vector depends on the atom state $|e\rangle$. Supposing now that our atom is prepared in a superposition of states $|g\rangle$ and $|e\rangle$, so that

$$|\psi_{atom}\rangle = \frac{|g\rangle + e^{i\phi}|e\rangle}{\sqrt{2}} \quad (1.99)$$

the initial state of the atom becomes

$$|\psi(0)\rangle = |\psi_{atom}\rangle |\alpha\rangle \quad (1.100)$$

The time evolution of this version of the system yields:

$$|\psi(t)\rangle = e^{-i\frac{H_{eff}t}{\hbar}} |\psi(0)\rangle = \frac{1}{\sqrt{2}} (|g\rangle |\alpha e^{i\chi t}\rangle + e^{-i(\chi t - \phi)} |e\rangle |\alpha e^{-i\chi t}\rangle) \quad (1.101)$$

The above equation clearly states that the time evolution in the far off-resonant case leads to an entanglement between the atom and the field. Choosing time to be $\chi t = \frac{\pi}{2}$ (in which we usually refer to as a $\frac{\pi}{2}$ pulse) we find that:

$$\left| \psi \left(\frac{\pi}{2\chi} \right) \right\rangle = \frac{1}{\sqrt{2}} (|g\rangle |i\alpha\rangle - ie^{i\phi} |e\rangle |-i\alpha\rangle) \quad (1.102)$$

The states $|g\rangle|i\alpha\rangle$ and $|-\alpha\rangle$ are separated by 180° in the phase space and they are called *maximally distinguishable states*. The magnitude of $|\alpha|$ defines whether they are macroscopically or mesoscopically distinguishable. The above process is used to prepare *Schrödinger cat states*. Another configuration that is widely used in experiments involves another energy level of the atom that is *far* from the levels $|e\rangle$ and $|g\rangle$, so that $E_f \ll E_g$, which let us suppose it is $|f\rangle$ and that the transition $|f\rangle \leftrightarrow |g\rangle$ is not supported in the experimental setup. This property doesn't allow the time evolution of the state $|f\rangle|\alpha\rangle$, so if we prepare the atom in a superposition of $|f\rangle$ and $|g\rangle$, this will lead to the time-evolution of the term containing the term $|g\rangle$ and will just contribute a phase factor ϕ . The analytical time evolution of this configuration yields:

$$|\Psi(0)\rangle = |\Psi_{\text{atom}}\rangle|\alpha\rangle \xrightarrow{\text{time evolution}} |\Psi(t)\rangle = (|g\rangle|\alpha e^{i\chi t}\rangle + e^{i\phi}|f\rangle|\alpha\rangle) \quad (1.103)$$

Setting the interaction time to be such that $\chi t = \frac{\pi}{2}$ we obtain:

$$\left| \psi \left(\frac{\pi}{2\chi} \right) \right\rangle = \frac{1}{2} (|g\rangle|-\alpha\rangle + e^{i\phi}|f\rangle|\alpha\rangle) \quad (1.104)$$

which is another way to obtain a *Schrödinger cat state*.

1.3.2 Dressed states approach

There is a wide variety of ways to obtain the solution of the Jaynes-Cummings model and getting an insight on its importance to light-matter interaction. Solving the time-dependent Schrödinger equation is not the only one. As we previously discussed, during the interaction of a two-level atom with a single-mode field there are two possible states of the system, ie. $|g\rangle|n+1\rangle$ and $|e\rangle|n\rangle$. We may use these states, also called *bare states* since they don't include an explicit limitation on the photon number as a *basis* to solve the dynamics of the problem in a more subtle manner. The fact that we are talking about states of an atom coupled to a field through the Jaynes-Cummings Hamiltonian, led to the term *dressed states of the atom or Jaynes-Cummings doublet*. The reason for introducing a new basis is the fact that through this process we obtain an expression that contains in simple terms, the eigenstates of the system. We start from the bare states of the system:

$$\begin{aligned} |\psi_{1n}\rangle &= |e\rangle|n\rangle \\ |\psi_{2n}\rangle &= |g\rangle|n+1\rangle \end{aligned} \quad (1.105)$$

Those states are orthogonal and writing down the Hamiltonian 1.65 matrix elements $\hat{H}_{ij}^{(n)} = \langle \psi_{in} | \hat{H} | \psi_{jn} \rangle$, we obtain:

$$\begin{aligned}\hat{H}_{11}^{(n)} &= \hbar \left[n\omega + \frac{1}{2}\omega_0 \right] \\ \hat{H}_{22}^{(n)} &= \hbar \left[(n+1)\omega - \frac{1}{2}\omega_0 \right] \\ \hat{H}_{12}^{(n)} &= \hbar\lambda\sqrt{n+1} = \hat{H}_{21}^{(n)}\end{aligned}\quad (1.106)$$

which leads us to a Hamiltonian of the form

$$H^{(n)} = \begin{bmatrix} n\omega + \frac{1}{2}\hbar\omega_0 & \hbar\lambda\sqrt{n+1} \\ \hbar\lambda\sqrt{n+1} & (n+1)\omega - \frac{1}{2}\omega_0 \end{bmatrix} \quad (1.107)$$

In figure 1.7 we show the energy split between the bare states $|\psi_{1n}\rangle, |\psi_{2n}\rangle$ and

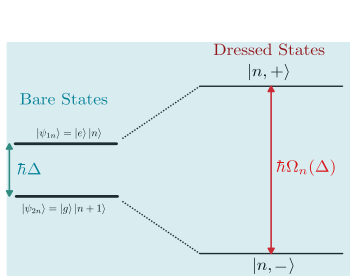


Figure 1.7: Split of the energy levels of the bare states (left) due to the interaction with a quantized field and the dressed states energy levels (right)

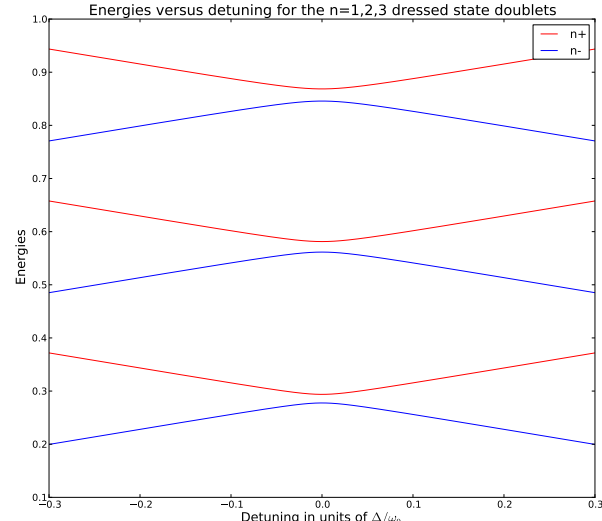


Figure 1.8: Dressed states energies versus detuning for the dressed states $|1, \pm\rangle, |2, \pm\rangle$ and $|3, \pm\rangle$.

the dressed states $|n,+\rangle, |n,-\rangle$ due to the interaction of the atom with the field, which is often referred to as *the Jaynes-Cummings splitting*. The expression of the the Hamiltonian involves only states that have a difference by ± 1 in the photon number, thus for a given n its eigenvalues become:

$$E_{\pm}(n) = \left(n + \frac{1}{2} \right) \hbar\omega \pm \hbar\Omega_n(\Delta) \quad (1.108)$$

where

$$\Omega_n(\Delta) = \sqrt{\Delta^2 + 4\lambda^2(n+1)}, (\Delta = \omega_0 - \omega) \quad (1.109)$$

is the Rabi frequency which now includes the detuning. In figure 1.8 we show the dependence of the dressed-states energy level with the detuning, for three different doublets. This expression for the Rabi frequency, enables us to write down a more general expression to describe the system, the *dressed states*:

$$\begin{aligned} |n, +\rangle &= \cos\left(\frac{\Phi_n}{2}\right) |\psi_{1n}\rangle + \sin\left(\frac{\Phi_n}{2}\right) |\psi_{2n}\rangle \\ |n, -\rangle &= -\sin\left(\frac{\Phi_n}{2}\right) |\psi_{1n}\rangle + \cos\left(\frac{\Phi_n}{2}\right) |\psi_{2n}\rangle \end{aligned} \quad (1.110)$$

where Φ_n is the mixture angle that intuitively describes the contribution of each of the basis vectors to the superposition of states and are defined as:

$$\begin{aligned} \Phi_n &= \tan^{-1}\left(\frac{2\lambda\sqrt{n+1}}{\Delta}\right) = \tan^{-1}\left(\frac{\Omega_n(0)}{\Delta}\right) \\ \sin\left(\frac{\Phi_n}{2}\right) &= \sqrt{\frac{\Omega_n(\Delta) - \Delta}{2 \cdot \Omega_n(\Delta)}} \\ \cos\left(\frac{\Phi_n}{2}\right) &= \sqrt{\frac{\Omega_n(\Delta) + \Delta}{2 \cdot \Omega_n(\Delta)}} \end{aligned} \quad (1.111)$$

Dressed states enable us to describe the dynamics of the system, for any initial state of it. Supposing we have a field in an initial state that is a superposition of other states, interacting with a two-level atom prepared in its excited state, the initial state of the atom-field system may be written as:

$$\begin{aligned} |\psi_{af}(0)\rangle &= |\psi_f(0)\rangle |e\rangle \\ &= \sum_n C_n |n\rangle |e\rangle \\ &= \sum_n C_n |\psi_{1n}\rangle \end{aligned} \quad (1.112)$$

Using equation 1.110 to express $|\psi_{1n}\rangle$ in terms of dressed states $|n, \pm\rangle$ we obtain:

$$|\psi_{1n}\rangle = \cos\left(\frac{\Phi_n}{2}\right) |n, +\rangle - \sin\left(\frac{\Phi_n}{2}\right) |n, -\rangle \quad (1.113)$$

Therefore the atom-field system state, is expressed by the wave function:

$$|\psi_{af}(0)\rangle = \sum_n C_n \left[\cos\left(\frac{\Phi_n}{2}\right) |n, +\rangle - \sin\left(\frac{\Phi_n}{2}\right) |n, -\rangle \right] \quad (1.114)$$

and the evolution of this system is described by the equation:

$$\begin{aligned} |\psi_{af}(t)\rangle &= e^{-\frac{i}{\hbar}\hat{H}t} \cdot |\psi_{af}(0)\rangle = \\ &= \sum_n C_n \left[\cos\left(\frac{\Phi_n}{2}\right) |n,+\rangle \cdot e^{-\frac{iE_+(n)t}{\hbar}} - \sin\left(\frac{\Phi_n}{2}\right) |n,-\rangle e^{-\frac{iE_-(n)t}{\hbar}} \right] \end{aligned} \quad (1.115)$$

1.4 Cavity QED experiments

So far we have discussed the theoretical model that describes the simplest light-matter interaction scenario, ie a two level atom interacting with a single mode quantized field. Like in most cases, theory predicts a lot of interesting results that have to be disproved or verified in the laboratory, in order to adopt, modify or completely reject a certain theoretical model.

Cavities or microcavities are the devices with the help of which we have managed to verify a plethora of phenomena of Quantum Physics.² The simplicity of the system, being not much different than a "photon box" combined with the detailed and remarkable work made from experimental groups around the world leaded by *S. Haroche, J. Kimble, D. Meschede, G. Rempe and H. Walther* [56],[57] and others, has added to the know-how of *preparing, controlling and manipulating* atoms in such states that we can use them as *qubits* in order to implement quantum algorithms using these setups.

Of course Cavity QED is not the sole candidate for the implementation of full scale algorithms. In fact, as we will see in the following chapters, there are lots of factors that restrict those systems from being ideal for quantum algorithms. The most prominent of those factors is decoherence, due to the interaction of a cavity-like setup with the environment [29]. In the last decade there has been a new generation of nanostructures where the predictions of Cavity QED could be tested in very different conditions in a solid state environment. These include *Photonic crystals* embeded with *Quantum Dots* and more recently *Circuit QED*. The latter technology exhibiting very low loss rates, is one of the most promising techniques regarding achieving the goal of creating a Quantum Computer.

²This remarkable work has led to the recognition of the founders of the field with the Nobelprize in Physics in 2012.

1.4.1 Tailoring spontaneous emission rates and atomic energies in confined space

Purcell's formula [8] for the spontaneous emission rate modification of a dipole in a cavity versus the case in free space, reads:

$$\frac{\Gamma_{\text{cavity}}}{\Gamma_{\text{free}}} = \frac{\rho_c(\omega_0)}{\rho_f(\omega_0)} = \frac{2\pi Q}{V_c \omega_0^3} = Q \frac{\lambda_0^3}{4\pi^2 V_c} \quad (1.116)$$

where Γ_{cavity} , Γ_{free} are the spontaneous emission rates inside the cavity and in free space respectively, $\rho_c(\omega_0)$, $\rho_f(\omega_0)$ are the densities of states for the cavity and the free space for the frequency ω_0 , Q is the cavity quality factor, λ_0 is the wavelength of the radiation in free space and V_c is the volume of the cavity.

Initially, cavities had been used in order to observe the modification of the spontaneous emission rate. For $V \simeq \lambda_0^3$, the spontaneous emission rate is increased by a factor almost equal to Q . Though, if the cavity is detuned, the decay-rate will decrease. The first observation of enhanced atomic spontaneous emission in a resonant cavity was published by Goy *et al* in 1983 [9], in whose experiment Rydberg atoms of sodium excited in the 23s state where injected in a niobium superconducting cavity resonant in 340 GHz. The cooling of the cavity had the advantage of suppressing the thermal field inside the cavity. Regarding optical transitions, in which the thermal-field is totally suppressed, the first experiments were conducted by Feld and collaborators in 1987 [58],[59] and in those was demonstrated the enhancement of spontaneous transitions in optical cavities.

As far as atomic energy shifts are concerned, the polarization of the atom by the non-resonant parts of the broadband electromagnetic field causes energy shifts, the Lamb shift being the most prominent one. Lamb shift may be described as being the result of the emission and re-absorption of virtual photons, so taking under consideration the fact that the real emission rate may be modified in confined space, the same should apply for those "virtual" photons, whereas the radiation energy shift results from vacuum fluctuations and is analogous to the result of Casimir effect [60].

1.4.2 Microwave cavities and the strong coupling regime

Selecting the appropriate region in which the phenomena under investigation are to be explored, gives two prominent candidates, ie. microwave frequencies and optical frequencies. In what follows we will deal mainly with microwave frequencies, though a very good review regarding optical cavity QED. may be found by Englert *et al*[56] Cavities should be imagined as a very small laser tube, with high reflectivity mirrors and dimensions such that the spontaneous

emission rate is modified for the desired frequencies. At microwave frequencies and low temperatures, the main technique of cavity QED involves high reflecting superconducting mirrors (niobium) able to impose to a single photon to bounce roughly 10^{10} times back and forth inside the cavity, before eventually getting out of it. Microwave photons are particularly difficult to detect, so the detection of the cavity field state is deduced from the resulting interaction on probe atoms. In optical QED configuration, the inverse process can also be used, namely the state of the field is used to deduce the atomic state.

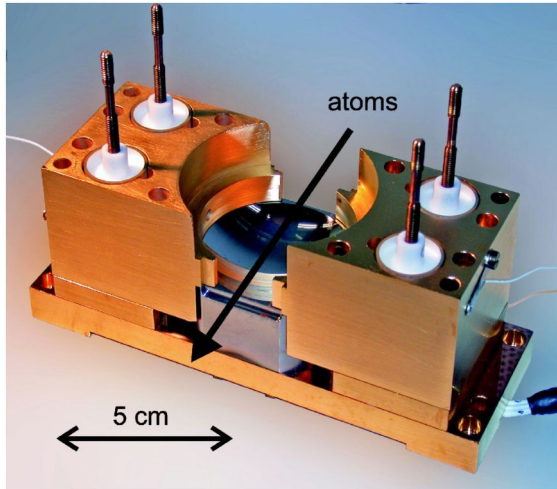


Figure 1.9: Photograph of the cavity assembly used in [61] with the top mirror removed. The atomic beam path is visualized by the arrow. The four posts are used to mount the upper mirror.

The flux of the atoms is controlled mainly by selecting their velocities or by using a chopping the atom beam using shutters.

In order to observe the effects described earlier, the atom field coupling constant g , must be larger than the atom and cavity relaxation rates T_a^{-1} and T_c^{-1} and much larger than the reciprocal of the atom-cavity interaction time. These conditions summarize the idea of the *strong coupling regime*. The *strong coupling* between the cavity and the atom implies that even a single photon inside the cavity is able to induce strong non-linear effects to the atom, as well as that a single atom in a cavity, is enough to sustain a laser oscillation. A parameter used to characterize the atom-cavity coupling is the *cooperativity*, which is defined as:

$$C = \frac{g^2}{\kappa\gamma} \quad (1.117)$$

where g is the atom-cavity coupling parameter, κ is the dissipation rate and γ is the spontaneous emission rate, as it is shown in figure 1.10.

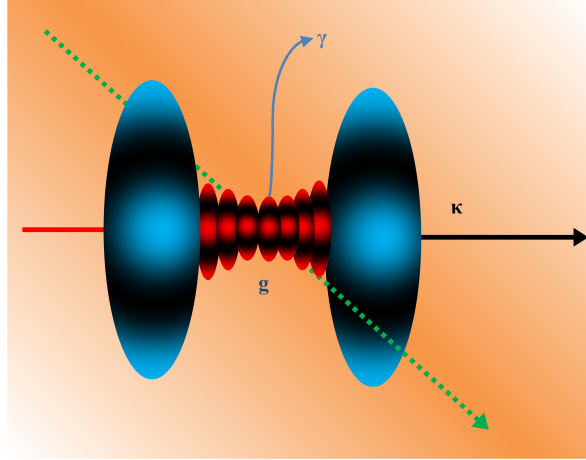


Figure 1.10: Representation of the main characteristics of cavity QED configuration

In [61] the fabrication of a state of the art superconducting cavity is described in detail. In this cavity the quality factor for the desired frequency (51.1 GHz) is $Q = 4.2 \times 10^{10}$, allowing photon storage time $T_c = 130ms$. For this setup, using the relation $Q = \frac{\omega_{cav}}{\kappa}$ we can calculate the rate of loss κ of the cavity to be $\kappa = 1,26\text{Hz}$. Previous experimental setups for the microwave region, were using cavities with a quality factor of the order of $Q = 310^8$ for the same frequency (51.1 GHz)[62].

Regarding the enhancement of the spontaneous emission rate when the atomic transition is resonant with the cavity, we can calculate using *Fermi's golden rule* (see for example [1]) that

$$\Gamma_{cav}^{resonant} = \Gamma_{free} \frac{3Q}{4\pi^2} \left(\frac{\lambda_0^3}{V} \right) \text{ with } \lambda_0 = 2\pi \frac{c}{\omega} \quad (1.118)$$

while for an atom off-resonant with the cavity

$$\Gamma_{cav}^{off\ resonant} = \Gamma_{free} \frac{3}{16Q\pi^2} \left(\frac{\lambda_0^3}{V} \right) \text{ with } \lambda_0 = 2\pi \frac{c}{\omega} \quad (1.119)$$

These relations resemble to Purcell's initial formula 1.116 for the enhancement of spontaneous emission rate. In order to have a reference of what are some typical values for the set of (g, κ, γ) we refer to [62] and [40], where we find:

$$\begin{aligned} (g, \kappa, \gamma) / 2\pi &= (120, 40, 5.2) \text{ MHz with } C = 69 \text{ for optical} \\ (g, \kappa, \gamma) / 2\pi &= (25, 0.36, 0.005) \text{ kHz with } C = 3.4 \times 10^5 \text{ for microwave} \end{aligned} \quad (1.120)$$

1.5 Cavity QED with lossy cavities

1.5.1 The empty cavity case

Using the techniques developed in Appendix B. Theoretical tools for cavity QED, we consider a cavity sustaining a frequency ω_c , while its field is ruled by the action of creation and annihilation operators, \hat{a}^\dagger and \hat{a} . Its environment (the reservoir) is a collection of harmonic oscillators with frequencies ω_j , while each mode of it is controlled by operators \hat{r}_j^\dagger and \hat{r}_j . Supposing that the cavity mode couples to the j^{th} reservoir oscillating mode via a coupling strength of κ_j , the Hamiltonians in the rotating wave approximation, neglecting the contribution of vacuum fluctuations will be:

$$\begin{aligned}\hat{H}_S &= \hbar\omega_c\hat{a}^\dagger\hat{a} \\ \hat{H}_R &= \sum_j \hbar\omega_j\hat{r}_j^\dagger\hat{r}_j \\ \hat{H}_{SR} &= \sum_j \hbar \left(\kappa_j^* \hat{a} \hat{r}_j^\dagger + h.c. \right) = \hbar \left(\hat{a} \hat{\Gamma}^\dagger + \hat{a}^\dagger \hat{\Gamma} \right)\end{aligned}\tag{1.121}$$

Using the general derivation of the master equation, we can identify the terms for the specific problem to be:

$$\begin{aligned}s_1 &= \hat{a} \\ s_2 &= \hat{a}^\dagger \\ R_1 &= \hat{\Gamma}^\dagger \\ R_2 &= \hat{\Gamma}\end{aligned}\tag{1.122}$$

Moving to the interaction picture, the expressions for the above operators, become:

$$\begin{aligned}\tilde{s}_1 &= \tilde{\hat{a}} e^{-i\omega_c t} \\ \tilde{s}_2 &= \tilde{\hat{a}}^\dagger e^{i\omega_c t} \\ \tilde{R}_1 &= \tilde{\hat{\Gamma}}^\dagger e^{i\omega_c t} \\ \tilde{R}_2 &= \tilde{\hat{\Gamma}} e^{-i\omega_c t}\end{aligned}\tag{1.123}$$

The reservoir correlation functions, under the Markov approximation are given by the relations:

$$\begin{aligned}\langle \tilde{\Gamma}(t)\tilde{\Gamma}(t') \rangle &= 0 \\ \langle \tilde{\Gamma}^\dagger(t)\tilde{\Gamma}^\dagger(t') \rangle &= 0 \\ \langle \tilde{\Gamma}^\dagger(t)\tilde{\Gamma}(t') \rangle &= \kappa \bar{n} \delta(t - t') \\ \langle \tilde{\Gamma}(t)\tilde{\Gamma}^\dagger(t') \rangle &= \kappa (\bar{n} + 1) \delta(t - t')\end{aligned}\tag{1.124}$$

In the above expressions, $\bar{n} = \left(e^{\frac{\hbar\omega_c}{kT}} - 1 \right)^{-1}$, κ is the decay rate of the cavity, k is the Boltzmann constant and T is the so-called *bath temperature*. In this specific case, the temperature T used, is the temperature of the environment of the cavity.

Using these correlation functions we obtain the master equation for the density matrix in the interaction picture as:

$$\dot{\tilde{\rho}} = -\kappa \bar{n} (\hat{a}\hat{a}^\dagger \tilde{\rho} - \hat{a}^\dagger \tilde{\rho} \hat{a}) - \kappa (\bar{n} + 1) (\hat{a}^\dagger \hat{a} \tilde{\rho} - \hat{a} \tilde{\rho} \hat{a}^\dagger) + \text{h.c.} \quad (1.125)$$

Further manipulation of this equation can allow us to separate terms containing the term \bar{n} , so the master equation becomes:

$$\dot{\tilde{\rho}}(t) = -\kappa (\hat{a}^\dagger \hat{a} \tilde{\rho} + \tilde{\rho} \hat{a}^\dagger \hat{a} - 2\hat{a} \tilde{\rho} \hat{a}^\dagger) - 2\kappa \bar{n} (\hat{a} \hat{a}^\dagger \tilde{\rho} + \hat{a}^\dagger \hat{a} \tilde{\rho} - \hat{a}^\dagger \tilde{\rho} \hat{a} - \hat{a} \tilde{\rho} \hat{a}^\dagger) \quad (1.126)$$

At the limit of zero temperature, $\bar{n} = 0$, the equation becomes:

$$\dot{\tilde{\rho}} = -\kappa (\hat{a}^\dagger \hat{a} \tilde{\rho} + \tilde{\rho} \hat{a}^\dagger \hat{a} - 2\hat{a} \tilde{\rho} \hat{a}^\dagger) \quad (1.127)$$

Essentially, numerical simulations that calculate the time evolution of a dissipating system using the master equation approach, converge to solving a system of differential equations with dimensions that depend mainly on the number of fock states that initially exist in the cavity.

Following the set of values as it was presented in 1.120, we can plot the time evolution of a state that consists of one excitation in a cavity, setting the values to be: $(g, \kappa, \gamma) = (1000, 10, 1)$, therefore keeping the requirements of the *strong coupling regime*.

1.5.2 Monte Carlo - Quantum Trajectory method

Another method of dealing numerically with the problem of a lossy cavity, is stochastically evolving the system in time and perform Monte Carlo simulation. In the case of a lossy cavity, we will describe an example to give the outline of the method, supposing a cavity with loss rate κ is coupled to a reservoir at $T = 0$. We begin writing down the master equation of the system, is given by:

$$\frac{d\rho}{dt} = \mathcal{L}\rho = -\frac{i}{\hbar} + \frac{\kappa}{2} (2\hat{a}\rho\hat{a}^\dagger - \hat{a}^\dagger\hat{a}\rho - \rho\hat{a}^\dagger\hat{a}) \quad (1.128)$$

Manipulating this expression in order to separate the reversible coherent part of the dynamics from the total dynamics, we obtain:

$$\frac{d\rho}{dt} = \mathcal{L}_0\rho + \kappa (2\hat{a}\rho\hat{a}^\dagger - \hat{a}^\dagger\hat{a}\rho - \rho\hat{a}^\dagger\hat{a}) \quad (1.129)$$

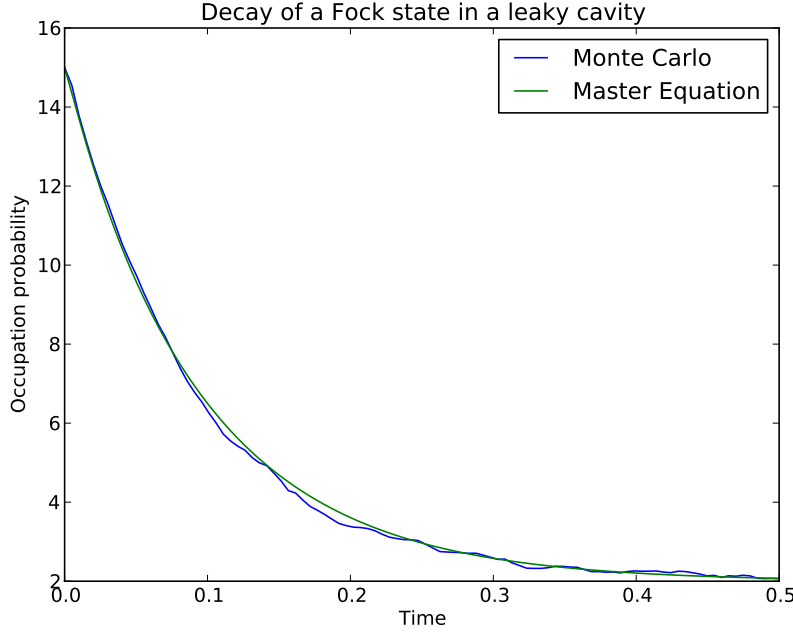


Figure 1.11: Decay of the Fock state $|15\rangle$ in a leaky cavity with $\kappa = 10$, using the master equation approach (green line) and quantum trajectories (blue line).

The formal solution of the Master equation is given by

$$\rho(t) = e^{\mathcal{L}t} \rho(0) \quad (1.130)$$

We can rewrite the Lindblad superoperator \mathcal{L} as

$$\mathcal{L} = \mathcal{T} + (\mathcal{L} - \mathcal{T}) \quad (1.131)$$

where the effect of the super-operator \mathcal{T} on density matrix is given by:

$$\mathcal{T} = \hat{C} \rho \hat{C}^\dagger \quad (1.132)$$

Operator \hat{C} is referred to as the *collapse operator* [29, 63]. Essentially it describes how the environment destroys the coherence within the cavity, leading the cavity field to collapse irreversibly. Its use, provides us with a non-unitary operation that gradually destroys the cavity field. It is proportional to the cavity annihilation operator and is given by the relation:

$$\hat{C} = \sqrt{2\kappa} \hat{a} \quad (1.133)$$

Now, we can use an identity for the super-operators

$$e^{(\mathcal{L}+a\mathcal{S})x} = \sum_{k=0}^{\infty} a^k \int_0^x dx_k \int_0^{x_k} dx_{k-1} \cdots \int_0^{x_2} (e^{\mathcal{L}(x-x_k)} \mathcal{S} e^{\mathcal{L}(x_k-x_{k-1})} \mathcal{S} \cdots \mathcal{S} e^{\mathcal{L}x_1}) dx_1 \quad (1.134)$$

in order to find an expression for the density matrix at a time t

$$\begin{aligned} \rho(t) &= e^{\mathcal{L}t} \rho(0) = e^{[\mathcal{T}+(\mathcal{L}-\mathcal{T})]t} \rho(0) = \\ &= \sum_{k=0}^{\infty} \int_0^t dt_m \int_0^{t_m} dt_{m-1} \cdots \int_0^{t_2} [\mathcal{S}(t-t_m) \mathcal{T} \mathcal{S}(t_m-t_{m-1}) \cdots \mathcal{T} \mathcal{S}(t_1) \rho(0)] dt_1 \end{aligned} \quad (1.135)$$

where we have defined \mathcal{S} as $\mathcal{S} = e^{(\mathcal{L}-\mathcal{T})t}$. The above expansion is valid for every \mathcal{T} . However, for this particular choice of $\mathcal{T} = \hat{C}\rho\hat{C}^\dagger$, the terms in the expansion of $\rho(T)$ have a unique physical significance. Probability for a perfect photo-detector installed in such a way so that it will detect all the photons that *leak out* from the cavity during a time interval $[0, t]$ to record exactly m events, one in each of the infinitesimal time interval times $[t_m, t_m + dt_m] \in [0, t]$ is given by:

$$p_m(t_1, t_2, \dots, t_m; [0, t]) = \text{Tr} [\mathcal{S}(t-t_m) \mathcal{T} \mathcal{S}(t_m-t_{m-1}) \cdots \mathcal{T} \mathcal{S}(t_1) \rho(0)] \quad (1.136)$$

In the above equation, $\rho(0)$ is the initial state of the cavity mode. We can define a non-normalized, conditional density matrix $\tilde{\rho}_c(t)$ of the system, conditioned on the measurement record defined above, by:

$$\tilde{\rho}_c(t) = \mathcal{S}(t-t_m) \mathcal{T} \mathcal{S}(t_m-t_{m-1}) \cdots \mathcal{T} \mathcal{S}(t_1) \rho(0) \quad (1.137)$$

This definition enables us to write down that

$$p_m(t_1, t_2, \dots, t_m; [0, t]) = \text{Tr} [\tilde{\rho}_c(t)] \quad (1.138)$$

If we have a normalized, conditional density matrix $\rho_c(t)$ of the system, it is related to the non-normalized density matrix by the relation:

$$\rho_c(t) = \frac{\tilde{\rho}_c(t)}{\text{Tr} [\tilde{\rho}_c(t)]} \quad (1.139)$$

Using these relations one can write the unconditioned density matrix $\rho(t)$ as:

$$\rho(t) = \sum_{m=0}^{\infty} \int_0^t dt_m \int_0^{t_m} dt_{m-1} \cdots \int_0^{t_2} dt_1 p_m(t_1, t_2, \dots, t_m; [0, t]) \rho_c(t) \quad (1.140)$$

After this mathematical discussion, we should point out the physical meaning. The conditional density operator $\rho_c(t)$ can be interpreted as the actual state of the system, if we know the photo-detection history exactly. To obtain the unconditional density matrix $\rho(t)$, we need to perform an ensemble average of these conditional density matrix weighted by the probabilities of recording the corresponding history of detection. The way to find the dynamics is to perform numerical simulation, which is referred to as **Quantum Trajectory Simulation**. To perform the numerical simulation with a finite time step Δt , one generates a random number r on the unit interval. The probability to detect a photon, which essentially is given by the expectation value of the collapse operator in this interval $[t, t + dt]$, while keeping track of the previous detection history, is:

$$p_c = \text{Tr} [\mathcal{T}\rho_c(t)] \quad (1.141)$$

The density matrix is then evolved forward deciding on the outcome of the comparison of a random number (let's say r) with the product $p_c\Delta t$. For the case $r \leq p_c\Delta t$, a photo detection occurred and the resulting state will be given by:

$$\tilde{\rho}_c(t + \Delta t) = \mathcal{T}\rho_c(t)\Delta t \quad (1.142)$$

In the opposite case, no photon was detected, thus the resulting state is given by:

$$\tilde{\rho}_c(t + \Delta t) = \mathcal{S}(\Delta t)\rho_c(t) \quad (1.143)$$

The meaning of the term "*trajectory*" should be now obvious. It states the *random outcome* of an event. After repeating this process for a series of random numbers r , we sum over them to get the output from the cavity and then normalize the result so that the trace of the normalised density matrix is equal to 1. This way of evolving stochastically a density matrix is also called stochastic master equation.

However, for an N-dimensional system, the density matrix contains N^2 elements, which makes it a demanding computational task. An easier way of obtaining the dynamics of the system is to solve the stochastic Schrödinger equation, which of course does not give the exact correct result, though it is a good approximation of the process. From the discussion of stochastic master equation, we know that we can write $\mathcal{S} = e^{(\mathcal{L}-\mathcal{T})t}$. To find the effect of this super-operator on a density matrix ρ , we first find:

$$\begin{aligned} [(\mathcal{L} - \mathcal{T})t]\rho &= (\mathcal{L}\rho)t - (\mathcal{T}\rho)t \\ &= -\frac{it}{\hbar}[H_0, \rho] + \kappa t(2\hat{a}\rho\hat{a}^\dagger - \hat{a}^\dagger\hat{a}\rho - \rho\hat{a}^\dagger\hat{a}) - t(\mathcal{T}\rho) \\ &= -\frac{it}{\hbar}[H_0, \rho] + \kappa t(2\hat{a}\rho\hat{a}^\dagger - \hat{a}^\dagger\hat{a}\rho - \rho\hat{a}^\dagger\hat{a}) - t(\mathcal{T}\rho) - t(\mathcal{T}\rho) \quad (1.144) \\ &= \left[\left(\frac{H_0}{i\hbar} - \kappa\hat{a}^\dagger\hat{a} \right) t, \rho \right] \end{aligned}$$

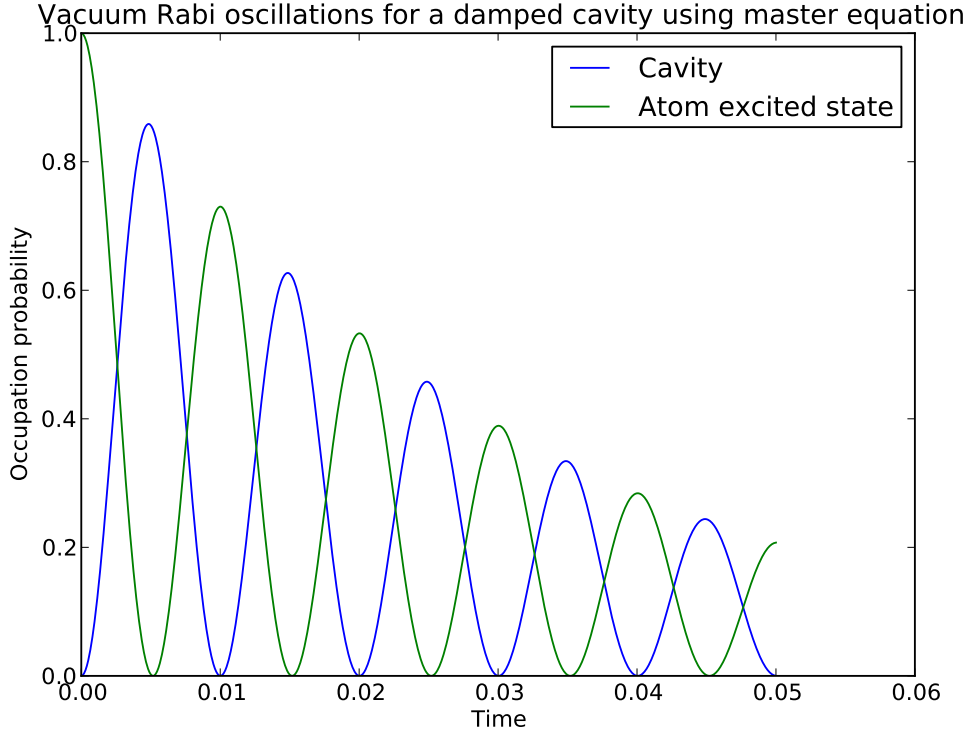


Figure 1.12: Jaynes Cummings model in a leaky cavity using the master equation. The parameters used here, are: $\omega_0 = \omega = 10000$, $g = 10^{-4}\omega_0$, $\kappa = 0.2g$.

Therefore, the effect of the super-operator can be written as:

$$\mathcal{S}(t)\rho = \hat{N}(t)\rho\hat{N}^\dagger(t) \quad (1.145)$$

where the operator $\hat{N}(t)$ is given by:

$$N(t) = \exp \left[\left(\frac{H_0}{i\hbar} - \kappa \hat{a}^\dagger \hat{a} \right) t \right] \quad (1.146)$$

Using the definition of the density matrix for a pure state, and the above relation we can write:

$$\rho(t) = |\psi(t)\rangle\langle\psi(t)| = \hat{N}\rho(0)\hat{N}(t) = \hat{N}(t)|\psi(0)\rangle\langle\psi(0)|\hat{N}^\dagger(t) \quad (1.147)$$

Therefore, we can also write the time evolution of $|\psi(t)\rangle$ as:

$$|\psi(t)\rangle = \hat{N}(t)|\psi(0)\rangle = \exp \left[\left(\frac{H_0}{i\hbar} - \kappa \hat{a}^\dagger \hat{a} \right) t \right] |\psi(0)\rangle \quad (1.148)$$

Denoting the effective Hamiltonian as

$$\begin{aligned}\hat{\mathcal{H}}_{eff} &= \hat{H}_0 - \frac{i\hbar}{2} \hat{C}^\dagger \hat{C} \\ &= \hat{H}_0 - i\hbar\kappa \hat{a}^\dagger \hat{a}\end{aligned}\quad (1.149)$$

we can finally write

$$|\psi(t)\rangle = \exp \left[\frac{\hat{\mathcal{H}}_{eff}}{i\hbar} t \right] |\psi(0)\rangle \quad (1.150)$$

In first sight, this may seem like a really hard way of deriving the Schrödinger equation. Though, since the Hamiltonian $\hat{\mathcal{H}}_{eff}$ contains non-unitary dynamics, this is not the same case. To numerically solve the stochastic Schrödinger equation we need a random number generator to obtain a number r and perform the comparison that will yield the trajectory, evolving the state in two different ways. Therefore the complexity is of order $O(N)$, in contrast to $O(N^2)$ for the evolution of the stochastic Master equation. The photo-detection probability and the rules for evolving the state, in terms of the conditional state $|\psi(t)\rangle$ are given by the following equations:

$$p_c = \langle \psi_c(t) | \hat{C}^\dagger \hat{C} | \psi_c(t) \rangle \quad (1.151)$$

Next we compare the product $p_c \Delta t$ with r . For $r \leq p_c \Delta t$, then there is a photo-detection, therefore the state is evolved as:

$$|\tilde{\psi}_c(t + \Delta t)\rangle = \hat{C} |\psi_c(t)\rangle \sqrt{\Delta t} \quad (1.152)$$

If $r > p_c \Delta t$, then there is no photo-detection, thus the state is evolved as:

$$|\tilde{\psi}_c(t + \Delta t)\rangle = \hat{N}(\Delta t) |\psi_c(t)\rangle \quad (1.153)$$

Chapter 2

Quantum Computation and Algorithms

In the last three decades, computers have changed our everyday lives. The main characteristic that established them in our everyday routines, was the power to perform repetitive tasks in a very small amount of time, therefore they were initially used to perform tasks as Signal Processing, Signal Encryption and thus Code Breaking, process of all kinds of data; from experimental data and numerical simulations to geo-informational data and military applications. One would say that Physics and Computer Science walk in parallel, hand by hand, and evolve almost simultaneously taking advantage of the new breakthroughs that come up every now and then in each field.

The first introduction of the notion of field of "Quantum Computation" is usually attributed to Richard Feynman in his 1982 paper [21], where he attempted to simulate quantum mechanics on classical machines. Actually, David Deutsch had circulated a preprint of his paper proposing a test of the many-universes interpretation in 1978 which was not published until 1985 [22], while Benioff in 1980 [20] published the first model for a computer based on quantum mechanical components. Unlike Feynmann, Benioff did the exact opposite: he tried to use quantum physics to simulate a classical computer.

The central idea behind "Quantum Computation" was to replace the 0's and 1's that are used in semiconductor devices stating a circuit's state regarding whether it is "on" or "off", by the superposition or entangled states of $|0\rangle$'s and $|1\rangle$'s which emerge in Quantum Mechanics.

After this statement that focused the attention of the scientific community to this emerging field, there have been splendid papers describing the abstract notion and functionality of a quantum computer. References for those may be found in the classical textbook of Nielsen and Chuang, *Quantum Computation and Quantum Information* [16], as well as in [24].

In the following we will briefly describe the main gates that are used in order to make use of the new resources that arise with the application of Quantum Mechanics to Computer Science, ie. the *Quantum Gates* which exhibit the principles that are used in order to perform Quantum Computational tasks, regardless of the system that is to be used for implementation.

Later we will describe three quantum algorithms that are of fundamental importance. *Deutsch-Jozsa algorithm* describes the process that is performed in a quantum system in order to specify whether a coin that is tossed, is biased or unbiased. It is of practical as well as of historical value to refer to it, since it was the first algorithm that made use of the new resources introduced in the begin of Quantum Computation Field. Grover's search algorithm is used in order to perform reverse search in a database, replacing the resource demanding classical algorithms and making computation times remarkably shorter. The wide variety of its applications makes it of fundamental importance in Encryption and Code Breaking applications. Shor's algorithm is probably dealing with one of the fundamental problems of number theory; search of the prime factors of a number. It is of a milestone importance since the problem of finding the prime factors of a number, is considered to be an index to the level of advancement of our civilization and the need for an efficient and fast algorithm has been of active mathematical interest for almost 2,000 years and is used in a variety of applications.

2.1 Quantum Bits and Gates

Creating quantum algorithms requires first specifying which is going to be the elementary piece of information that is going to be processed. In classical computation, this quantity is defined by the state of the circuit ie. whether the circuit is on (1) or off (0), enabling us to have a straightforward basis of communication with the circuit and thus command it to perform certain operations that are defined using **classical gates**.

In quantum computation, things are a little counter-intuitive. Having lots of physical systems that have many different quantum states, we need to define in each system what is going to be our $|0\rangle$ or $|1\rangle$, which frivolously guides us to the logical assumption that we need a **two state system**. This is a good start and the frivolity of this deduction, will not become a hardle until later on this discussion.

In Chapter 1 (Introduction to Cavity Q.E.D) we discussed what happens in the simple case of light-matter interaction and went through the two-level system model. Since the first steps of quantum computation, cavity QED seemed a to be a splendid candidate for creating quantum gates, involving two level systems

and the possibility to perform measurements and deduce the state of the system. Thus, in cavity QED we can make use of the $|e\rangle$ state to symbolize $|1\rangle$ and $|g\rangle$ to symbolize $|0\rangle$.

Having a new physical resource that comes with the heritage of its quantum nature, we are able to make use of it and perform various operations, much different than in Classical Computation, which in Computer Science language we call **gates**. We should point out the fact that a qubit can be visualised with the notion of the Bloch-sphere. Bloch-sphere is a sphere that represents the evolution of a state under unitary operations.

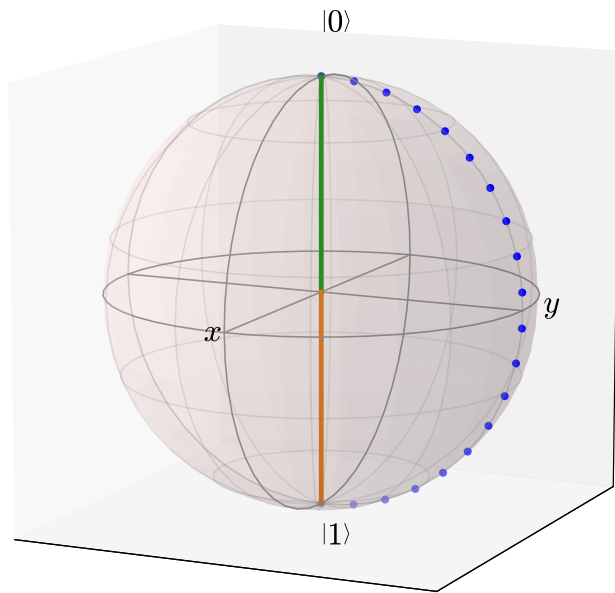


Figure 2.1: Bloch-sphere representation of the operation performed by Pauli X gate. A ket $|0\rangle$ (green line) is rotated by π over the x axis without modification of its length.

Reviewing the basic operations involved during the various stages of a quantum computation algorithm and describing their main features, is what follows. We will present them regarding the number of qubits involved and will briefly discuss the operations those gates represent in physical terms.

2.1.1 One qubit operations

In order to build a quantum algorithm, the qubits should undergo unitary transformations. Single qubit operations essentially perform rotations of the state vector on the surface of the Bloch sphere.

Gate	Name	Matrix
	Pauli X	$\begin{bmatrix} 0 & 1 \\ 1 & 0 \end{bmatrix}$
	Pauli Y	$\begin{bmatrix} 0 & -i \\ i & 0 \end{bmatrix}$
	Pauli Z	$\begin{bmatrix} 1 & 0 \\ 0 & -1 \end{bmatrix}$
	Hadamard	$\frac{1}{\sqrt{2}} \begin{bmatrix} 1 & 1 \\ 1 & -1 \end{bmatrix}$
	Phase	$\begin{bmatrix} 1 & 0 \\ 0 & i \end{bmatrix}$
	$\frac{\pi}{8}$	$\begin{bmatrix} 1 & 0 \\ 0 & e^{\frac{i\pi}{4}} \end{bmatrix}$

Table 2.1: One qubit gates

Pauli-X gate performs a rotation over the x axis by π . Essentially, it is the quantum NOT gate, since it maps $|0\rangle$ to $|1\rangle$ and vice versa. Its operation is visualized in figure 2.1.

Pauli Y gate, performs a rotation over the y axis by π , mapping eg. $|0\rangle$ to $i|1\rangle$ and $|1\rangle$ to $-i|0\rangle$.

Pauli Z gate, represents a rotation over the z axis by π . Rotations performed around z-axis, change the *phase* of the qubit, ie. the angle θ on the Bloch sphere. Pauli Z gate, leaves the basis state $|0\rangle$ unchanged and maps $|1\rangle$ to $-|1\rangle$. Hadamard gate is one of the most important gates . In terms of Bloch-sphere representation, it performs a rotation over the x and z axes by π . This actually means that the basis state $|0\rangle$ is mapped to the state $\frac{|0\rangle+|1\rangle}{\sqrt{2}}$ and $|1\rangle$ to the state $\frac{|0\rangle-|1\rangle}{\sqrt{2}}$, creating the *maximally entangled states*. Phase gate S, leaves $|0\rangle$ unchanged and changes the **phase** of $|1\rangle$ to $e^{i\pi/2}|1\rangle$. It belongs to the family of the **phase shift gates**, that leave the basis state $|0\rangle$ unaltered and map $|1\rangle$ to $e^{i\theta}|1\rangle$, which doesn't alter the probability of measuring $|0\rangle$ or $|1\rangle$, but essentially is equivalent to tracing a horizontal circle on the Bloch sphere for θ radians. For the phase gate (S) it is $\theta = \frac{\pi}{2}$. Note, that Pauli-Z gate, is the case for phase shift gate, for $\theta = \pi$. One more usual case for the phase shift gate is the $\frac{\pi}{8}$ gate, where $\theta = \frac{\pi}{4}$. It leaves $|0\rangle$ unchanged and changes the phase of $|1\rangle$ to $e^{i\pi/4}|1\rangle$. In

Table 2.1 we present the symbols, names and matrix representations of the most important single-qubit operations.

2.1.2 Two qubit operations

Two qubit operations are fundamental for the functionality of any algorithm. In classical computation, we use certain gates in order to state for example "*If A is true, then do B*". In quantum computation, things are a little more complicated, since there are certain limitations regarding the processes that are involved in quantum algorithms in order to avoid **destroying** the quantum information. More details on those limitations may be found in the classical textbook of Nielsen and Chuang [16] and in John Preskill's lecture notes. It will suffice to say that copying a quantum state is prohibited (also known as the *no-cloning theorem*), thus we should create reversible operations that do not destroy the quantum states involved in the operations. Thankfully, reversible computing had been a matter of debate long before the rise of quantum computation and it proved to help overcome what seemed to be an insurmountable obstacle. Another feature that is not allowed, is loops over the circuit, so we say that quantum algorithms are *acyclic*.

The first two qubit gate we will present is the *control-NOT gate*, also referred to as C-NOT gate. It involves two input qubits, which perform certain roles as control and target qubits respectively. The operation performed by CNOT gate is $|c\rangle|t\rangle \rightarrow |c\rangle|t \oplus c\rangle$, where of course $|c\rangle$ is the control qubit and $|t\rangle$ is the target qubit. The \oplus symbol states modulo 2, which means that *if the control qubit is $|1\rangle$, the target qubit is flipped, otherwise it is left alone*.

SWAP gate, performs the operation explicitly stated by its name; it swaps two qubits. This may seem quite simple, though it will prove later that it is quite useful. Controlled Z gate, is similar to CNOT gate, though instead of performing the NOT operation, it performs a Z operation on the target qubit if it is found on state $|1\rangle$, else it leaves it the same. Generalising we may construct any *Controlled-U gate*, where U is any unitary transformation. One more example is the Controlled-Phase gate, that works exactly the same way as CNOT, and C-U gates, but it performs a phase operation on the target qubit should it be in state $|1\rangle$, taking it to $i|1\rangle$, thus changing its phase by $\frac{\pi}{2}$.

2.1.3 Three qubit operations

The requirement for reversible processes demands the replacement of the classical logical gates which in general are irreversible, from reversible quantum gates as it was stated earlier as well.

Gate	Name	Matrix
	Control NOT	$\begin{bmatrix} 1 & 0 & 0 & 0 \\ 0 & 1 & 0 & 0 \\ 0 & 0 & 0 & 1 \\ 0 & 0 & 1 & 0 \end{bmatrix}$
	SWAP	$\begin{bmatrix} 1 & 0 & 0 & 0 \\ 0 & 0 & 1 & 0 \\ 0 & 1 & 0 & 0 \\ 0 & 0 & 0 & 1 \end{bmatrix}$
	Controlled Z	$\begin{bmatrix} 1 & 0 & 0 & 0 \\ 0 & 1 & 0 & 0 \\ 0 & 0 & 1 & 0 \\ 0 & 0 & 0 & -1 \end{bmatrix}$
	Controlled -Phase	$\begin{bmatrix} 1 & 0 & 0 & 0 \\ 0 & 1 & 0 & 0 \\ 0 & 0 & 1 & 0 \\ 0 & 0 & 0 & i \end{bmatrix}$

Table 2.2: Two qubit gates

A logic gate \mathbf{L} is *reversible* if, for any output y , there is a unique input x such that applying $L(x) = y$. If a gate L is reversible, there is an inverse gate L' which maps y to x for which $L'(y) = x$. From common logic gates, NOT is reversible. The common AND gate for instance, is not reversible. However there is a way to compute an arbitrary function. Two outstanding examples are the Toffoli gate and the Fredkin gate which are described below.

Toffoli gate, also CCNOT gate, was suggested by Tommaso Toffoli in 1980 and is a universal reversible logic gate, which means that any arbitrary function may be built using only Toffoli gates. It uses three input qubits (let's say $|a\rangle, |b\rangle, |c\rangle$) and it maps them to $|a\rangle, |b\rangle$ and $|c\rangle \text{XOR } (|a\rangle \text{ AND } |b\rangle)$. As it was shown later, a Toffoli gate may be constructed using 5 two-qubit quantum gates [64].

Fredkin gate, is another universal reversible logic gate. As it is shown in Table 2.3, it swaps the last two qubits if the control qubit is $|1\rangle$.

2.2 Deutsch-Jozsa algorithm

Having described and defined the basic elements of a quantum algorithm, it is time to describe the first quantum algorithm that we will deal with in this thesis. We refer to Deutsch-Jozsa algorithm. The problem it solves is not a really intriguing problem, though through it, the power of quantum computation was

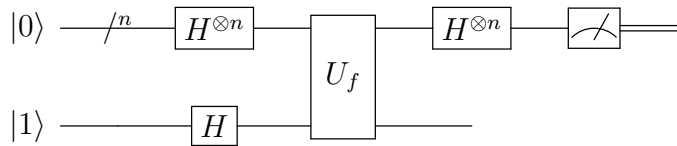
Gate	Name	Matrix
	Toffoli Gate	$\begin{bmatrix} 1 & 0 & 0 & 0 & 0 & 0 & 0 & 0 & 0 \\ 0 & 1 & 0 & 0 & 0 & 0 & 0 & 0 & 0 \\ 0 & 0 & 1 & 0 & 0 & 0 & 0 & 0 & 0 \\ 0 & 0 & 0 & 1 & 0 & 0 & 0 & 0 & 0 \\ 0 & 0 & 0 & 0 & 1 & 0 & 0 & 0 & 0 \\ 0 & 0 & 0 & 0 & 0 & 1 & 0 & 0 & 0 \\ 0 & 0 & 0 & 0 & 0 & 0 & 1 & 0 & 0 \\ 0 & 0 & 0 & 0 & 0 & 0 & 0 & 0 & 1 \\ 0 & 0 & 0 & 0 & 0 & 0 & 1 & 0 & 0 \end{bmatrix}$
	Fredkin (Control Swap)	$\begin{bmatrix} 1 & 0 & 0 & 0 & 0 & 0 & 0 & 0 & 0 \\ 0 & 1 & 0 & 0 & 0 & 0 & 0 & 0 & 0 \\ 0 & 0 & 1 & 0 & 0 & 0 & 0 & 0 & 0 \\ 0 & 0 & 0 & 1 & 0 & 0 & 0 & 0 & 0 \\ 0 & 0 & 0 & 0 & 1 & 0 & 0 & 0 & 0 \\ 0 & 0 & 0 & 0 & 0 & 0 & 1 & 0 & 0 \\ 0 & 0 & 0 & 0 & 0 & 0 & 0 & 1 & 0 \\ 0 & 0 & 0 & 0 & 0 & 0 & 0 & 0 & 1 \end{bmatrix}$

Table 2.3: Three qubit gates

made clear.

The problem: Supposing we have a function $f(x)$ taking as an input $x = 0$ or $x = 1$ and maps it to 0, 1, we want to know if f has a constant value or not.

A simple example to get grip on the problem is to imagine having a coin and we want to know if it is false ie. it has on both sides heads or tails. The original publication by Deutsch [22] described a non-deterministic algorithm, which gave the correct answer with a $\frac{1}{2}$ chance. Deutsch's algorithm improvement came in 1992 in what we now know as "*Deutsch-Jozsa algorithm*"[30]. Later, it was improved by Artur Ekert, Richard Cleve and Michele Mosca [23]

**Figure 2.2:** Deutsch-Jozsa algorithm

The algorithm begins taking as input the $n + 1$ state $|0\rangle^{\otimes n}|1\rangle$. That is, the first n qubits are each in the state $|0\rangle$ and the final qubit is $|1\rangle$. A Hadamard gate

is applied to each qubit to obtain the state

$$\frac{1}{\sqrt{2^{n+1}}} \sum_{x=0}^{2^n-1} |x\rangle (|0\rangle - |1\rangle) \quad (2.1)$$

The U_f gate, is the heart of the system. It maps the state $|x\rangle|y\rangle$ to $|x\rangle|y \oplus f(x)\rangle$. Applying U_f gives the state

$$\frac{1}{\sqrt{2^{n+1}}} \sum_{x=0}^{2^n-1} |x\rangle (|f(x)\rangle - |1 \oplus f(x)\rangle) \quad (2.2)$$

For each x , $f(x) = 0$ or 1 , thus we may write

$$\frac{1}{\sqrt{2^{n+1}}} \sum_{x=0}^{2^n-1} (-1)^{f(x)} |x\rangle (|0\rangle - |1\rangle) \quad (2.3)$$

At this point, the auxiliary qubit initially prepared in state $|1\rangle$ may be ignored. Applying a Hadamard transformation to each qubit we obtain

$$\frac{1}{2^n} \sum_{x=0}^{2^n-1} (-1)^{f(x)} \sum_{y=0}^{2^n-1} (-1)^{x \cdot y} |y\rangle = \frac{1}{2^n} \sum_{y=0}^{2^n-1} \left[\sum_{x=0}^{2^n-1} (-1)^{f(x)} (-1)^{x \cdot y} \right] |y\rangle \quad (2.4)$$

where $x \cdot y = x_0y_0 \oplus x_1y_1 \oplus \dots \oplus x_{n-1}y_{n-1}$ is the sum of the bitwise product. Finally we examine the probability of measuring $|0\rangle^{\otimes n}$

$$\left| \frac{1}{2^n} \sum_{x=0}^{2^n-1} (-1)^{f(x)} \right|^2 \quad (2.5)$$

which evaluates to 1 if $f(x)$ is **constant** and 0 if $f(x)$ is **balanced**.

It's worth mentioning that even for the simple case we have one qubit, we also need the auxiliary qubit. This is the cost of reversible computation, that requires extra input in order to perform the computational task.

The improvement of Deutsch-Jozsa algorithm that was contributed by Ekert et al [23], used as an auxiliary qubit the state $|0\rangle - |1\rangle$ and removed the need for the Hadamard transformation on it.

The preparation of the input qubits into the superposition, is that enables us to make use of the feature of quantum computation called *quantum parallelism*. In this given example, the algorithm iterates just once to give the outcome, since the use of the Hadamard gate creates a superposition of states $|0\rangle$ and $|1\rangle$, thus enabling us to simultaneously treat the input qubits and obtain the outcome of the unitary operation. Deutsch-Jozsa algorithm was the first example where the feature of quantum parallelism was used and it was made clear that this feature would change the classical way of designing algorithms.

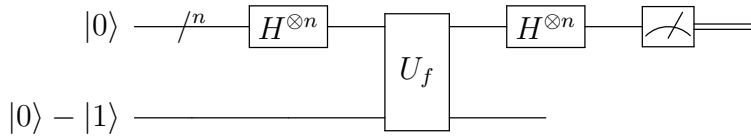


Figure 2.3: Improved version of Deutsch-Jozsa algorithm [23]

2.3 Grover's search algorithm

Deutsch's algorithm gave birth to new perspectives regarding the possible problems that were able to be solved using quantum algorithms. In previous section we used a unitary transformation U_f in order to **place the enquiry** of whether our function was balanced or constant. The same idea, for a purpose of advanced complexity was used in one of the most promising quantum algorithms; Grover's search algorithm.

The problem: Given an unsorted database of size $N = 2^n$, find the item labeled with i .

A practical example is the reverse telephone registry search ie. if one knows the telephone number and wishes to find using the telephone registry, to which individual it corresponds. This is a demanding computational task. Classically, if we examine k records in the registry, then we have a probability $\frac{k}{N}$ to find the item labeled with i . The best classical algorithm requires on average $O(n/2)$ iterations in order to locate the desired item.

Grover's algorithm [31],[32] is essentially an extension to Deutsch-Jozsa algorithm. The basic idea is creating a function that will operate as an "**oracle**", that points out the desired object. Thus, for each object we need a different function, in order to complete the algorithm successfully. Grover's algorithm is also deterministic, which means that will always give the correct result, while the number of the repeats required, as we will see is significantly less than that of the classical algorithms, which makes it one of the most interesting algorithms in the field of Quantum Computation.

We should first discuss certain properties of the *oracle* operation that is performed in Grover's algorithm. A good intuitive interpretation of the function of the algorithm was given in 1999 by Jozsa [34]. This function is unitary, as every function that is involved during quantum computation algorithms. It is defined by the relation:

$$I_{x_0} |x\rangle = \begin{cases} |x\rangle & \text{if } x \neq x_0 \\ -|x_0\rangle & \text{if } x = x_0 \end{cases} \quad (2.6)$$

For simplicity we will use the symbolism I_τ to identify the oracle that locates the element τ from the database. As it may be seen from its definition, the operator

I_τ , inverts the element $|\tau\rangle$. We may prove that

$$U \cdot I_{|\tau\rangle} \cdot U^{-1} = I_{U|\tau\rangle} \quad (2.7)$$

and also

$$-I_v = I_{v^\perp} \quad (2.8)$$

One more usefull form of the oracle operator is:

$$I_\tau = I_n - 2|\tau\rangle\langle\tau| \quad (2.9)$$

where I_n is the identity matrix with dimesnions n . If we use $|0\rangle$ in the above expression we obtain:

$$I_0 = I_n - 2|0\rangle\langle 0| \quad (2.10)$$

which is called **diffusion operator**.

The steps of the algorithm for locating an item are as follows:

1. Create a superposition of all the items in the list
2. Apply the oracle operator in order to identify the desired object by inverting its amplitude.
3. Apply the diffusion operator in order to amplify the probability amplitude of the desired state.

The geometrical proof of the functionality of the Grover algorithm will give us insight on how the algorithm works and why the operators I_τ and I_0 have the above form [18].

Consider the plane spanned by $|s'\rangle$ and $|\omega\rangle$, where $|s'\rangle$ is a ket in the subspace perpendicular to $|\omega\rangle$. We will consider the first iteration, acting on the initial ket $|s\rangle$. Since $|\omega\rangle$ is one of the basis vectors in $|s\rangle$ the overlap is

$$|s'\rangle = \sqrt{\frac{N-1}{N}}$$

In geometric terms, the angle $\theta/2$ between $|s\rangle$ and $|s'\rangle$ is given by:

$$\sin \theta/2 = \frac{1}{\sqrt{N}}$$

The operator U_ω is a reflection at the hyperplane orthogonal to $|\omega\rangle$ for vectors in the plane spanned by $|s'\rangle$ and $|\omega\rangle$; i.e. it acts as a reflection across $|s'\rangle$. The operator U_s is a reflection through $|s\rangle$. Therefore, the state vector remains in the plane spanned by $|s'\rangle$ and $|\omega\rangle$ after each application of the operators U_s and U_ω ,

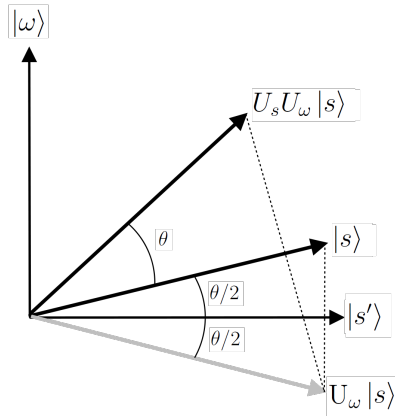


Figure 2.4: Geometric Proof of the function of Grover's algorithm

and it is straightforward to check that the operator $U_s U_\omega$ of each Grover iteration step rotates the state vector by an angle of $\theta = 2 \arcsin \frac{1}{\sqrt{N}}$.

We need to stop when the state vector passes close to $|\omega\rangle$; after this, subsequent iterations rotate the state vector "away" from $|\omega\rangle$, reducing the probability of obtaining the correct answer. The exact probability of measuring the correct answer is:

$$\sin^2 \left(\left(r + \frac{1}{2} \right) \theta \right)$$

where "r" is the (integer) number of Grover iterations. The earliest time that we get a near-optimal measurement is therefore $r \approx \frac{\pi\sqrt{N}}{4}$.

After describing how the oracle leads us to the desired result, we are ready to describe the process which allows us to obtain the desired result. First of all, we need to prepare our system in a superposition of all possible states which should be described in an appropriate basis. On this superposition of states, we act the oracle for element τ i.e. I_τ which inverts the amplitude of the desired state. The operation of the algorithm makes use of quantum parallelism feature, which demands entanglement. In order to entangle two (or more qubits) we use a Hadamard gate. The following step is to apply the diffusion operator $I_0 = I - 2|0\rangle\langle 0|$, in order to amplify the state that was inverted by operator I_τ and finally apply one more Hadamard gate in order to read the outcome of the algorithm.

Therefore, Grover's algorithm is essentially a repetition of the unitary transformation

$$Q = -H I_0 H I_\tau \quad (2.11)$$

where $I_0 = I - 2|0\rangle\langle 0|$, $I_\tau = I - 2|\tau\rangle\langle \tau|$ and $H = \prod_{i=1}^n H_i$ is the product of Hadamard gates acting on the i -th qubit. This expression of Grover's

algorithm[34] transformation is equivalent to the original form [31],[32]

$$Q^{GR} = -I_0 H I_\tau H \quad (2.12)$$

The explicit expression of the transformation performed by a Hadamard gate is

$$H_i = \begin{cases} |0\rangle_i \rightarrow \frac{1}{\sqrt{2}}(|0\rangle_i + |1\rangle_i) \\ |1\rangle_i \rightarrow \frac{1}{\sqrt{2}}(|0\rangle_i - |1\rangle_i) \end{cases} \quad (2.13)$$

In fact, Grover's algorithm can make use of any unitary transformation instead of Hadamard gate, which in the worst case causes a constant slowdown in the number of iterations the algorithm needs to converge to the wanted state [33], thus it may be expressed in the general form

$$Q = -U I_0 U^{-1} I_\tau \quad (2.14)$$

The simplest case of use of Grover's algorithm:

Let's imagine the simple problem where we have four coloured cards (Red, Green, Blue and Yellow) that are hidden and we want to locate the green card for example.

Classically this problem requires on average 2.25 trials in order to locate the wanted card, though Grover's algorithm promises that we can locate it in one step.

First of all we need to define a suitable basis for our problem. This basis can be expressed as:

$$\begin{aligned} |Y\rangle &= |0\rangle = (1 \ 0 \ 0 \ 0)^\perp \\ |G\rangle &= |1\rangle = (0 \ 1 \ 0 \ 0)^\perp \\ |B\rangle &= |2\rangle = (0 \ 0 \ 1 \ 0)^\perp \\ |R\rangle &= |3\rangle = (0 \ 0 \ 0 \ 1)^\perp \end{aligned} \quad (2.15)$$

After defining the basis we need to create a superposition $|\Psi\rangle$ of all the states of the basis, as:

$$|\Psi\rangle = \frac{|0\rangle + |1\rangle + |2\rangle + |3\rangle}{\sqrt{4}} \quad (2.16)$$

Since we want to find the green card, we define the respective oracle as

$$I_G = I_4 - 2|G\rangle\langle G| \quad (2.17)$$

whereas the diffusion operator I_0 is defined as

$$I_0 = I_4 - 2|\Psi\rangle\langle\Psi| \quad (2.18)$$

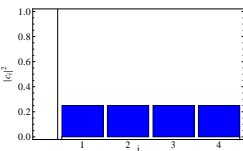


Figure 2.5: Probability amplitudes of the four plitudes after applying the initial states in the superposition version operator

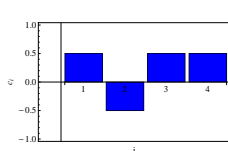


Figure 2.6: Probability amplitudes of the four plitudes after applying the inverse unitary operator

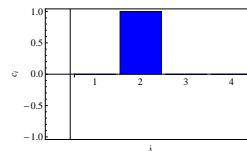


Figure 2.7: Probability amplitudes after applying the diffusion operator.

2.4 Shor's Algorithm

Encryption and decryption has been as old as the need for protecting sensitive information. During World War II, it was made quite clear that in order to gain advantage in a certain period, intelligence efficiency and the ability of monitoring enemy communications would be crucial for the outcome of the War. Encrypting information and making sure that only the desired target will be able to decipher the message is of grave importance today as well. The RSA algorithm (see for extra details [65]), on which modern encryption methods are based upon, uses three steps: **Key generation, encryption and decryption**. The process of generating the keys, encrypting and decrypting a message let's say **M**, between two individuals (let's say **Alice** and **Bob**) is as follows:

1. Choose two distinct prime numbers **p** and **q**. For security purposes the integers **p** and **q** should be chosen at random and should be of similar bit-length.
2. Compute $n = pq$
3. Compute $\phi(n) = (p - 1)(q - 1)$ where ϕ is Euler's totient function
4. Choose an integer e such that $1 < e < \phi(n)$ and greatest common divisor of $(e, \phi(n)) = 1$ (coprimes). **e is released as the public key exponent**
5. Determine **d** as: $d = e^{-1}(\text{mod } \phi(n))$. **d** is kept as the private key exponent. During the **encryption** the following procedure happens:
6. **Alice** transmits her public key **(n,e)** to **Bob** and keeps the private key secret.
7. **Bob** then wishes to send a message **M** to **Alice**, so he first turns message **M** into an integer **m**, such that $0 < m < n$ by using an agreed protocol, and then computes the ciphertext **c** corresponding to $c = m^e(\text{mod } n)$

8. Having decrypted the message, **Bob** transmits the message c to **Alice**. Alice can recover m from c via computing $m = c^d \pmod{n}$ and using the agreed protocol to convert it to \mathbf{M} .

It is clear that the power of RSA algorithm is based on the fact that *there are no classical algorithms efficient enough to factorize large prime numbers*, since the best classical algorithm for a b -bit number n (larger than 100 digits) is for the *general number field sieve* algorithm, $O\left(\exp\left(\left(\frac{64}{9}b\right)^{1/3}(\log b)^{2/3}\right)\right)$ (sub-exponential). Shor's algorithm takes only $O(b^3)$ time (polynomial) and $O(b)$ space on b -bit number inputs. The efficiency of Shor's algorithm is due to the efficiency of the *Quantum Fourier Transform* as we will shortly discuss.

Number Theory provides us with a shortcut for factorizing large numbers. It involves the *period of a certain function*. We will give a simple example, to see how this method works.

Let's say that we want to factorize 15.

1. Find a coprime of 15 (let's say 11).
2. Divide 11 by 15 to get 0 with a remainder of 11
3. Square the remainder, getting 121.
4. Divide 121 by 15 to get 8 with a remainder of 1.
5. Cube 11 to get 1331.
6. Divide 1331 by 15, to get 88 with a remainder of 11.
 - We observe that the remainders 11 and 1 alternate with a period 2.
So, we say that *the period of 11 with respect to being divided by 15 is 2*
7. Knowing the period (2) we raise 11 to the power given by its period to obtain $11^2 = 121$.
8. Take the square root of $\sqrt{121} = 11$.
9. Subtract and add 1 to get the pair of numbers 10 and 12.
10. Find the greatest common divisor of pairs $(10, 15) = 5$ and $(12, 15) = 3$ (using Euclidean algorithm).

This process is quite long for the given example, though, for very large numbers, the power of *Quantum Fourier Transform* for period finding makes the difference. Before describing this sub-routine of Shor's algorithm let's give the

general form of the algorithm. **The problem:** Given an odd (even numbers have the trivial divisor of two), composite number N , find an integer d strictly between 1 and N that divides N . **The solution:**

1. Run a primality test in order to verify that N is indeed a composite number and not a prime number.
2. Pick a random number $a < N$
3. Compute $\gcd(a, N)$ using Euclidean algorithm
4. If $\gcd(a, N) \neq 1$ then there is a nontrivial factor of N , so we are done.
5. Otherwise, use the *period finding sub-routine* to find r , the period of the following function:

$$f(x) = a^x \bmod N$$

ie. the order r of a in $(\mathbb{Z}_N)^\times$, which is the smallest positive integer r for which $f(x+r) = f(x)$ or $f(x+r) = a^{x+r} \bmod N = a^x \bmod N$.

6. If r is odd, go back to step 1.
7. If $\sqrt{a} \equiv -1 \pmod{N}$ go back to step 1.
8. $\gcd(\sqrt{a} \pm 1, N)$ is a nontrivial factor if N and we are done.

2.4.1 The Quantum Fourier Transform

The importance of Quantum Fourier Transform in quantum computation, makes it enough to define a whole set of problems that can be solved by using it. Such problems, apart from Shor's algorithm, are the quantum phase estimation algorithm that allows the estimation of the eigenvalues of a unitary operator and the hidden subgroup problem[66],[67].

Quantum Fourier Transform is the quantum analog of Discrete Fourier Transform. Classical DFT takes acts on a vector in \mathbb{C}^N , $(x_0, x_1, x_2, \dots, x_{N-1})$ and maps it to a vector $(y_0, y_1, y_2, \dots, y_{N-1})$ according to the formula:

$$y_k = \frac{1}{\sqrt{N}} \sum_{j=0}^{N-1} x_j \omega^{jk} \quad (2.19)$$

Remembering Euler's identity $e^{i\pi} + 1 = 0$ we set ω to be the primitive N -th root of unity, ie: $\omega = e^{\frac{2\pi i}{N}}$

Similarly, QFT transforms a vector

$$|\psi\rangle = a_0|\psi\rangle + a_1|\psi\rangle + \dots a_{N-1}|\psi\rangle$$

by applying a DFT on its amplitudes, giving us:

$$|\psi\rangle = \beta_0|\psi\rangle + \beta_1|\psi\rangle + \dots \beta_{N-1}|\psi\rangle \quad (2.20)$$

Given a random state vector $|\psi\rangle$

$$|\psi\rangle = \sum_{x=0}^{2^n-1} a_x|x\rangle \quad (2.21)$$

where n is the number of qubits, $QFT|\psi\rangle$ is defined as:

$$|\psi'\rangle = QFT|\psi\rangle = \sum_{x=0}^{2^n-1} \sum_{y=0}^{2^n-1} \frac{a_x e^{\frac{2\pi i}{2^n} xy}}{\sqrt{2^n}} |y\rangle \quad (2.22)$$

Rewriting the previous summation setting $M_{xy} = e^{2\pi i xy/2^n}$ we find that

$$\sum_{x=0}^{2^n-1} \sum_{y=0}^{2^n-1} \frac{a_x e^{\frac{2\pi i}{2^n} xy}}{\sqrt{2^n}} |y\rangle = \frac{1}{\sqrt{2^n}} \sum_{x=0}^{2^n-1} \left(\sum_{y=0}^{2^n-1} M_{xy} a_x \right) |\psi\rangle \quad (2.23)$$

Thus the QFT transformation matrix is composed from the elements M_{xy} and we can calculate it to be:

$$F_N = \frac{1}{\sqrt{N}} \begin{bmatrix} 1 & 1 & 1 & 1 & \dots & 1 \\ 1 & \omega & \omega^2 & \omega^3 & \dots & \omega^{N-1} \\ 1 & \omega^2 & \omega^4 & \omega^6 & \dots & \omega^{2(N-1)} \\ 1 & \omega^3 & \omega^6 & \omega^9 & \dots & \omega^{3(N-1)} \\ \vdots & \vdots & \vdots & \vdots & & \vdots \\ 1 & \omega^{N-1} & \omega^{2(N-1)} & \omega^{3(N-1)} & \dots & \omega^{(N-1)(N-1)} \end{bmatrix} \quad (2.24)$$

A circuit implementing QFT is presented in 2.8.

2.4.2 Finding the period of a function using QFT

The implementation of Shor's algorithm, as it is stated by the problem itself, requires customized circuits for each problem. In the general case for a number N and the random a , we require two registers (input and output) consisting of L qubits, so that $N^2 \leq 2^L \leq 2N^2$. This requirement ensures that there are at least N different x , which produce the same $f(y)$, even as the period r approaches $N/2$. The procedure for finding the period is as follows:

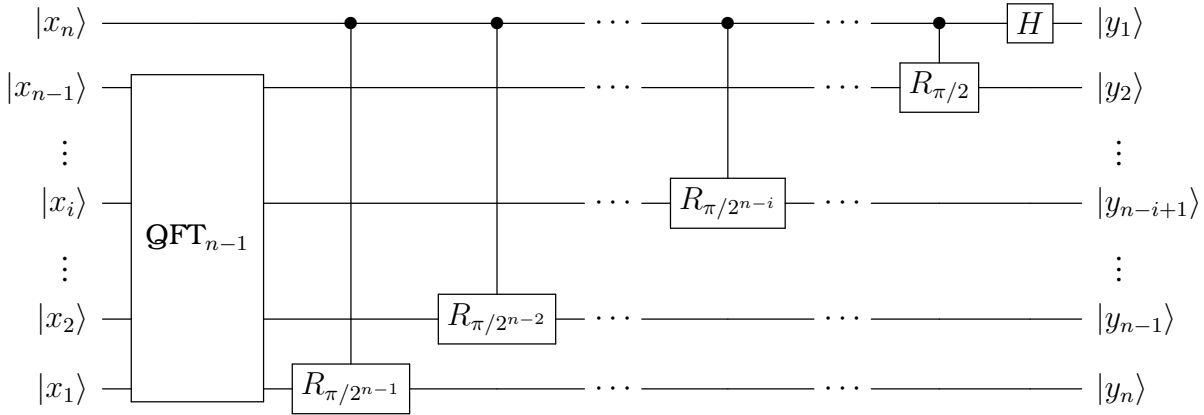


Figure 2.8: Quantum circuit representing the Quantum Fourier Transform for n qubits.
Image rebuilt using Qcircuit from Wikipedia

1. Prepare 2 L-qubit registries in the initial state

$$\left(\frac{1}{\sqrt{2^L}} \sum_{x=0}^{2^L-1} |x\rangle \right) |0\rangle \quad (2.25)$$

2. Apply the unitary transformation U_f that defines $f_{a,N}(x) = a^x \bmod N$:

$$\left(\frac{1}{\sqrt{2^L}} \sum_{x=0}^{2^L-1} |x\rangle \right) |0\rangle \rightarrow \left(\frac{1}{\sqrt{2^L}} \sum_{x=0}^{2^L-1} |x\rangle \right) |f_{a,N}(x)\rangle \quad (2.26)$$

3. Apply the QFT to the first register:

$$\left(\frac{1}{\sqrt{2^L}} \sum_{x=0}^{2^L-1} |x\rangle \right) |f_{a,N}(x)\rangle \rightarrow \frac{1}{2^L} \sum_{y=0}^{2^L-1} \left(\sum_{x=0}^{2^L-1} e^{2\pi i xy/2^L} |y\rangle \right) |f(x)\rangle \quad (2.27)$$

4. Make a measurement on the first register obtaining y .
5. Find the period of the function r by constructing continued fractions for $\frac{y}{2^L}$.
In case this step fails return to step 1.

Chapter 3

Implementation of quantum algorithms on cavity QED systems

The discussed quantum circuits required for quantum algorithms are essentially guidelines that explain which transformations are required to be performed on a set of qubits in order to obtain a running algorithm. The versatility of quantum systems, allows a great variety of possible experimental set-ups that implement those algorithms. In the past few years there has been intense activity on designing and developing systems that allow the manipulation of qubits, which is the key to creating devices that will perform with high fidelity quantum algorithms.

Those set-ups include ion traps ([68, 47]), Nuclear Magnetic Resonance systems (NMR) [50], photonic systems ([69],[70]), the promising circuit QED platform [51],[52],[53] and of course microwave cavity QED. In what follows we will discuss how the search algorithms that were presented in the previous chapter are implemented on cavity QED, following the papers of Serge Haroche [37] on Grover's algorithm and Marlan O. Scully on Shor's algorithm [36].

The first thing we need to mention in order to proceed forward, is the fact that on cavity QED systems we have the freedom of choosing between atomic levels or cavity states when it comes to defining "what the qubit is". This fact allows cavity QED systems to be versatile and adjustable to many modifications as long as those adjustments are allowed by the limitations of the experimental setup.

There is a big heritage of techniques that have been developed in cavity QED setups that allow us to precisely create entangled states on demand [71], perform Quantum Non-Demolition (QND) measurements [72], [73] and precisely manipulate the state of both atoms and cavity-fields using techniques that are described in detail in [6].

3.1 Grover's search algorithm

The challenge regarding the implementation of Grover's algorithm is setting up a series of pulses that will perform the oracle operator which is essentially a conditional phase gate operation that inverts the amplitude of the desired state.

The freedom in the choice of appropriate unitary transformations in order to perform the equivalent process in Grover's algorithm as it was expressed in equation 2.14, suggests that we may search for an expression which can be implemented in cavity QED systems using simple rotations that can be performed with high accuracy using Ramsey zones and external microwave sources. The qubits that are used in this process are two circular Rydberg atoms A_1 and A_2 that are prepared by an oven. They come out with specific velocities, that define the interaction time with every subsystem of the setup and they are both initially in their ground states.

In order to handle every atom separately, we need to define in which state of the two atoms correspond the states $|0\rangle$ and $|1\rangle$.

For A_1 , state $|g\rangle$ is defined as $|0\rangle$ and state $|e\rangle$ as $|1\rangle$. Since the pulses have to act at the same time on both atoms, states $|0\rangle$ and $|1\rangle$ for A_2 need to be defined in a different way to avoid errors on the manipulation of each atom. Thus, the use of the lower energy level $|i\rangle$ to encode $|1\rangle$ for A_2 and $|g\rangle$ for $|0\rangle$ resolves this issue.

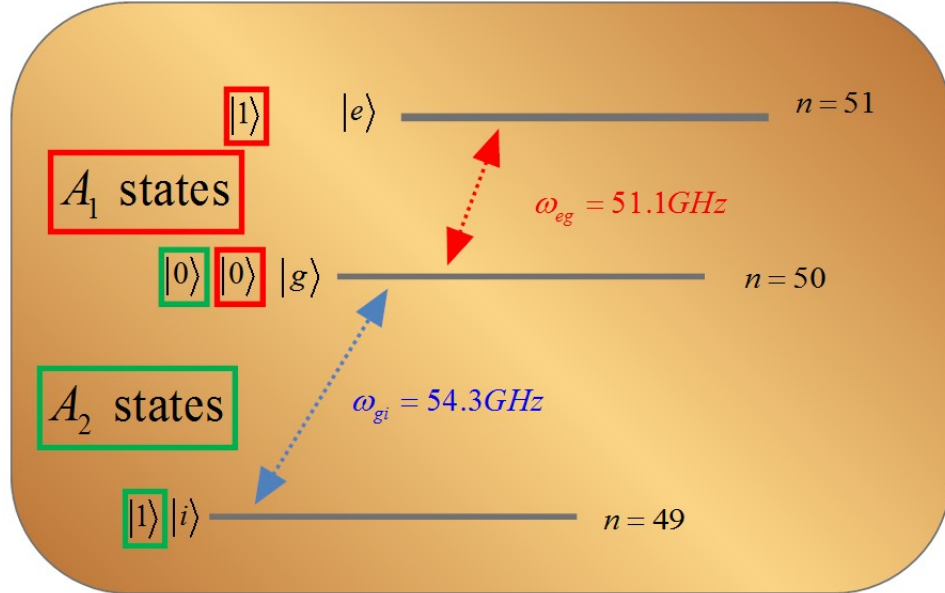


Figure 3.1: Qubit definition for Grover's algorithm.

The simplest case in which the algorithm can be performed, involves 2 qubits

(n=2), thus this case corresponds to the example we discussed in the previous chapter, giving us four states:

$$\begin{aligned} |0\rangle &= \begin{pmatrix} 1 & 0 & 0 & 0 \end{pmatrix}^\perp \\ |1\rangle &= \begin{pmatrix} 0 & 1 & 0 & 0 \end{pmatrix}^\perp \\ |2\rangle &= \begin{pmatrix} 0 & 0 & 1 & 0 \end{pmatrix}^\perp \\ |3\rangle &= \begin{pmatrix} 0 & 0 & 0 & 1 \end{pmatrix}^\perp \end{aligned} \quad (3.1)$$

Hadamard gates are single-qubit gates that can be performed using $\pi/2$ pulses, thus we concentrate on the realization of the I_τ inversion and diffusion I_0 operations. Since we can handle every atom separately, we have to find equivalent expressions for the Grover operation Q , that will perform rotations in every single qubit. The required angle of rotation for each qubit will depend on the kind of oracle that is realized, thus we define the angles θ_1 and θ_2 by which each one of the atoms (qubits) is rotated, using the following convention:

Rotations for:	θ_1	θ_2
$ 0\rangle$	π	π
$ 1\rangle$	0	π
$ 2\rangle$	π	0
$ 3\rangle$	0	0

Table 3.1: Definition of the angle of rotation for the realization of the oracles.

Next, the operation $X_j(\theta)$ is defined (index j declares on which qubit it is performed), by the explicit expression:

$$X_j(\theta) : \begin{cases} |0_j\rangle \rightarrow \cos \frac{\theta}{2} |0_j\rangle + i \sin \frac{\theta}{2} |1_j\rangle \\ |1_j\rangle \rightarrow i \sin \frac{\theta}{2} |0_j\rangle + \cos \frac{\theta}{2} |1_j\rangle \end{cases} \quad (3.2)$$

The action of one Hadamard operation before and after the operation X_j , leads to the operation:

$$Z_i(\pm\theta) = H_i X_i(\mp\theta) H_i \quad (3.3)$$

The equivalent expression for the operators I_τ regarding the convention of 3.1 and the use of the quantum phase gate that is defined by the unitary matrix

$$I_{QPG} = \begin{pmatrix} 1 & 0 & 0 & 0 \\ 0 & 1 & 0 & 0 \\ 0 & 0 & 1 & 0 \\ 0 & 0 & 0 & -1 \end{pmatrix} \quad (3.4)$$

may now be written as:

$$I_\tau = I_{QPG}[Z_1(\theta_1)H_1][Z_2(\theta_2)H_2] \quad (3.5)$$

It is easy to show that the operation of the quantum phase gate (I_{QPG}) can be performed either after or before the rotations of the atoms, so that:

$$I_{QPG}[Z_1(\theta_1)][Z_2(\theta_2)] = [Z_1(\theta_1)][Z_2(\theta_2)]I_{QPG} \quad (3.6)$$

Thus, the I_0 operator of Grover's algorithm may be written setting $\theta_1 = \pi$ and $\theta_2 = \pi$ as:

$$[H_1 Z_1(\pi)] [H_2 Z_2(\pi)] I_{QPG} \quad (3.7)$$

Using the abbreviations

$$S_i = X_i(-\pi)H_i \quad (3.8)$$

$$P_i(\theta) = H_i X_i(-\theta) \quad (3.9)$$

we may rewrite the Grover operation (Q) as:

$$Q = S I_{QPG} H I_{QPG} P \quad (3.10)$$

The explicit expression for the abbreviations S_j and P_j are:

$$S_j : \begin{cases} |0_j\rangle \rightarrow \frac{i}{\sqrt{2}} (-|0_j\rangle - |1_j\rangle) \\ |1_j\rangle \rightarrow \frac{i}{\sqrt{2}} (|0_j\rangle - |1_j\rangle) \end{cases} \quad (3.11)$$

$$P_j : \begin{cases} |0_j\rangle \rightarrow \frac{1}{\sqrt{2}} \left(e^{-i\frac{\theta}{2}} |0_j\rangle + e^{i\frac{\theta}{2}} |1_j\rangle \right) \\ |1_j\rangle \rightarrow \frac{1}{\sqrt{2}} \left(e^{-i\frac{\theta}{2}} |0_j\rangle - e^{i\frac{\theta}{2}} |1_j\rangle \right) \end{cases} \quad (3.12)$$

The matrix form of the oracle operator I_τ is:

$$I_\tau = \begin{bmatrix} e^{-\frac{i}{2}(\theta_1+\theta_2)} & 0 & 0 & 0 \\ 0 & e^{-\frac{i}{2}(\theta_1-\theta_2)} & 0 & 0 \\ 0 & 0 & e^{\frac{i}{2}(\theta_1-\theta_2)} & 0 \\ 0 & 0 & 0 & -e^{\frac{i}{2}(\theta_1+\theta_2)} \end{bmatrix} \quad (3.13)$$

Using the matrix form of all the operators as we discussed previously we may write the Grover operation as:

$$Q = \frac{1}{2} \begin{pmatrix} e^{-\frac{1}{2}i(\theta_1+\theta_2)} & -e^{-\frac{1}{2}i(\theta_1-\theta_2)} & -e^{\frac{1}{2}i(\theta_1-\theta_2)} & e^{\frac{1}{2}i(\theta_1+\theta_2)} \\ -e^{-\frac{1}{2}i(\theta_1+\theta_2)} & e^{-\frac{1}{2}i(\theta_1-\theta_2)} & -e^{\frac{1}{2}i(\theta_1-\theta_2)} & e^{\frac{1}{2}i(\theta_1+\theta_2)} \\ -e^{-\frac{1}{2}i(\theta_1+\theta_2)} & -e^{-\frac{1}{2}i(\theta_1-\theta_2)} & e^{\frac{1}{2}i(\theta_1-\theta_2)} & e^{\frac{1}{2}i(\theta_1+\theta_2)} \\ -e^{-\frac{1}{2}i(\theta_1+\theta_2)} & -e^{-\frac{1}{2}i(\theta_1-\theta_2)} & -e^{\frac{1}{2}i(\theta_1-\theta_2)} & -e^{\frac{1}{2}i(\theta_1+\theta_2)} \end{pmatrix} \quad (3.14)$$

Admittedly, the most intriguing part of the proposed experiment is the realization of the Quantum Phase Gate. In order to perform this operation, the team of Haroche made use of the van der Waals interaction of the two Rydberg atoms, which is assisted by the cavity. A detailed description of this specific experiment may be found in [74].

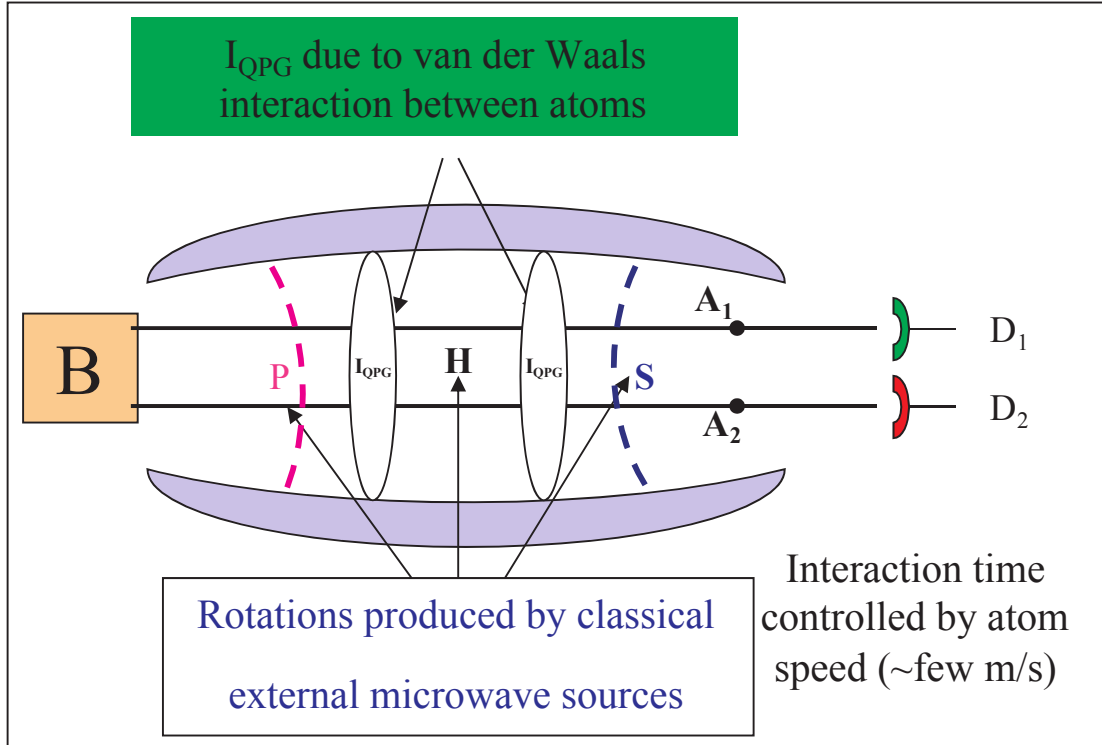


Figure 3.2: Experimental setup for the realization of Grover algorithm in cavity QED. Atoms 1 and 2 cross the cavity with the same velocities but on different positions and undergo pulses S,H,P from external microwave sources and interact together twice inside the cavity via assisted van der Waals interactions.

The interaction Hamiltonian describing the interaction of two atoms with the cavity field, in the interaction picture is

$$H_i = g \sum_{j=1,2} \left(e^{-i\delta t} \hat{a}^\dagger \hat{S}_j^- + e^{i\delta t} \hat{a} \hat{S}_j^+ \right) \quad (3.15)$$

where $\hat{S}_j^+ = |e_j\rangle\langle g_j|$ and $\hat{S}_j^- = |g_j\rangle\langle e_j|$ with $|g_j\rangle$ and $|e_j\rangle$ ($j=1,2$) being the ground and excited states respectively of atoms j. In the case $\delta \gg g$ (dispersive regime), there is no energy exchange between the atoms and the cavity, thus the atoms may interact with each other.

The effective Hamiltonian of this interaction is given by

$$H_i = \lambda \left[\sum_{j=1,2} (|e_j\rangle\langle e_j|\hat{a}\hat{a}^\dagger - |g_j\rangle\langle g_j|\hat{a}^\dagger\hat{a}) + (\hat{S}_1^+ \hat{S}_2^- + \hat{S}_1^- \hat{S}_2^+) \right] \quad (3.16)$$

where $\lambda = g^2/\delta$. The first two terms describe the photon number dependent Stark shifts, while the last two terms describe the energy exchange between the two atoms.

If the cavity is initially in the vacuum state the Hamiltonian becomes (see for example Chapter 19 of [14] and [75]):

$$H_{eff} = \lambda \left[\sum_{j=1,2} |e_j\rangle\langle e_j| + (\hat{S}_1^+ \hat{S}_2^- + \hat{S}_1^- \hat{S}_2^+) \right] \quad (3.17)$$

In this expression the first term describes the Lamb shift, whereas the second term the energy exchange between the two atoms assisted by the cavity. When the interaction time is chosen so that $\lambda t = \pi$, the system undergoes the transition:

$$\begin{aligned} |g_1\rangle|g_2\rangle &\rightarrow |g_1\rangle|g_2\rangle \\ |g_1\rangle|i_2\rangle &\rightarrow |g_1\rangle|i_2\rangle \\ |e_1\rangle|g_2\rangle &\rightarrow |e_1\rangle|g_2\rangle \\ |e_1\rangle|i_2\rangle &\rightarrow -|e_1\rangle|i_2\rangle \end{aligned} \quad (3.18)$$

The process described corresponds to the realization of the quantum phase gate.

Describing the details of the experiment, we have to note that the cavity is initially in the vacuum state, its temperature is droped to 1.3K with the mean number of thermal photons to 0.7. In order to further cool it, a series of atoms in ground state $|g\rangle$ absorb the residual thermal field, thus providing $\bar{n} = 0.12$ [76]. In state of the art systems an average thermal photon number of 0.05 is achieved. The cavity is constructed by superconducting niobium mirrors allowing high Q values ($Q = 3 \times 10^8$), while values of Q in the order of 10^{10} have been achieved [61]. The coupling of the atoms to the cavity field is $\Omega/2\pi = 50kHz$, whereas the detuning $\delta/2\pi = 200kHz$ which satisfies the requirements of the dispersive regime and the H_{eff} as it is described in equation 3.17.

In order to obtain sufficient time for two quantum phase gates (atom-cavity interaction time 2.5×10^{-4}) the atoms crossing the cavity should have velocities $\sim 40m/s$. The total interaction time with the mode is $120\mu s$, short compared to the photon lifetime which is 1ms for a cavity with $Q = 3 \times 10^8$.

3.1.1 An alternative realization of the quantum phase gate

The challenge for the realization of a two qubit quantum phase gate, has led to various proposed experiments. Of special interest is the setup proposed in [77],

where the authors describe a setup that will realize the quantum phase gate and give an example of how it may be used for the implementation of Grover's algorithm.

The transformation performed by a 2-qubit quantum phase gate, may be written in the form:

$$Q_\eta |\alpha_1, \beta_2\rangle = \exp [i\eta \delta_{\alpha_1,1} \delta_{\beta_2,1}] |\alpha_1, \beta_2\rangle \quad (3.19)$$

where $|\alpha_1\rangle$ and $|\beta_2\rangle$ stands for the the basis states $|0\rangle$ or $|1\rangle$ of the qubits 1 and 2 respectively. The explicit form of Q_η is:

$$\begin{aligned} Q_\eta = & |0_1, 0_2\rangle\langle 0_1, 0_2| + |0_1, 1_2\rangle\langle 0_1, 1_2| + \\ & + |1_1, 0_2\rangle\langle 1_1, 0_2| + e^{i\eta} |1_1, 1_2\rangle\langle 1_1, 1_2| \end{aligned} \quad (3.20)$$

Using the relations $|0\rangle\langle 0| = (1 + \sigma_z)/2$ and $|1\rangle\langle 1| = (1 - \sigma_z)/2$, the matrix representation of Q_η is:

$$Q_\eta = I_1 I_2 - \frac{1}{4} (1 - e^{i\eta}) (I_1 I_2 - I_1 \sigma_{z2} - \sigma_{z1} I_2 + \sigma_{z1} \sigma_{z2}) \quad (3.21)$$

The case we are interested in, is for $\eta = \pi$.

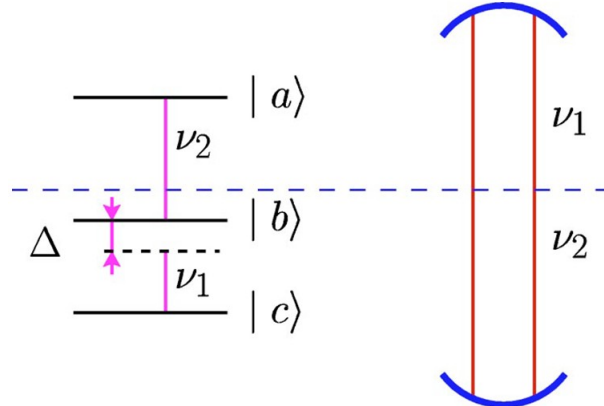


Figure 3.3: Three level system

Figure 3.3 describes the proposed setup. A cavity supporting two resonant frequencies ν_1 and ν_2 and in this case the photon number states of the cavity $|0\rangle$ and $|1\rangle$ represent logic 0 and 1 respectively.

If the vacuum Rabi frequencies associated with the frequencies supported by the cavity modes ν_1 and ν_2 are g_1 and g_2 and we have a detuning Δ such that $\omega_{ab} = \nu_2$ and $\omega_{bc} = \nu_2 + \Delta$, then a quantum phase gate may be realized when a three level atom initially in its ground state $|c\rangle$ passes through the cavity so that:

a) The detuning $\Delta = g_2$.

b) The interaction time of the atom with the cavity is such that $g_1\tau = \sqrt{2}\pi$.

In the case where the cavity has one photon in each of its modes, the effective Hamiltonian for the interaction in the dipole and rotating wave approximation is:

$$\mathcal{H} = \mathcal{H}_0 + \mathcal{H}_1 \quad (3.22)$$

where

$$\mathcal{H}_0 = \hbar\nu_1\hat{a}_1^\dagger\hat{a}_1 + \hbar\nu_2\hat{a}_2^\dagger\hat{a}_2 + \hbar\omega_{bc}|b\rangle\langle b| + \hbar\omega_{ac}|a\rangle\langle a| \quad (3.23)$$

$$\mathcal{H}_1 = \hbar g_1 \left(\hat{a}_1|b\rangle\langle c| + \hat{a}_1^\dagger|c\rangle\langle b| \right) + \hbar g_2 \left(\hat{a}_2|a\rangle\langle b| + \hat{a}_2^\dagger|b\rangle\langle a| \right) \quad (3.24)$$

Moving to the interaction picture we obtain:

$$\mathcal{H}_I = e^{-\frac{i\mathcal{H}_0 t}{\hbar}} \mathcal{H}_1 e^{\frac{i\mathcal{H}_0 t}{\hbar}} = H_1 + H_2 \quad (3.25)$$

Since the only allowed states for the atom-cavity system are those that preserve the energy and the total number of excitations, the only allowed states are $|a, 0, 0\rangle, |b, 0, 1\rangle$ and $|c, 1, 1\rangle$, so the terms H_1 and H_2 are:

$$\begin{aligned} H_1 &= \hbar g_1 \left(\hat{a}_1|b\rangle\langle c|e^{-i\Delta t} + \hat{a}_1^\dagger|c\rangle\langle b|e^{i\Delta t} \right) \\ &= \hbar g_1 (|b, 0, 1\rangle\langle c, 1, 1|e^{-i\Delta t} + |c, 1, 1\rangle\langle b, 0, 1|e^{i\Delta t}) \end{aligned} \quad (3.26)$$

and

$$\begin{aligned} H_2 &= \hbar g_2 \left(\hat{a}_2|a\rangle\langle b| + \hat{a}_2^\dagger|b\rangle\langle a| \right) \\ &= \hbar g_2 (|a, 0, 0\rangle\langle b, 0, 1| + |b, 0, 1\rangle\langle a, 0, 0|) \end{aligned} \quad (3.27)$$

If we define the dressed states that correspond to the field mode supporting the frequency ν_2 , as:

$$\begin{aligned} |+\rangle &\equiv \frac{1}{\sqrt{2}} (|a, 0, 0\rangle + |b, 0, 1\rangle) \\ |-\rangle &\equiv \frac{1}{\sqrt{2}} (|a, 0, 0\rangle - |b, 0, 1\rangle) \end{aligned} \quad (3.28)$$

we may rewrite the expression for H_2 as:

$$H_2 = \hbar g_2 (|+\rangle\langle +| - |-\rangle\langle -|) \quad (3.29)$$

with eigenvalues $\hbar g_2$ and $-\hbar g_2$. Writing down the Hamiltonian H_1 in the interaction picture of H_2 yields:

$$H_{1I} = \frac{\hbar g_1}{\sqrt{2}} (|+\rangle\langle c, 1, 1| e^{-i(\Delta+g_2)t} - |-\rangle\langle c, 1, 1| e^{-i(\Delta-g_2)t} + |c, 1, 1\rangle\langle +| e^{i(\Delta+g_2)t} - |c, 1, 1\rangle\langle -| e^{i(\Delta-g_2)t}) \quad (3.30)$$

If we set $g_2 = \Delta$, then the above expression simplifies to:

$$H_{1I} = \frac{\hbar g_1}{\sqrt{2}} (|+\rangle\langle c, 1, 1| e^{-i2\Delta t} - |-\rangle\langle c, 1, 1| + |c, 1, 1\rangle\langle +| e^{-i2\Delta t} - |c, 1, 1\rangle\langle -|) \quad (3.31)$$

If the detuning is large, we can ignore the oscillating terms, thus

$$H_{1I} = -\frac{\hbar g_1}{\sqrt{2}} (|-\rangle\langle c, 1, 1| + |c, 1, 1\rangle\langle -|) \quad (3.32)$$

The Rabi frequency between the levels $|-\rangle$ and $|c, 1, 1\rangle$ is $g_1/\sqrt{2}$, which means that selecting the interaction time so that $g_1\tau = \sqrt{2}\pi$, gives the transformation

$$|c, 1, 1\rangle \rightarrow -|c, 1, 1\rangle \quad (3.33)$$

This means that the above process yields the quantum phase gate Q_π .

3.2 Implementation of the quantum Fourier transform

A similar approach to the alternative described previously for Grover's algorithm, was described in [36] in order to describe a setup able to realize the heart of Shor's algorithm, ie. the Quantum Fourier Transform. The QFT is in general more demanding when one considers the number of qubits involved.

Supposing we want to act the quantum Fourier transform operation on a state $|a\rangle$ for which $2^q < a < 2^{q-1}$, we would obtain:

$$N_{QFT} = \frac{1}{\sqrt{2^q}} \sum_{c=0}^{2^q-1} e^{2\pi i ac/2^q} |c\rangle \quad (3.34)$$

In order to realize the algorithm it is enough to describe the operation of a one-qubit gate and a quantum phase gate.

¹If we wanted to map $|9\rangle \equiv |1, 0, 0, 1\rangle$ we would require 4 qubits, since $2^4 < 9 < 2^3$

One qubit gates are easily realizable in cavity QED setups since they are rotations precisely performed by Ramsey zones. In terms of Pauli spin matrices it is written as:

$$\hat{U}_{\theta,\phi} = \cos(\theta)\mathbf{I} - \cos(\phi)\sin(\theta)\hat{\sigma}_x - i\sin(\phi)\sin(\theta)\hat{\sigma}_y \quad (3.35)$$

For two qubits j and k , the quantum phase gate for $\eta = \pi$ is given similar to equation 3.20 as:

$$Q_{\pi}^{j,k} = |0_j, 0_k\rangle\langle 0_j, 0_k| + |0_j, 1_k\rangle\langle 0_j, 1_k| + |1_j, 0_k\rangle\langle 1_j, 0_k| + e^{i\pi}|1_j, 1_k\rangle\langle 1_j, 1_k| \quad (3.36)$$

In order to obtain the QFT for $q=3$, we need to perform the transformations

$$A_0 B_{01} B_{02} A_1 B_{12} A_2 \quad (3.37)$$

where $A_i \equiv U_{\pi/4, \pi/2}$ represent the one bit gates and $B_{jk} \equiv Q_{\pi/2^{k-j}}$ represent the two-qubit quantum phase gates.

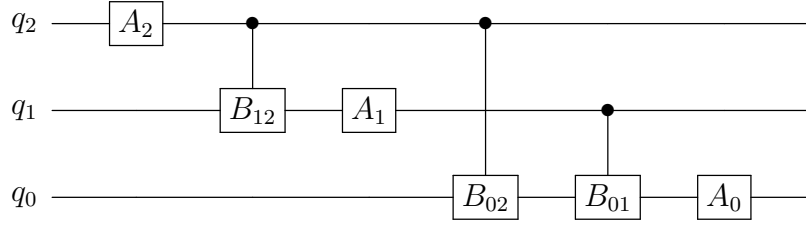


Figure 3.4: Quantum circuit realizing the quantum Fourier transform for $q=3$. $A_i \equiv U_{\pi/4, \pi/2}$ represent the one bit gates and $B_{jk} \equiv Q_{\pi/2^{k-j}}$ represent the two-qubit quantum phase gates.

The unitary one-bit gate can be implemented by applying a classical field to a two-level atom, which results to a Hamiltonian given by:

$$H = \frac{\hbar\Omega}{2} (e^{-i\phi}|a\rangle\langle b| + e^{i\phi}|b\rangle\langle a|) \quad (3.38)$$

where $|a\rangle$ is the excited state and $|b\rangle$ the ground state. The time evolution operator of this system is:

$$\begin{aligned} U_I(t) &= \exp\left[-\frac{i}{\hbar}Ht\right] \\ &= \cos(\Omega t/2) (|a\rangle\langle a| + |b\rangle\langle b|) - i \sin(\Omega t/2) (e^{-i\phi}|a\rangle\langle b| + e^{i\phi}|b\rangle\langle a|) \end{aligned} \quad (3.39)$$

In the above equation, the transformation described is an one-bit unitary gate with $\theta = \frac{\Omega t}{2}$.

Regarding the quantum phase gate, since it is necessary to perform more than one specific gates for the case of $q = 3$, one may consider the case of a three level atom in V configuration as shown in 3.5. Transition $|b\rangle \rightarrow |a\rangle$ is completely off resonant with the cavity field, while $|b\rangle \rightarrow |c\rangle$ is dispersively coupled to the cavity.

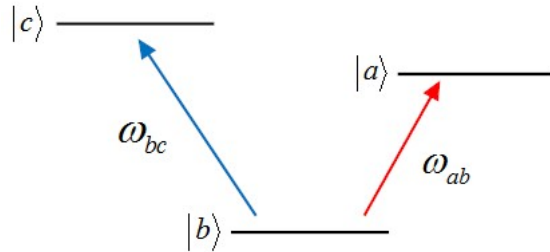


Figure 3.5: Atom in V configuration. Transition $|b\rangle \rightarrow |a\rangle$ is completely off resonant with the cavity field, while $|b\rangle \rightarrow |c\rangle$ is dispersively coupled to the cavity.

The effective Hamiltonian of the system is given by:

$$\mathcal{H}_{eff} = -\frac{\hbar g^2}{\Delta} (\hat{a}\hat{a}^\dagger|c\rangle\langle c| - \hat{a}^\dagger\hat{a}|b\rangle\langle b|) \quad (3.40)$$

where $\Delta = \omega_{cb} - \nu$ is the detuning. Supposing an initial state of the atom-field system described by

$$\frac{1}{2} (|0, a\rangle + |0, b\rangle + |1, a\rangle + |1, b\rangle) \quad (3.41)$$

the passage of the atom through the cavity results in a phase change $\eta = g^2\tau/\Delta$ of the term $|1, b\rangle$, ie:

$$\frac{1}{2} (|0, a\rangle + |0, b\rangle + |1, a\rangle + e^{i\eta}|1, b\rangle) \quad (3.42)$$

Setting appropriate values for detuning Δ and interaction time τ allows the realization of the quantum phase gate for $\eta = \pi$.

Returning to the realization of Shor's algorithm for the case of $q = 3$, in order to realize the phase gates that are required (B_{01}, B_{02}, B_{12}) one would suggest that three different types of atoms are required. One of the main advantages of manipulating Rydberg atoms is the capability of making use of their atomic sublevels by applying an external magnetic field, thus lifting the degeneracy and allowing the proper level spacings between the atomic levels. For example, using an external magnetic field we can achieve the atomic level diagram of figure 3.6. The ground state $|b\rangle$ of the atoms corresponds to $|1\rangle$ and states $|a_i\rangle$ to $|0\rangle$. In this way we can ensure that the transitions $|b\rangle \rightarrow |a_i\rangle$ are resonant only in cavity i

which supports the frequency ν_i , while the one-bit gates $A_i \equiv U_{\pi/4,\pi/2}^i$ realized by classical fields of frequency ν_i perform the necessary transformations. Pulses $U_{\pi/2,0}^i$ are used to flip the states $|a_i\rangle$ and $|b\rangle$ before atom i enters the cavity and are essential, since states $|b\rangle$ were defined as $|1\rangle$ and $|a_i\rangle$ as $|0\rangle$. The setup is presented in figure 3.7.

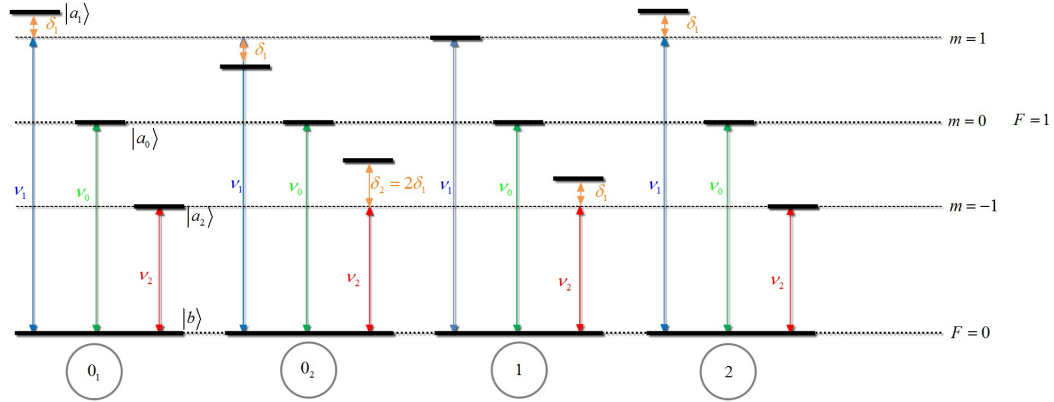


Figure 3.6: Atomic levels under the influence of the magnetic field. For each atom the ground state $|b\rangle$ corresponds to $|1\rangle$ and $|a_i\rangle$ to $|0\rangle$.

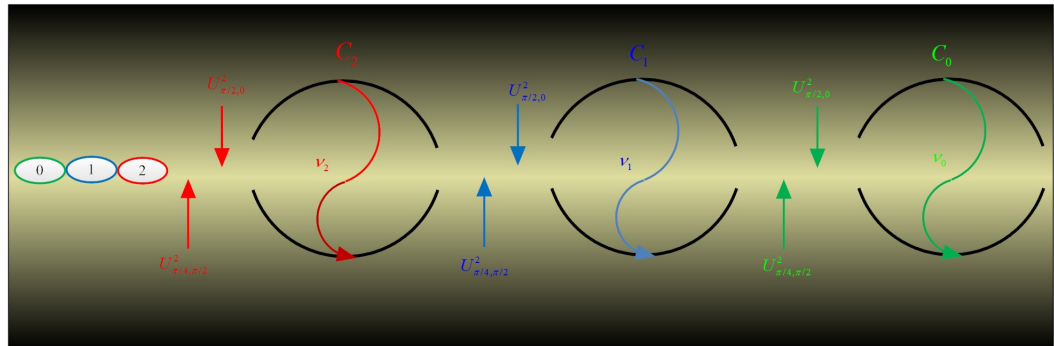


Figure 3.7: Experimental setup for the realization of QFT for 3 qubits.

The interaction times τ , the coupling constant g and the detunings δ_i are chosen so that $\frac{g^2\tau}{\delta_{j-k}} = \pi/2^{j-k}$. Especially, regarding the interaction time and coupling constants they are chosen so that when atom i passes through cavity C_i , will transfer its coherence to the cavity and leave in the ground state, so that the QFT is stored in the cavities.

The readout requires a triplet of atoms prepared in the ground state and resonant to each cavity, in order to measure the field inside the cavity. If one

atom comes in the ground state the output is 0, whereas if it comes in an excited state it will correspond to 1.

This scheme can be theoretically generalized for any number n of qubits. In the next chapter, we will discuss how extended cavity QED setups, where on top of the atom-cavity interaction, the cavities are allowed to interact directly through photon hopping, can be exceptional models for other applications, including quantum simulations.



Chapter 4

Implementing quantum gates in coupled cavity arrays

Describing an experimental setup for the realization of Shor's algorithm, we discussed how a system of three separate cavities could be used in order to perform the required two qubit transformations. In that setup, the cavities were supporting different frequencies, thus interacting with specific atoms each time, to perform the necessary operations on qubits. Moreover, we didn't require any field transfer from one cavity to the other, but required that the cavities allowed the passage of the atoms, as well as that the atoms had the appropriate velocities to achieve the desirable interaction time with the cavity they would interact.

In parallel to the developments of implementing QIP with quantum optical systems, the idea of using quantum systems for quantum simulation attracted a lot of attention. *Quantum Simulations* [21],[38],[78],[79],[80], is the use of specifically engineered systems with controllable local interactions, in order to simulate complex physical phenomena where both classical computers modelling and experimental attempts fail.

In this way it was shown that is possible, to determine the behaviour of a lot of phenomena lacking full theoretical explanation, like phase transitions in solid state physics and quantum magnetism. More recently, there have been efforts in describing exotic physical theories from high energy physics, like the Thirring model and the renormalization of mass [81, 82].

The platforms for quantum simulation initially included optical lattices with cold atoms [83, 84, 85, 86] , ion traps [47, 87, 88, 89, 90], and NMR setups [91, 92]. The idea of using coupled cavities each containing one two-level-system (TLS) as a quantum simulator was initially proposed for the study of phenomena like Mott transitions and XY spin models [39]. This was followed by studies of the phase diagram of the system and applications in simulating exotic effects in condensed matter physics have been developed [93, 94, 95, 96, 97, 98, 99] .

Lately, studies of driven dissipative Jaynes-Cummings arrays have emerged analyzing the Jaynes-Cummings-Hubbard model out of equilibrium and the signatures of the underlying many body effects, in the steady states of the system [100, 101, 102, 103, 104, 105].

This fascinating new perspective has stimulated works that encouraged the experimental progress on specific structures, also for the purpose of performing quantum computation. The most spectacular development was definitely in Circuit QED platforms [106].

In this final chapter of the present thesis we will study the simple and easier to experimentally implement case, of a system of two coupled cavities and discuss a scheme for implementing the quantum phase gate there.

4.1 Quantum dynamics in the two coupled cavities model

The Jaynes-Cummings model for the description of the interaction of a two-level atom with a single mode electromagnetic field, is described by the Hamiltonian

$$\hat{H}_{J-C} = \frac{1}{2}\hbar\omega_0\hat{\sigma}_3 + \hbar\omega\hat{a}^\dagger\hat{a} + \hbar g (\hat{\sigma}_+\hat{a} + \hat{\sigma}_-\hat{a}^\dagger) \quad (4.1)$$

If we consider a system of two empty cavities, each one of them supporting a frequency ω_i , evanescently coupled, this allows the photons from C_1 to hop to C_2 and vice versa, then we have a Hamiltonian of the form:

$$\hat{H} = \hbar\omega_1\hat{a}_1^\dagger\hat{a}_1 + \hbar\omega_2\hat{a}_2^\dagger\hat{a}_2 + J (\hat{a}_1^\dagger\hat{a}_2 + \hat{a}_2^\dagger\hat{a}_1) \quad (4.2)$$

where \hat{a}_i , \hat{a}_i^\dagger are the annihilation and creation operators for the field modes and J is the "hopping" parameter that describes how a field state from C_1 can move to C_2 and vice versa. It's worth mentioning that the coupling parameter between the cavities has frequency dimensions [107], [108], is defined as the overlap between the two fields that are sustained in the cavities and is proportional to the quantity

$$J \propto \int d\vec{r} \vec{u}_1(\vec{r} - \vec{r}_1) \cdot \vec{u}_2(\vec{r} - \vec{r}_2) \quad (4.3)$$

where $\vec{u}_i(\vec{r} - \vec{r}_i)$ is the vector field distribution of the mode, \vec{r} is a position vector in the cavity and \vec{r}_i is a reference position within each cavity. Supposing

$\omega_1 = \omega_2 = \omega$ ¹ we may define the quantities:

$$\begin{aligned}\hat{A}_1 &= \frac{1}{\sqrt{2}} (\hat{a}_1 + \hat{a}_2) \\ \hat{A}_2 &= \frac{1}{\sqrt{2}} (\hat{a}_1 - \hat{a}_2)\end{aligned}\quad (4.4)$$

leading to the equation

$$\hat{\mathcal{H}}_{field} = \hbar\omega_{c1}\hat{A}_1^\dagger\hat{A}_1 + \hbar\omega_{c2}\hat{A}_2^\dagger\hat{A}_2 \quad (4.5)$$

The new frequencies $\omega_{c1,2} = \omega \pm J$ correspond to the two normal modes of a mechanical system of two 1D coupled oscillators. The general case is treated in [107]. One may easily verify that those delocalised field modes, obey the bosonic operators commutation relations

$$[A_i, A_j^\dagger] = 1, \quad i = 1, 2, \dots \quad (4.6)$$

Supposing each cavity now contains a fixed two-level atom, the total hamiltonian of the system is given by:

$$\begin{aligned}\hat{\mathcal{H}} &= \hat{H}_{J-C,1} + \hat{H}_{J-C,2} + J \left(\hat{a}_1^\dagger \hat{a}_2 + \hat{a}_2^\dagger \hat{a}_1 \right) \Leftrightarrow \\ \hat{\mathcal{H}} &= \sum_{j=1,2} \left[\frac{\hbar\omega_0 \hat{\sigma}_{j3}}{2} + \omega_j \hat{a}_j^\dagger \hat{a}_j + g \left(\hat{a}_j \hat{\sigma}_{j+} + \hat{a}_j^\dagger \hat{\sigma}_{j-} \right) \right] + J \left(\hat{a}_1^\dagger \hat{a}_2 + \hat{a}_2^\dagger \hat{a}_1 \right)\end{aligned}\quad (4.7)$$

This Hamiltonian describes fully the interaction in the two cavities system. As it is clearly seen, the total number of excitations is conserved. In this case, we will study the dynamics of the one excitation case for simplicity. In this case we consider a general state:

$$|\psi(t)\rangle = a(t)|g_1g_210\rangle + b(t)|g_1g_201\rangle + c(t)|e_1g_200\rangle + d(t)|g_1e_200\rangle \quad (4.8)$$

The first two terms in each ket represent the state of atoms 1 and 2 respectively, whereas the last two represent the cavity field states in cavities 1 and 2. The time evolution of this one-excitation state is given by the Schrödinger equation with the use of the delocalised modes ($j = 1, 2$):

$$\begin{aligned}\alpha_j(t) &= a(t) + (-1)^j b(t) \\ \beta_j(t) &= c(t) + (-1)^j d(t)\end{aligned}\quad (4.9)$$

¹In this degenerate case the coupling parameter is limited by $|J| < \omega/2$

The Schrödinger equation, using the above delocalised modes gives

$$\begin{aligned}\alpha_j(t) &= e^{-i(\omega_0 - \Omega_j/2)t} \left[\alpha_j(0) \cos(\nu_j t) + \frac{i}{\nu_j} \left(\frac{\Omega_j}{2} \alpha_j(0) - g \beta_j(0) \right) \sin(\nu_j t) \right] \\ \beta_j(t) &= e^{-i(\omega_0 - \Omega_j/2)t} \left[\beta_j(0) \cos(\nu_j t) - \frac{i}{\nu_j} \left(\frac{\Omega_j}{2} \beta_j(0) - g \alpha_j(0) \right) \sin(\nu_j t) \right]\end{aligned}\quad (4.10)$$

where

$$\nu_j = \sqrt{\left(\frac{\Omega_j}{2}\right)^2 + g^2} \quad (4.11)$$

and we have set

$$\Omega_{1,2} = \Delta \pm J \quad (4.12)$$

Using the relation 4.4 and a new set of operators that describe the atomic modes defined as:

$$\begin{aligned}\hat{S}_{1+} &= \frac{1}{\sqrt{2}} (\hat{\sigma}_{1+} + \hat{\sigma}_{2+}) \\ \hat{S}_{2+} &= \frac{1}{\sqrt{2}} (\hat{\sigma}_{1+} - \hat{\sigma}_{2+})\end{aligned}\quad (4.13)$$

we may rewrite the total Hamiltonian of the system in the form:

$$\hat{\mathcal{H}} = \sum_{j=1,2} \left[\omega_0 \hat{S}_{j+} \hat{S}_{j-} + \omega_{ej} \hat{A}_j^\dagger \hat{A}_j + g \left(\hat{A}_j \hat{S}_{j+} + \hat{A}_j^\dagger \hat{S}_{j-} \right) \right] \quad (4.14)$$

In order to investigate the region of parameters that will allow us to use the two coupled cavities setup as a quantum phase gate, we resort to analytical calculations and numerical simulations, that are presented in the following.

4.2 Analytical treatment

The form of the equation 4.14 resembles to the form of 4.1. Indeed, some algebra can verify that if we consider the interaction Hamiltonian

$$\hat{H}_I = \sum_{j=1,2} \left[g \left(\hat{A}_j \hat{S}_{j+} + \hat{A}_j^\dagger \hat{S}_{j-} \right) \right] \quad (4.15)$$

and move to the interaction picture in respect to the term,

$$\hat{H}_0 = \sum_{j=1,2} \left(\omega_0 \hat{S}_{j+} \hat{S}_{j-} + \Omega_j \hat{A}_j^\dagger \hat{A}_j \right) \quad (4.16)$$

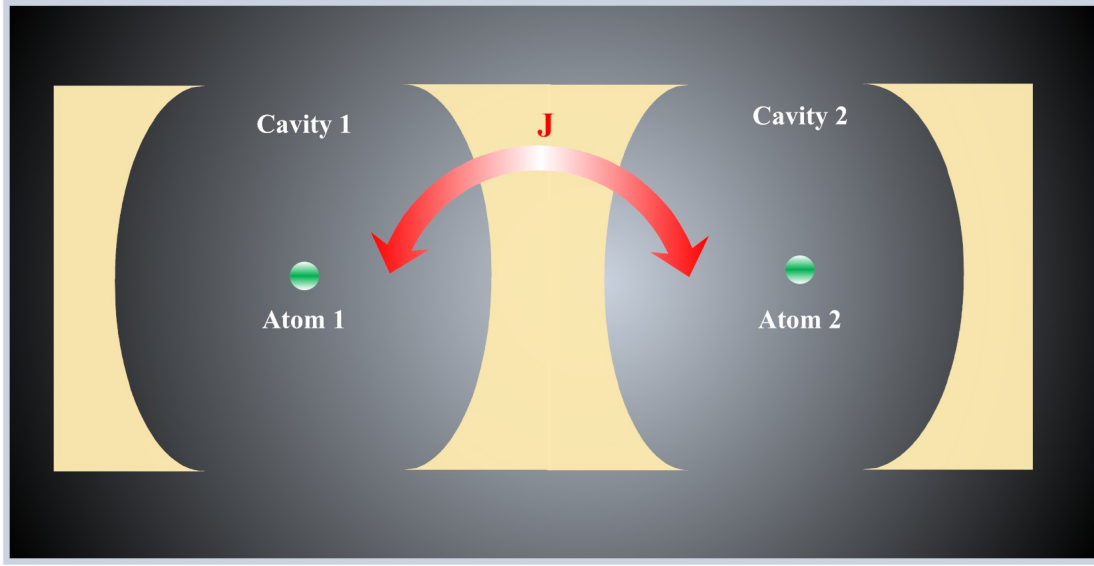


Figure 4.1: Two coupled cavities interacting with fixed atoms.

then, we have a similar procedure like the one we did in order to derive the state evolution for the Jaynes-Cummings model. Indeed, since $[\hat{H}_0, \hat{H}_I] = 0$, the interaction Hamiltonian in the interaction picture takes the form:

$$\hat{\mathcal{H}}_I = g \left(\hat{A}_1^\dagger \hat{S}_1 e^{-i\Omega_1 t} + \hat{A}_2^\dagger \hat{S}_2 e^{-i\Omega_2 t} + \text{Hermitian Conjugate} \right) \quad (4.17)$$

This form shows that each term of the interaction Hamiltonian oscillates at the respective frequency Ω_i , though, this form does not allow a clear overview of the state transfer between the atoms, which is the basic feature that could allow the operation of a quantum phase gate. In order to obtain this expression in [109] Ogden et al follow the process described in [110] to derive the effective Hamiltonian of the system, which simplifies the Hamiltonian but doesn't eliminate the atom-field interaction terms. The effective Hamiltonian is defined from the time derivative of the time-averaged evolution operator.

$$i \frac{\partial}{\partial t} \overline{\hat{U}(t)} = \hat{\mathcal{H}}_{eff} \overline{\hat{U}(t)} \quad (4.18)$$

The time average of an operator $\hat{\mathcal{O}}$ is defined as:

$$\overline{\hat{\mathcal{O}}(t)} = \int_{-\infty}^{\infty} f(t - t') \hat{\mathcal{O}}(t') dt' \quad (4.19)$$

The function $f(t - t')$ is real valued and serves the purpose of eliminating the fast oscillating terms, acting as a ((low-pass filter)). We need to specify that we

use only its generic properties in order to exclude high-frequency terms in this time-averaging process, therefore we do not need to explicitly specify its form. Comparison with the Schrödinger equation $i\frac{\partial}{\partial t}\hat{U}(t) = \hat{H}_I\hat{U}(t)$ for the non-time-averaged evolution operator allows us to write down the effective Hamiltonian as a series of \hat{H}_I and \hat{U} . Discarding the terms of this expansion beyond second order in respect to \hat{H}_I gives the expression:

$$\hat{\mathcal{H}}_{eff} = \overline{\hat{\mathcal{H}}_I(t)} + \frac{1}{2} \left\{ \overline{[\hat{\mathcal{H}}_I(t), \hat{U}_1(t)]} - \overline{[\hat{\mathcal{H}}_I(t), \hat{U}_1(t)]} \right\} \quad (4.20)$$

Replacing $\hat{U}_1(t)$ by the expression deriving from the expansion in terms of $\hat{\mathcal{H}}_I(t)$ of the time evolution operator $\hat{U}(t)$ yields:

$$\hat{U}_1(t) = \frac{1}{i} \int_{t_0}^t \hat{\mathcal{H}}_I(t') dt' \quad (4.21)$$

Directly calculating this integral for the interaction Hamiltonian of equation 4.17 leads us to a unitary operator of the form

$$\hat{V}(t) = g \left(\frac{\hat{A}_1^\dagger \hat{S}_{1-} e^{-i\Omega_1 t}}{\Omega_1} + \frac{\hat{A}_2^\dagger \hat{S}_{2-} e^{-i\Omega_2 t}}{\Omega_2} - \text{Herm. Conj.} \right) \quad (4.22)$$

Following the above process, in order to obtain the expression for the effective Hamiltonian we need to calculate the commutator $[\hat{\mathcal{H}}_I(t), \hat{V}(t)]$:

$$\begin{aligned} [\hat{\mathcal{H}}_I(t), \hat{V}(t)] &= \frac{2g^2}{\Omega_1} [\hat{A}_1 \hat{S}_{1+}, \hat{A}_1^\dagger \hat{S}_{1-}] + \frac{2g^2}{\Omega_2} [\hat{A}_2 \hat{S}_{2+}, \hat{A}_2^\dagger \hat{S}_{2-}] + \\ &\quad + g^2 e^{2iJt} \left(\frac{1}{\Omega_1} + \frac{1}{\Omega_2} \right) [\hat{A}_1 \hat{S}_{1+}, \hat{A}_2^\dagger \hat{S}_{2-}] + \\ &\quad + g^2 e^{2iJt} \left(\frac{1}{\Omega_1} + \frac{1}{\Omega_2} \right) [\hat{A}_2 \hat{S}_{2+}, \hat{A}_1^\dagger \hat{S}_{1-}] \end{aligned} \quad (4.23)$$

The form of the commutator of equation 4.23 cannot be totally treated analytically, thus we need to make certain approximations.

4.2.1 Case A: Large intercavity hopping regime

First we consider the case for which $J \gg \{\Delta, g\}$. The last two terms of the above expression both oscillate at a frequency of $2J$. As it was done throughout the derivation of the above expression terms rotating at frequencies proportional to Ω_i or J have a zero time average since they oscillate too fast, thus we will keep only the first two terms.

Consequently, under the above approximation, the expression obtained for $\hat{\mathcal{H}}_{eff}$ is given by

$$\hat{\mathcal{H}}_{eff} = \frac{g^2}{\Omega_1} \left[\hat{A}_1 \hat{S}_{1+}, \hat{A}_1^\dagger \hat{S}_{1-} \right] + \frac{g^2}{\Omega_2} \left[\hat{A}_2 \hat{S}_{2+}, \hat{A}_2^\dagger \hat{S}_{2-} \right] \quad (4.24)$$

Yet this form of the Hamiltonian is not useful for studying the system's quantum dynamics. The evolution of the system imposes the use of the Hamiltonian in the Schrödinger picture. After some tedious algebra we obtain

$$\begin{aligned} \hat{\mathcal{H}}' = \hat{H}_0 + & \underbrace{\sum_{i,j=1}^2 \frac{g^2}{2\Omega_i} \left(\hat{A}_i \hat{A}_i^\dagger |e\rangle_j \langle e| - \hat{A}_i^\dagger \hat{A}_i |g\rangle_j \langle g| \right)}_{\text{dispersive interaction between atoms and delocalized field modes}} + \\ & \underbrace{+ \frac{g^2}{\Omega_1 \Omega_2} J (\hat{\sigma}_{1+} \hat{\sigma}_{2-} + \hat{\sigma}_{2+} \hat{\sigma}_{1-})}_{\text{transfer of states between atoms without excitation of the field modes}} \end{aligned} \quad (4.25)$$

The term \hat{H}_0 corresponds to the energy of the bare atomic and delocalized field modes and is the term we derived in equation 4.16. The second term describes the dispersive interaction between atoms and the delocalized field modes. As we discussed in previous cases where we were studying dispersive interactions between cavities and single field modes, there is no energy transfer, though the atoms experience a Stark shift. The final term is the one that describes the transfer of energy between atoms without excitation of the field modes.

Setting $G = g^2/\Omega_1 \Omega_2$ and using the equations of motion 4.9 and 4.10 we obtain:

$$\begin{aligned} a(t) &= e^{-i(\omega - G\Delta)t} [a(0) \sin(Jt) - b(0) \cos(Jt)] \\ b(t) &= e^{-i(\omega - G\Delta)t} [-ia(0) \cos(Jt) + ib(0) \sin(Jt)] \\ c(t) &= e^{-i(\omega_0 + G\Delta)t} [c(0) \cos(GJt) - id(0) \sin(GJt)] \\ d(t) &= e^{-i(\omega_0 + G\Delta)t} [-ic(0) \sin(GJt) + d(0) \cos(GJt)] \end{aligned} \quad (4.26)$$

Therefore, we expect the probability amplitudes to oscillate with a period $T = \frac{2\pi}{GJ}$, where

$$G = \frac{g^2}{\Omega_1 \Omega_2} = \frac{g^2}{(\Delta + J)(\Delta - J)} \quad (4.27)$$

A valid choice of parameters for this large intercavity hopping regime is $J = 10g, \Delta = 0.1g, g = 5.10^{-3}\omega_0$. Setting the initial state of the system to $|\psi(0)\rangle = |eg00\rangle$ and using the full Hamiltonian for the time evolution of the system, we obtain the probabilities for the excitation to pass from Atom 1 to

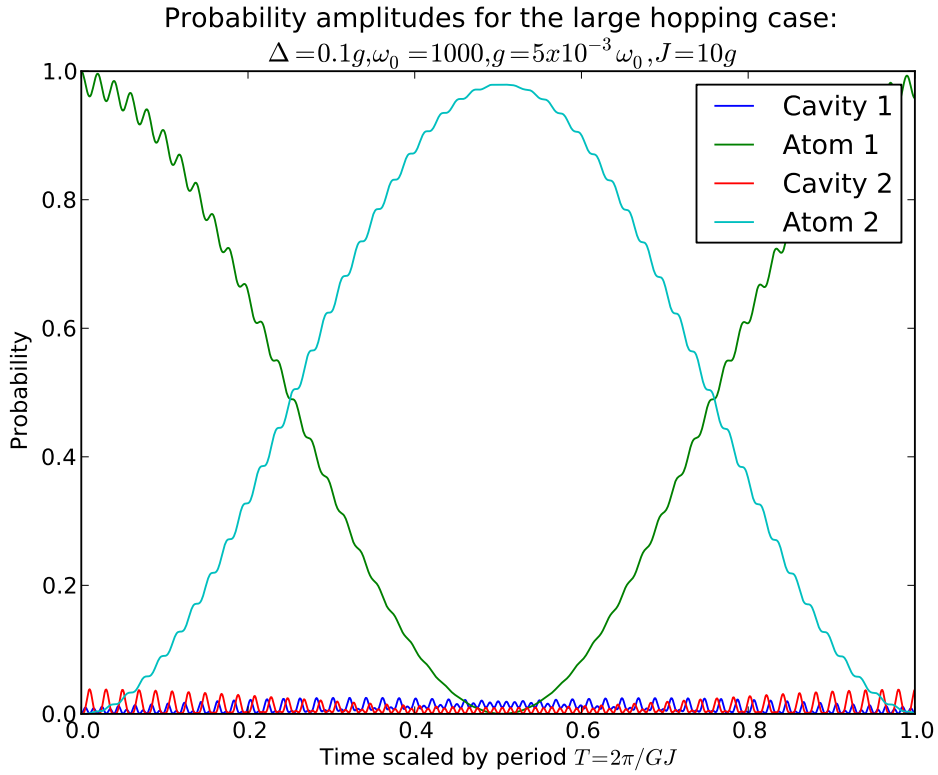


Figure 4.2: Probability amplitudes corresponding to exciting a specific cavity mode or a specific atom as a function of time, for the case of large hopping assuming the system started from the state $|eg00\rangle$. Here, $J = 10g$, $\Delta = 0.1g$ and $\omega = 1000g$, while the time is scaled by period $T = \frac{2\pi}{GJ}$

Atom 2 and the probability for the excitation to pass to the field modes. Those probabilities are plotted versus time, in figure 4.2.

The plot clearly shows that in this large hopping case, the excitation has much higher probability to be found in one of the atoms, than transferring to the cavity field. The latter will be important for the case where the cavity is lossy and photons leak to the environment (we study this case later). This atom-atom excitation exchange happens with a frequency GJ as predicted by the analytical solution 4.26.

Setting the values for this case of parameters in the quantity GJ we can calculate that the period of the oscillation for the probability amplitudes regarding

the excitation transfer from atom 1 to atom 2, to be:

$$\begin{aligned} T_{LH} &= \frac{2\pi}{GJ} = \frac{2\pi}{\frac{g^2}{\Omega_1\Omega_2}J} = \frac{2\pi}{\frac{g^2}{(\Delta+J)(\Delta-J)}J} \\ &= \frac{2\pi(\Delta^2 - J^2)}{g^2J} \simeq \frac{2\pi J}{g^2}, \text{since } \Delta \ll J \end{aligned} \quad (4.28)$$

4.2.2 Case B: Large Detuning regime

Following the same procedure as in the case of large hopping, we come again facing the problem of defining the effective Hamiltonian. Since we consider the detuning to be much bigger than the coupling strength between atom-cavity and the cavities (ie. $\Delta \gg \{J, g\}$), terms rotating at rates Ω_1 or Ω_2 need to be eliminated from the time averaging process. Thus, the effective Hamiltonian in the Schrödinger picture becomes:

$$\begin{aligned} \hat{H}' &= \hat{H}_0 + \sum_{j=1}^2 \frac{g^2\Delta}{\Omega_1\Omega_2} \left(\hat{a}_j \hat{a}_j^\dagger |e\rangle_j \langle e| - \hat{a}_j^\dagger \hat{a}_j |g\rangle_j \langle g| \right) + \frac{g^2J}{2\Omega_1\Omega_2} \left(\hat{A}_2^\dagger \hat{A}_2 - \hat{A}_1^\dagger \hat{A}_1 \right) (\hat{\sigma}_{1z} + \hat{\sigma}_{2z}) + \\ &\quad + \frac{g^2J}{\Omega_1\Omega_2} (\hat{\sigma}_{1+}\hat{\sigma}_{2-} + \hat{\sigma}_{2+}\hat{\sigma}_{1-}) \end{aligned} \quad (4.29)$$

The last term of this expression is the same as the one we obtained for the large hopping case and describes the atom-atom interaction. Though, we observe that the Stark shift terms are altered. In the previous case, each atom would interact with the delocalised field modes, but now, since the atom-cavity detuning is much larger than the coupling strength between the cavities the shift splits into two terms.

The first one describes the interaction of each atom with its cavity field and the second one describes the interaction of each atom with the delocalised field modes and is much smaller than the local field effect.

This second term vanishes for large values of detuning. Regarding the equations of motion, they will have exactly the same form as 4.26. Therefore, we can verify the fact that there is no state transfer exchange between the field modes and the atoms and the excitation oscillates between the atoms at a constant rate.

Setting the limits for this case, in order to calculate the period of the probability amplitudes oscillations, we find that the period is $T = \frac{2\pi}{GJ}$.

Following the same procedure as in the large hopping case, but taking this case's approximation, we find the period to be:

$$T_{disp} \simeq \frac{\pi\Delta^2}{g^2J} \quad (4.30)$$

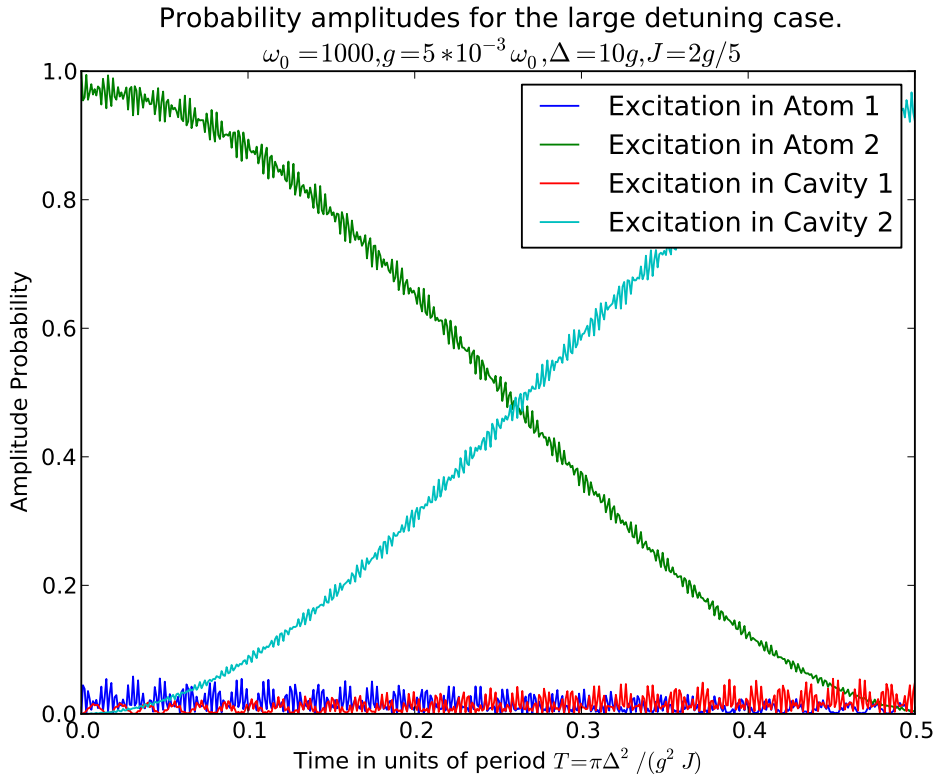


Figure 4.3: Probability amplitudes corresponding to exciting a specific cavity mode or a specific atom as a function of time, for the case of large detuning, assuming the system started from the state $|eg00\rangle$. Here we chose $\Delta = 10g$, $g = 5 \times 10^{-3} \omega_0$, $J = 2g/5$, while the time is scaled by period $T = \frac{\pi\Delta^2}{g^2 J}$

The requirements for the dispersive regime are $\Delta \gg \{J, g\}$, thus a valid choice of parameters that fulfils this requirement and is experimentally viable, is $\Delta = 50 \times 10^{-2} \omega_0$, $g = 5 \times 10^{-3} \omega_0$, $J = 2 \times 10^{-3} \omega_0$ with $\omega_0 = 10^3$. In figure 4.3 we present the numerical results for this case. We can verify that there is very small probability for the excitation to pass to the field modes, just like in the large hopping case.

However, the time required for the excitation to transfer from atom 1 to atom 2 is greatly increased, thus compromising the response of the system. We observe that the period of the state transfer is $T = \frac{\pi\Delta^2}{g^2 J}$. Setting different values for the parameters, we observed (not shown here), that for small values of Δ , as it is expected, there is a considerable probability for the excitation to pass to the field modes, though as detuning increases (with g and J being stable), we observed that even this probability diminishes. This is explained by the fact that the energy transfer from atomic modes to field modes requires a considerable amount of

energy, therefore it is greatly suppressed.

4.2.3 Case C: Resonant interaction regime

The last case we need to investigate is the resonant case, for which we need to suppose that $J = \Delta$. The main reason that guides us on this selection is the fact that with this choice of parameters the terms Ω_i of equation 4.14 become zero, which allows only in the last term of this expression to affect the state evolution. Another reason to expect this behaviour is the fact that for $J = \Delta$, there is resonance between the cavity field and the collective field modes, thus allowing energy transfer between atom and field states, in contrast to the previous two cases where the direct exchange of energy between the atoms was the dominant procedure. In order to derive the effective Hamiltonian in the Schrödinger picture, now we eliminate the terms that contain frequencies $2J$ and Ω_1 . The Hamiltonian for this case is proved to be

$$\hat{\mathcal{H}}' = \hat{H}_0 + g \left(\hat{A}_2^\dagger \hat{S}_{2-} + \hat{A}_2 \hat{S}_{2+} \right) + \frac{g^2}{2\Omega_1} \left[\hat{A}_1 \hat{A}_1^\dagger (|e\rangle_1 \langle e| + |e\rangle_2 \langle e|) - \hat{A}_1^\dagger \hat{A}_1 (|g\rangle_1 \langle g| + |g\rangle_2 \langle g|) - (\hat{\sigma}_{1+} \hat{\sigma}_{2-} + \hat{\sigma}_{2+} \hat{\sigma}_{1-}) \right] \quad (4.31)$$

The second term describes the energy exchange between the resonant delocalised atomic and field modes \hat{S}_2 and \hat{A}_2 . The third term describes dispersive interaction between modes \hat{S}_1 and \hat{A}_1 since they are highly detuned. We also observe a Stark shift of the atoms dependent on the population of \hat{A}_1 , whereas the final term describes the direct transfer of energy between the atoms, without the mediation of the cavity field. For this case, the equations of motion will give the exact behaviour of the system. Since the dispersive interaction may be neglected ($\frac{g^2}{2\Omega_1} \ll g$) for times smaller than Ω_1/g^2 , we expect a behaviour similar to the case of one atom coupled to one cavity. The difference here is that the role of the single mode field is assigned to the delocalised field mode (\hat{A}_2) and the role of the atom to the delocalised atom mode (\hat{S}_2). If the field modes contain at $t = 0$ no excitation ($\alpha_j(0) = 0$) the evolution of the atomic modes is:

$$\begin{aligned} \beta_1(t) &= e^{-i(\omega_0 + g^2/\Omega_1)t} \beta_1(0) \\ \beta_2(t) &= e^{-i(\omega_0 + g^2/\Omega_2)t} \beta_2(0) \cos \left[\left(g + \frac{\Omega_2^2}{8g} \right) t \right] \end{aligned} \quad (4.32)$$

The dispersive coupling of mode \hat{S}_1 to the field keeps its population constant, while atomic mode \hat{S}_2 oscillates at rate almost g (since the term $\frac{\Omega_2^2}{8g}$ is negligible) due to the excitation transfer between \hat{A}_2 and \hat{S}_2 . The phase difference between

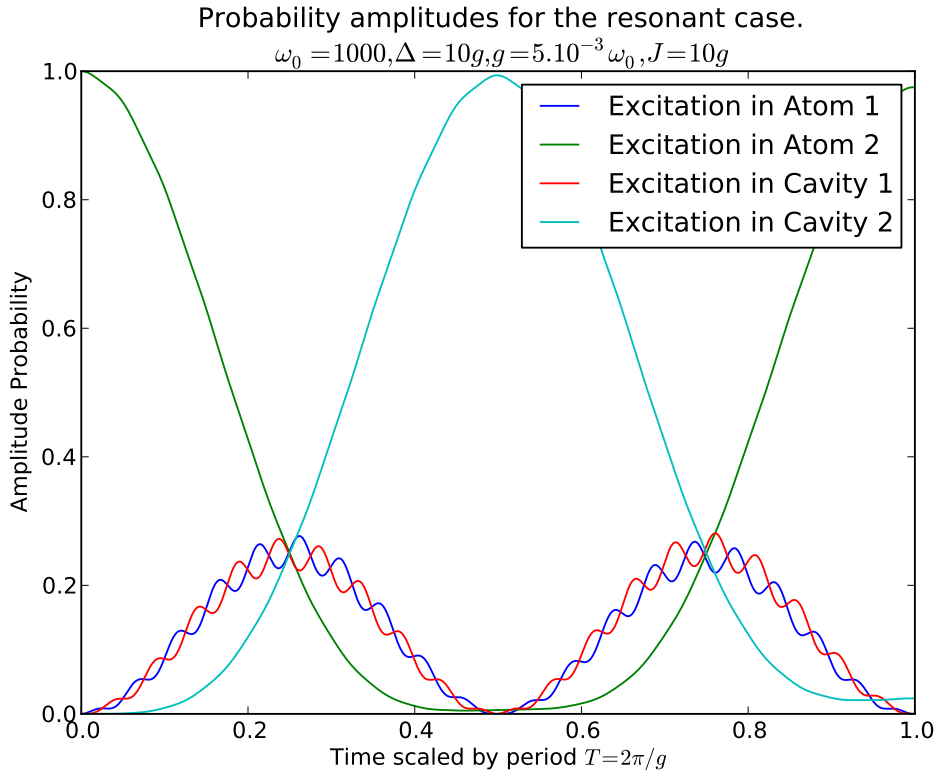


Figure 4.4: Probability amplitudes corresponding to exciting a specific cavity mode or a specific atom as a function of time, for the resonant case, assuming the system started from the state $|eg00\rangle$. In this case, $\Delta = 10g$, $g = 10^{-3}\omega_0$, $J = 10g$, while the time is scaled by period $T = \frac{2\pi}{g}$

them is

$$\delta = \frac{\Omega_2}{2} + \frac{g^2}{\Omega_1} \quad (4.33)$$

Taking the exact resonance case so that $\Omega_2 = 0$ and $g^2/\Omega_1 \ll 1$ this phase difference is almost zero, therefore the two delocalised modes oscillate with approximately same frequencies. Taking the initial conditions $a(0) = 0, b(0) = 0, d(0) = 0$ we find that:

$$\begin{aligned} a(t) &= b(t) = -\frac{ic(0)}{2} e^{-i\omega_0 t} \sin(gt) \\ c(t) &= c(0) e^{-i\omega_0 t} \cos^2\left(\frac{gt}{2}\right) \\ d(t) &= c(0) e^{-i\omega_0 t} \sin^2\left(\frac{gt}{2}\right) \end{aligned} \quad (4.34)$$

The transfer of the atomic state between the atoms through this mechanism is much faster than any of the two cases we previously described, having a period $T = \frac{2\pi}{g}$. Though, this significant increase of responsiveness comes with the cost of exposing the system to decoherence via cavity loss, since the cavity modes mediate this process. For the numerical simulations we have chosen the set of parameters: $\Delta = 10g$, $g = 5.10^{-3}\omega_0$, $J = 10g$. This set of values apply to the condition of $J = \Delta$ and as it can be seen by figure 4.4, the period of the probability amplitudes regarding the atoms is as predicted by the analytical results $T = \frac{2\pi}{g}$. Moreover, we observe that the probability for the excitation to pass to the field modes, is greatly increased compared to the dispersive and large hopping case, which is expected if we consider that in this case, the cavity field is resonant *with the collective cavity field modes*.

4.3 Quantum Dynamics in a two cavity system with dissipation

Returning to realistic situations, as it was made clear in the discussion we made in the final section of **Chapter 1**, we are not able to ignore the effect of the dissipation on our system. We have mentioned earlier the fact that if we want to realize this experimental setup we will have to make sure that we use the dispersive regime or the large hopping regime of parameters, in order to avoid, or at least, reduce the effects of the unavoidable process of decoherence.

The master equation for this system, now has to take under consideration the fact that both cavities can lose photons via their exchange with the environment. It will have the form:

$$\begin{aligned} \frac{d\rho}{dt} &= -i[H, \rho] + \frac{\kappa}{2}(\mathcal{L}[\hat{a}_1] + \mathcal{L}[\hat{a}_2]) = \\ &= -i[H, \rho] + \frac{\kappa}{2} \left[\left(2\hat{a}_1\rho\hat{a}_1^\dagger - \hat{a}_1\hat{a}_1\rho - \rho\hat{a}_1^\dagger\hat{a}_1 \right) + \left(2\hat{a}_2\rho\hat{a}_2^\dagger - \hat{a}_2\hat{a}_2\rho - \rho\hat{a}_2^\dagger\hat{a}_2 \right) \right] \end{aligned} \quad (4.35)$$

For our numerical simulations we have used the set of collapse operators

$$\begin{aligned} \hat{C}_1 &= \hat{a}_1\sqrt{2\kappa} \\ \hat{C}_2 &= \hat{a}_2\sqrt{2\kappa} \end{aligned} \quad (4.36)$$

Comparing the expressions for T_{LH} with T_R , and substituting all the parameters but g , one may find that:

$$\frac{T_{LH}}{T_R} \simeq \frac{J_{LH}}{g} \gg 1 \text{ for the large hopping regime} \quad (4.37)$$

This means that the large hopping interaction requires almost $J \times T_R$ time. Regarding the dispersive case, if we compare its period to the large hopping case, we find it is:

$$\frac{T_{disp}}{T_R} = \frac{\Delta_{disp}^2}{g J_{disp}} \quad (4.38)$$

Using the sets of parameters for the three regions as in the non-dissipative case, we have:

1. Large Hopping regime: $g = 5 \times 10^{-3}\omega_0$, $J = 10g$, $\Delta = 0.1g$, $T_{LH} = 2\pi J/(g^2)$
2. Dispersive regime: $g = 5.10^{-3}\omega_0$, $J = 2/5g$, $\Delta = 10g$, $T_{disp} = 2\pi\Delta^2/g^2J$
3. Resonant regime: $g = 5.10^{-3}\omega_0$, $J = 2/5g$, $\Delta = 10g$, $T_R = 2\pi/g$

This means that for our numerical values the periods, expressed via T_R , are:

$$\begin{aligned} T_{LH} &\simeq 10 \times T_R \\ T_{disp} &\simeq 100 \times T_R \end{aligned} \quad (4.39)$$

Comparing the periods of the three regimes we find that the resonant case has the smallest period. It's small period, allows to sustain more oscillations initially, though since the excitation passes to the field modes there is a very small probability over time for the excitation to pass from one atom to the other. In the following we plot the amplitudes of the probabilities showing the ideal case and the dispersive case. From figures 4.5-4.7, we observe that the system in the resonant case is susceptible to decoherence, as it is predicted by theory, since the cavity field modes mediate the process.

The numerical simulation for the large hopping case in figures 4.8-4.10, shows that this case has better dynamical behaviour when dissipation is taken under account. As expected, there is significant probability for the excitation to pass from one atom to another, even for $\kappa = g$, despite the fact that it is a slower process than the resonant case.

Regarding the dispersive case, from figures 4.11-4.13, we observe the effect the greater time scale has on the system. Specifically, the fact that figure 4.9 for the large hopping case with $\kappa = 1$ resembles to figure 4.11 for the dispersive case for $\kappa = 0.1$, implies that the large hopping regime yields better behaviour in lossy systems, since it involves faster dynamics.

In the next section we will calculate exactly what is the effect of losses on implementing the required entangling non-local gates through this mechanism. This will be done within the description of the implementation of Deutch-Josza algorithm in this system.

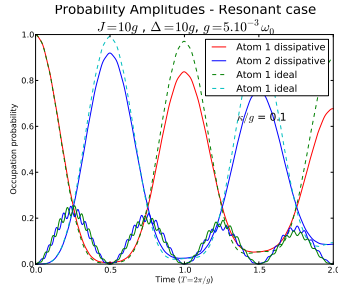


Figure 4.5: Resonant case with $\kappa = 0.1g$

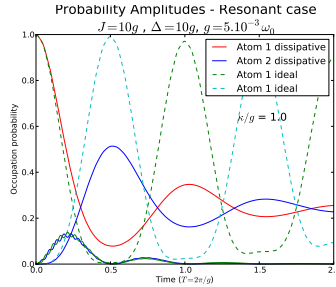


Figure 4.6: Resonant case with $\kappa = g$

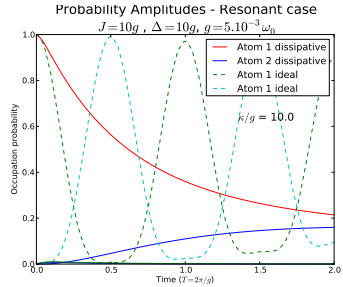


Figure 4.7: Resonant case with $\kappa = 10g$

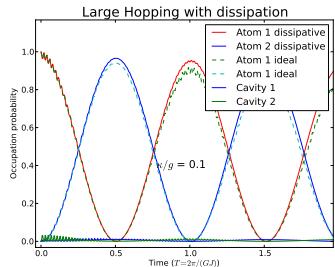


Figure 4.8: Large hopping case with $\kappa = 0.1g$

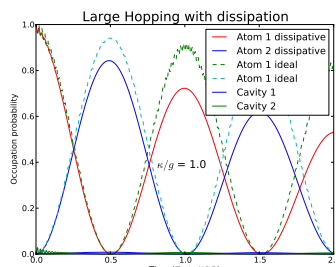


Figure 4.9: Large hopping case with $\kappa = 1g$

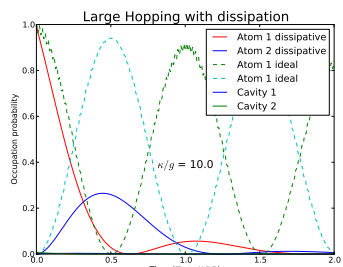


Figure 4.10: Large hopping case with $\kappa = 10g$

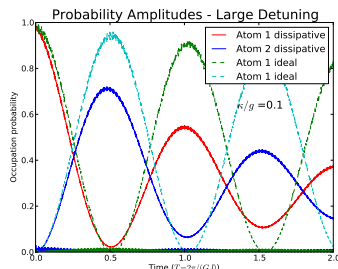


Figure 4.11: Dispersive case with $\kappa = 0.1g$

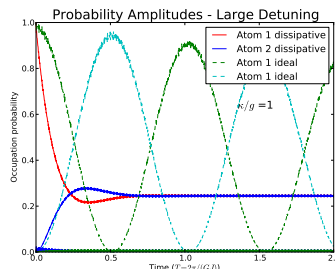


Figure 4.12: Dispersive case with $\kappa = 1g$

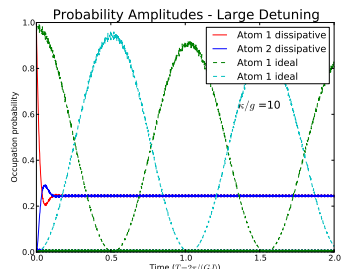


Figure 4.13: Dispersive case with $\kappa = 10g$

4.4 A proposal for Deutsch-Jozsa algorithm in a two cavity system

In the previous section we derived both analytically and numerically the quantum dynamics of a system of coupled cavities interacting with fixed atoms both in the dissipative and in the ideal case. It's worth mentioning, that this specific setup could be realized using photonic crystals doped with quantum dots and circuit

QED[106, 111].

In order to examine how efficiently this mechanism could be used in order to realize a CNOT gate, which is performed by non-local interactions like the one of our case, we will estimate the fidelity of the system [16], for each of the cases, supposing there is no spontaneous emission rate in our system:

$$F(\rho_{ideal}, \rho_{dissipative}) = Tr \left[\sqrt{\sqrt{\rho_{id}} \rho_{dis} \sqrt{\rho_{id}}} \right] \quad (4.40)$$

From our previous discussion, we know that our system can implement a *SWAP* gate. Though, \sqrt{SWAP} gate which is realized when we choose the time to be equal to $T/4$ is a universal two qubit gate[112]. In figure 4.14, we show how the CNOT gate can be obtained using \sqrt{SWAP} gates and local pulses. In order to implement the algorithm we also need a single qubit gate, realizable in the present setup. In order to implement the X gate, we choose a π pulse from an external classical source tuned with the atom frequency ω_0 , while for the Hadamard gate we use a $\pi/2$ pulse from a classical source. In the following we assume those operations can be perfectly performed, since they are fast local operations realized by controlled external sources tuned to the desirable Rabi frequencies.

The transformation of \sqrt{SWAP} gate to CNOT that allows the algorithm, is shown in figure 4.14 Using the matrix representation of \sqrt{SWAP}

$$\sqrt{SWAP} = \begin{pmatrix} 1 & 0 & 0 & 0 \\ 0 & \frac{1}{2} + \frac{i}{2} & \frac{1}{2} - \frac{i}{2} & 0 \\ 0 & \frac{1}{2} - \frac{i}{2} & \frac{1}{2} + \frac{i}{2} & 0 \\ 0 & 0 & 0 & 1 \end{pmatrix}, \quad (4.41)$$

as well as the ones for the X,H, gates

$$X = \begin{pmatrix} 0 & 1 \\ 1 & 0 \end{pmatrix} \quad H = \frac{1}{\sqrt{2}} \begin{pmatrix} 1 & 1 \\ 1 & -1 \end{pmatrix} \quad (4.42)$$

We can verify that the circuit of 4.14, is indeed equivalent to a CNOT gate. Therefore, the circuit that implements the algorithm is the one in 4.15. Regarding the readout of the process, it can be experimentally realised using the shelving technique [113] that provides reliable readouts. As we saw in the previous section, in the large hopping and dispersive cases, the system remains coherent for relatively longer times which indicates that even in the presence of strong dissipation (equal to the coupling rate), one could implement the required non-local gate at least a few times before the system eventually decoheres.

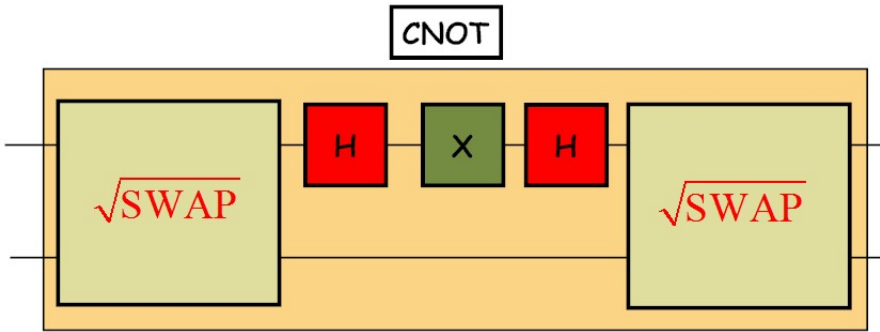


Figure 4.14: Quantum circuit representing the operations required in order to obtain the CNOT gate using \sqrt{SWAP} gate.

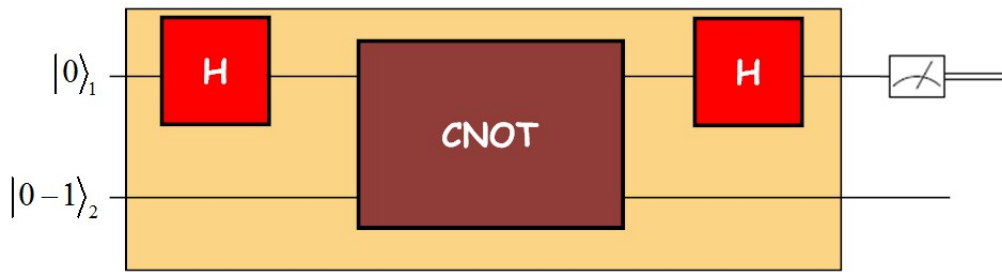


Figure 4.15: Representation of the quantum circuit for the Deutsch-Jozsa algorithm.

In order to calculate the fidelity of the \sqrt{SWAP} for each regime, we will have to define the desirable time interval that the interaction is on, ie. the $1/4$ of the period of each case and evolve the lossy case in order to obtain $\rho_{dissipative}(T/4)$ using the Master Equation of equation 4.35. The ideal case will yield a density matrix $\rho_{ideal}(T/4)$, which in our case is the density matrix of the maximally entangled state $\frac{|eg00\rangle - |ge00\rangle}{\sqrt{2}}$. Therefore the required times in the parameter regimes we are assuming, are:

$$\begin{aligned} T_{LH}/4 &= \pi J/2(g^2) \\ T_{disp}/4 &= \pi \Delta^2/2g^2J \\ T_R/4 &= \pi/2g \end{aligned} \quad (4.43)$$

The numerical calculations for the fidelity of the \sqrt{SWAP} gate using the appropriate times , allow us to plot the dependence of the fidelity versus κ rate, which is plotted in 4.16.

We observe that the fidelity in the resonant case falls rapidly as κ increases, which is justified by the stronger dissipation occurring in the resonant regime due to the existence of population in the cavity modes. We would expect the dispersive case to sustain higher fidelity values, though, watching closer we see

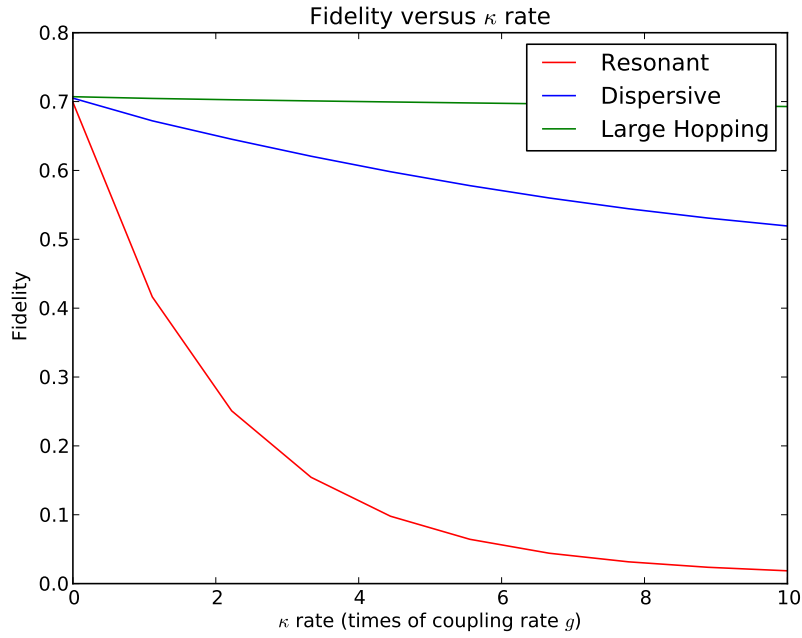


Figure 4.16: Fidelity of \sqrt{SWAP} gate versus κ , with κ expressed using coupling rate g of the cavities for the dispersive case (blue line $g = 5.10^{-3}\omega_0$, $J = 2/5g$, $\Delta = 10g$, $T_{disp}/4 = \pi\Delta^2/2g^2J$), resonant case (red line, $g = 5.10^{-3}\omega_0$, $J = 10g$, $\Delta = 10g$, $T_R/4 = \pi/2g$) and large hopping case (green line $g = 5 \times 10^{-3}\omega_0$, $J = 10g$, $\Delta = 0.1g$, $T_{LH}/4 = \pi J/2(g^2)$).

that the time required for the \sqrt{SWAP} gate in the dispersive case is much larger than the large hopping case ($T_{disp} \simeq 10T_{LH}$). This means that the system in the latter case is exposed to environment for smaller times, thus the highest fidelity values.

Chapter 5

Conclusions and Future work

In this thesis we made a detailed overview of the most important theoretical aspects of cavity QED focusing on the region of microwave QED. As we have seen throughout the text, it is possible using the basic principles that apply on single Cavity QED, to extend our discussion on other setups involving arrays of coupled resonators.

We initially discussed analytically how single cavity systems can be used in different ways in the implementation of Quantum Information Algorithms and reviewed some of the early results in the field.

We then dealt analytically and numerically with the model of two identical coupled cavities both in the ideal case of zero κ, γ and in the dissipative case. We proved that this configuration can be used in order to implement a Quantum Phase Gate, while we gave an outline of how Deutsch-Jozsa algorithm could be performed.

Cavity QED ideas have recently been extended in other experimental realizations, such as Circuit QED. The latter we plan to explore in more detail in future studies.

We would like to note that numerical simulations of Open Quantum Systems, an important aspect of this thesis, will provide the background for our future work in the direction of modelling specific experimental setups. We would like to study how constant driving the atoms or the field, effects the steady state observables and explore the possibility for robust QIP there. We will also explore different platforms including waveguide arrays and specific Circuit QED implementations.

Appendix A

1 Useful packages for Quantum Optics

One of the most important aspects of this thesis, was gaining a more extensive and thorough approach regarding numerical tasks. It might be easier to use programs like *Mathematica* and indeed *Mathematica* was really useful throughout all this thesis.

During the past few years, there has been a magnificent progress in programming and the way the new generation of programmers work, thus giving rise to *Open Source Software*. Apart from commercial packages like *Mathematica* or *MatLab* there has been developed a variety of open source tools that are widely used. In order to use a reliable and tested package that is focused in Quantum Optics, we used **QuTiP**[114] which is a *toolbox* of frequently used routines that uses *Python* programming language. In what follows we will give some programming details that we consider worth mentioning.

2 Details on Mathematica code

The ability of various mathematical packages to efficiently perform numerical calculations, combined with the flexibility of Quantum Mechanics to express operators and vector states in matrix expressions, makes it quite easy for one to investigate complex setups, like coupled cavity arrays. We will describe the more important steps of the process we followed, defining numerically the physical system of two coupled cavities with fixed atoms, which may prove really time consuming if someone has not an insight on the internal doings of various packages.

Mathematica has difficulty handling matrices that are defined as normal arrays and contain lots of zeros. Thus, we will use the following commands to define the basis vectors and one of creation/annihilation operators.

First of all, we need to set a basis of vectors on which we are going to perform our operations. In this procedure we performed a general case scenario, rather

than just restricting ourselves to the one-excitation case, in order to have a more versatile form for future work:

```
Basis[n_, i_]:=Normal[SparseArray[{i+1, 1}→1, {n, 1}]];
e=Basis[2, 1]; g=Basis[2, 0];
f[n_]:=Basis[Ne+1, n-1];
sigmap=e.gT; sigmam=g.eT; sigmaz=e.eT-g.gT;
Destroy[n_]:=SparseArray[{Band[{1, 2}]\rightarrow Sqrt[Range[n-1]]}, {n, n}];
Id[n_]:=IdentityMatrix[n];
(1)
```

In those lines we defined a function $Basis[n_, i_]$ that will be able to create the basis vectors for an n dimensional space. Making use of it we defined the atom states $|e\rangle$ and $|g\rangle$. This direct way of defining vector states for two level atoms, cannot be kept for the cavity states for higher values of the excitation number (N_e), so we defined with another way ($f[n_]$) the cavity state vectors to keep things more general. The definition of the $\hat{\sigma}_+, \hat{\sigma}_-$ and $\hat{\sigma}_3$ atomic operators is followed by the annihilation operator \hat{a} , whereas we used a shorter way for the *Identity Matrix* command of *Mathematica*.

This is all we need to numerically investigate the problem. In order to define all operators and states, we make use of the command **KroneckerProduct** which is the way of handling the four different spaces involved in this procedure. For example the state $|gg10\rangle$ will be written as

```
gg10=KroneckerProduct[g, g, f[2], f[1]];
```

The operator $\hat{\sigma}_{+,2}$ will be declared as:

```
sp2=KroneckerProduct[Id[2], sigmap, Id[Ne+1], Id[Ne+1]];
```

which clearly states that the action of the operator is confined on the subspace of **Atom 2**.

Keeping in mind those basic principles, we are able to set up a Hamiltonian and then defining some initial state, use the **Expm[...]** command to study the time evolution of the system by applying the unitary operator.

3 Python code used for plots.

The dynamical study of the systems discussed throughout the text, was initially done in Mathematica and later was verified using the Python programming language. In the following pages, we present some of the scripts used during this thesis.

Jaynes Cummings model with dissipation using master equation or quantum trajectories

```
# -*- coding: utf-8 -*-

#
# Vacuum Rabi oscillations in the Jaynes-Cummings model with dissipation
#
from qutip import *
from pylab import *

def run():

    # Configure parameters
    wc = 10000 # cavity frequency
    wa = 10000 # atom frequency
    g = 0.001*wc # coupling strength
    kappa = 0.2*g # cavity dissipation rate
    gamma = 0 # atom dissipation rate
    N = 2 # for two possible states of the field
    use_rwa = True

    # initial state for the system cavity-atom
    psi0 = tensor(basis(N,0), basis(2,1)) # start with an excited atom

    # Hamiltonian operators
    a = tensor(destroy(N), qeye(2))
    sm = tensor(qeye(N), destroy(2))

    if use_rwa:
        # use the rotating wave approximation
        H = wc * a.dag() * a + wa * sm.dag() * sm + g * (a.dag() * sm + a * sm.dag())
    else:
        H = wc * a.dag() * a + wa * sm.dag() * sm + g * (a.dag() + a) * (sm + sm.dag())

    # collapse operators for non-unitary dynamics
    c_op_list = []

    n_th_a = 0.0 # zero temperature
    rate = kappa * (1 + n_th_a)
    if rate > 0.0:
        c_op_list.append(sqrt(rate) * a)

    rate = kappa * n_th_a
    if rate > 0.0:
        c_op_list.append(sqrt(rate) * a.dag())

    rate = gamma
    if rate > 0.0:
        c_op_list.append(sqrt(rate) * sm)

    # evolve and calculate expectation values
    tlist = linspace(0,5*pi/g,1000)
```

```
output = mesolve(H, psi0, tlist, c_op_list, [a.dag() * a, sm.dag() * sm])

# plot the results
plot(tlist/(g*pi), output.expect[0])
plot(tlist/(g*pi), output.expect[1])
legend(("Cavity", "Atom_excited_state"))
xlabel('Time')
ylabel('Occupation_probability')
title('Vacuum_Rabi_oscillations_for_a_damped_cavity_using_master_equation')
show()

if __name__=='__main__':
    run()
```

Two coupled cavities without dissipation for large hopping case.

```

from qutip import *
from pylab import *

def run():

    # Define constants
    G = 5
    omega_atom = 1000
    detuning = 0.1*G
    omega_field = omega_atom + detuning
    J = 10*G
    N = 2 # number of possible states for cavity 1

    # Define basis. In total we have 4 Hilbert space dimensions to describe the system.
    #
    # choose an order for composite system: A1-A2-C1-C2
    # then compute the operators for the full Hilbert space and use them to
    # construct the hamiltonian.
    #

    # cavity operators in full hilbert space
    a1 = tensor([qeye(2), qeye(2), destroy(N), qeye(N)])
    a2 = tensor([qeye(2), qeye(2), qeye(N), destroy(N)])

    # atomic operators in full hilbert space C1-A1-C2-A2
    e=basis(2,0)
    g=basis(2,1)
    f1=basis(N,0)
    f2=basis(N,1)

    e1e = tensor([e.dag(), qeye(2), qeye(N), qeye(N)])
    e2e = tensor([qeye(2), e.dag(), qeye(N), qeye(N)])
    sp1 = tensor([sigmap(), qeye(2), qeye(N), qeye(N)])
    sm1 = tensor([sigmam(), qeye(2), qeye(N), qeye(N)])
    sp2 = tensor([qeye(2), sigmap(), qeye(N), qeye(N)])
    sm2 = tensor([qeye(2), sigmam(), qeye(N), qeye(N)])

    # Write the Hamiltonians in 4 separate terms to avoid mistakes.
    H1 = omega_atom * (e1e + e2e)
    H2 = omega_field * (a1.dag()*a1 + a2.dag()*a2)
    H3 = G * (a1 * sp1 + a1.dag() * sm1) + G * (a2 * sp2 + a2.dag() * sm2)
    H4 = J * (a1.dag() * a2 + a1 * a2.dag())

    H = H1 + H2 + H3 + H4

    #Time evolution of the system
    gg01 = tensor([g, g, f1, f2])
    gg10 = tensor([g, g, f2, f1])
    eg00 = tensor([e, g, f1, f1])
    ge00 = tensor([g, e, f1, f1])

    psi0=eg00 #initially excitation in atom 1

    # evolve and calculate expectation values
    Gkap=abs(G**2/((detuning + J)*(detuning - J)))
    T=pi/(Gkap*J)
    tlist = linspace(0,T,1000)
    output = mesolve(H, psi0, tlist, [], [])

```

```
# plot the results
plot(tlist/T, expect(a1.dag()*a1, output.states))
plot(tlist/T, expect(s1.dag() * s1, output.states))
plot(tlist/T, expect(a2.dag()*a2, output.states))
plot(tlist/T, expect(s2.dag() * s2, output.states))

legend(("Cavity_1", "Atom_1","Cavity_2", "Atom_2"))
xlabel('Time_scaled_by_period$\mathcal{T}=2\pi/G_J$')
ylabel('Probability')
title('Probability_amplitudes_for_the_large_hopping_case:$\Delta=0.1g,\omega_0=1000,g=5\times10^{-3}\omega_0,J=10g$')
show()

if __name__=='__main__':
    run()
```

Fidelity versus κ for large hopping

```

# Calculate the fidelity of a system of two coupled cavities under dissipation
from qutip import *
from pylab import *

#collapse operators for non-unitary dynamics

def rho_compute(Ham,psi0,tlist,kappa_max,kappalist, cav1, cav2,rho_ideal):

    #fid_list=zeros((len(kappalist)))
    rho_dis_list= []
    index=0
    for kappa in kappalist:
        c_op_list = []
        c_op_list.append(sqrt(kappa) * cav1)
        c_op_list.append(sqrt(kappa) * cav2)
        dissipative = mesolve(Ham, psi0, tlist, c_op_list, [])
        rho_dissipative = dissipative.states
        rho_dissipative_final=rho_dissipative[-1]
        rho_dis_list.append(rho_dissipative_final)
        index +=1
    return rho_dis_list

# Define constants
G=5
omega_atom = 1000
detuning = 0.1*G
omega_field = omega_atom - detuning
J = 10*G
kappa_max = 10*G # cavity dissipation rate
kappalist = linspace(0,kappa_max,10)
gamma = 0.0 # atom dissipation rate

N = 1 # number of excitations

# cavity operators in full hilbert space
a1 = tensor([qeye(2), qeye(2), destroy(N+1), qeye(N+1)])
a2 = tensor([qeye(2), qeye(2), qeye(N+1), destroy(N+1)])

# atomic operators in full hilbert space C1-A1-C2-A2
e=basis(2,0)
g=basis(2,1)
f1=basis(N+1,0)
#f2=basis(N+1,1)
eg00=tensor(e,g,f1,f1)
ge00=tensor(g,e,f1,f1)

e1e = tensor([e*dag(e), qeye(2), qeye(N+1), qeye(N+1)])
e2e = tensor([qeye(2), e*dag(e), qeye(N+1), qeye(N+1)])
g1g = tensor([g*dag(g), qeye(2), qeye(N+1), qeye(N+1)])
g2g = tensor([qeye(2), g*dag(g), qeye(N+1), qeye(N+1)])
s1 = tensor([sigmap(), qeye(2), qeye(N+1), qeye(N+1)])
s1m = tensor([sigmam(), qeye(2), qeye(N+1), qeye(N+1)])
s2 = tensor([qeye(2), sigmap(), qeye(N+1), qeye(N+1)])
s2m = tensor([qeye(2), sigmam(), qeye(N+1), qeye(N+1)])
s1z = tensor([sigmaz(), qeye(2), qeye(N+1), qeye(N+1)])
s2z = tensor([qeye(2), sigmaz(), qeye(N+1), qeye(N+1)])

```

```

# Define the Hamiltonian terms
H1 = omega_atom * (e1e + e2e)
H2 = omega_field * (a1.dag()*a1 + a2.dag()*a2)
H3 = G * (a1 * sp1 + a1.dag() * sm1) + G * (a2 * sp2 + a2.dag() * sm2)
H4 = J * (a1.dag() * a2 + a1 * a2.dag())
H = H1 + H2 + H3 + H4

psi0 = tensor([e, g, f1, f1])

#Set the time interval for the evolution of the system
Gkap=abs(G**2/((detuning + J)*(detuning - J)))
T=pi/(Gkap*J)
tlist = linspace(0,T/4,500)

#Calculate the density matrix for the ideal case
ideal=(eg00-ge00)/sqrt(2)
#psi_ideal_list = ideal.states
#psi_ideal=psi_ideal_list[-1]
rho_ideal = ket2dm(ideal)
#n1_ideal= expect(sm1.dag() * sm1,ideal.states)
#n2_ideal= expect(sm2.dag() * sm2,ideal.states)
#pf1_ideal = expect(a1.dag() * a1, ideal.states)
#pf2_ideal = expect(a2.dag() * a2, ideal.states)

#Use the rho_compute function to calculate the density operators at t=T
rho_list=rho_compute(H,psi0,tlist,kappa_max,kappalist,a1,a2,rho_ideal)
flist=[]
for i in range (0,10):
    flist.append(fidelity(rho_ideal,rho_list[i]))
output_data = vstack((kappalist/G, flist))
file_data_store('large_hopping.dat', output_data.T, numtype="real")

plot(kappalist,flist)
show()

```

Appendix B. Theoretical tools for cavity QED

1 Review of the harmonic oscillator

In the following pages we review the basic notions of quantum harmonic oscillator and build on it according to [3], [4], [5], presenting the main techniques used throughout the text and refer to quantum harmonic oscillator.

In classical mechanics, a particle of mass m moving in the potential $V(x) = \kappa x^2$ oscillates at a frequency $\omega = \sqrt{\frac{\kappa}{m}}$, where κ is the force constant. The Hamiltonian for this one-dimensional harmonic oscillator consists of two discrete terms referring to kinetic and potential energy, therefore we can write

$$H = T + V = \frac{p_x^2}{2m} + \frac{m\omega^2}{2}x^2 \quad (1)$$

where the x-directed particle momentum p_x is defined by the relation $m\frac{dx}{dt}$. In quantum mechanics, the classical momentum is replaced by the operator $\hat{p}_x = -i\hbar\frac{\partial}{\partial x}$, therefore the Hamiltonian becomes

$$\hat{H} = \frac{\hat{p}_x^2}{2m} + \frac{m\omega^2}{2}\hat{x}^2 \quad (2)$$

From a pure algebraic point of view one may observe that in this equation we have the two operators appearing as simple squares, which suggests that we may factor the equation so that it is linear in terms of \hat{p}_x and \hat{x} . With this in mind, we define two new operators:

$$\hat{a} = \sqrt{\frac{m\omega}{2\hbar}} \left(\hat{x} + \frac{i\hat{p}_x}{m\omega} \right) \quad (3)$$

$$\hat{a}^\dagger = \sqrt{\frac{m\omega}{2\hbar}} \left(\hat{x} - \frac{i\hat{p}_x}{m\omega} \right) \quad (4)$$

The set of equations 3 and 4 describes the so-called *creation and annihilation* operators of the harmonic oscillator. The inverse set of relations expressing the position \hat{x} and momentum \hat{p}_x operators in terms of the creation and annihilation operators can be expressed as

$$\hat{x} = \sqrt{\frac{\hbar}{2m\omega}} (\hat{a} + \hat{a}^\dagger) \quad (5)$$

$$\hat{p}_x = \sqrt{\frac{\hbar}{2m\omega}} (\hat{a} - \hat{a}^\dagger) \quad (6)$$

$$(7)$$

The Hamiltonian described by Equation 2 expressed using the creation and annihilation operators is

$$\hat{H} = \frac{\hbar\omega}{2} (\hat{a}\hat{a}^\dagger + \hat{a}^\dagger\hat{a}) \quad (8)$$

and it is straight-forward to show that the commutation relation between the creation and annihilation operators is $[\hat{a}, \hat{a}^\dagger] = 1$. where we use the commutation relation $[\hat{p}_x, \hat{x}] = -i\hbar$. Using this commutation relation we are capable of rewriting the equation 8 as

$$\hat{H} = \frac{\hbar\omega}{2} (\hat{a}\hat{a}^\dagger + \hat{a}^\dagger\hat{a}) = \frac{\hbar\omega}{2} (\hat{a}\hat{a}^\dagger - \hat{a}\hat{a}^\dagger + 2\hat{a}^\dagger\hat{a}) = \frac{\hbar\omega}{2} (1 + 2\hat{a}^\dagger\hat{a}) \quad (9)$$

It is important at this point to write explicitly how the creation and annihilation operators can be used in terms of matrices, since this is a very important procedure when one needs to perform numerical simulations using programming languages.

First of all we need to specify that the eigenstates $\psi_n = |n\rangle$ of the harmonic oscillator are orthonormal, which is expressed by the relation

$$\langle n' | n \rangle = \delta_{n',n} \quad (10)$$

In this notation $\langle n' | \hat{a}^\dagger | n \rangle$ is a matrix element. One may show that these matrix elements are non-zero when they involve adjacent states of the harmonic oscillator, so that

$$\langle n' | \hat{a}^\dagger | n \rangle = \sqrt{n+1} \delta_{n'=n+1} \quad (11)$$

$$\langle n' | \hat{a} | n \rangle = \sqrt{n} \delta_{n'=n-1} \quad (12)$$

If we write all the matrix elements for the different states of the harmonic oscillator with N states, we obtain a matrix of the form

$$a = \begin{pmatrix} 0 & \sqrt{1} & 0 & 0 & 0 \\ 0 & 0 & \sqrt{2} & 0 & 0 \\ 0 & 0 & 0 & \ddots & \vdots \\ \vdots & 0 & 0 & \ddots & \sqrt{N-1} \\ 0 & 0 & 0 & 0 & 0 \end{pmatrix} \quad (13)$$

$$a^\dagger = \begin{pmatrix} 0 & 0 & 0 & 0 & 0 \\ \sqrt{1} & 0 & 0 & 0 & 0 \\ \vdots & \sqrt{2} & 0 & \ddots & \vdots \\ \vdots & 0 & \ddots & \ddots & \vdots \\ 0 & 0 & 0 & \sqrt{N-1} & 0 \end{pmatrix} \quad (14)$$

As it was expected, the matrix representations of creation and annihilation operators are transpose, which actually allows us to define only one of those matrices in our numerical applications. For example if we would like to define the annihilation matrix in *Mathematica* we can use the command:

```
Destroy[n_] := SparseArray[{Band[{1, 2}] → Sqrt[Range[n-1]]}, {n, n}]
```

In fact, this way of defining matrices with lots of zeros in *Mathematica*, is the most effective in terms of computational resources as suggested in [115].

Returning to the commutator algebra of the harmonic oscillator, we should point out the need to define one more operator that appears in the whole spectrum of the problems that are dealt in this context. Of course, we refer to the *number operator*, which is defined by the relation

$$\hat{N} = \hat{a}^\dagger \hat{a} \quad (15)$$

For the number operator, we can easily show the commutation relations for \hat{a} and \hat{a}^\dagger

$$[\hat{N}, \hat{a}] = -\hat{a} \quad (16)$$

$$[\hat{N}, \hat{a}^\dagger] = -\hat{a}^\dagger \quad (17)$$

The problem of the harmonic oscillator has only one obvious limitation. This limitation concerns the fact that there is one ground state of energy with a wavefunction that describes it. We will describe the procedure of calculating this ground state energy and the corresponding wave-function, in order to explain what exactly the creation and annihilation operators help us with.

To derive the ground state wave-function and energy of the one-dimensional quantum harmonic oscillator, we should start using the Scrödinger equation:

$$\hat{H}\psi_n = \hbar\omega \left(\hat{a}^\dagger \hat{a} + \frac{1}{2} \right) \psi_n = E_n \psi_n \quad (18)$$

Multiplying from the left by \hat{a} we obtain

$$\hbar\omega \left(\hat{a}^\dagger \hat{a} + \frac{\hat{a}}{2} \right) \psi_n = E_n \hat{a} \psi_n \quad (19)$$

and taking under consideration the commutation relation

$$[\hat{a}^\dagger, \hat{a}] = 1 \Leftrightarrow \hat{a} \hat{a}^\dagger = \hat{a}^\dagger \hat{a} + 1 \quad (20)$$

we obtain the equation

$$\hbar\omega \left((1 + \hat{a} \hat{a}^\dagger) \hat{a} + \frac{\hat{a}}{2} \right) \psi_n = E_n \hat{a} \psi_n \quad (21)$$

Factoring out the term $\hat{a} \psi_n$ on the left-hand side of the previous equation we find that

$$\hbar\omega \left((1 + \hat{a} \hat{a}^\dagger) + \frac{1}{2} \right) (\hat{a} \psi_n) = E_n (\hat{a} \psi_n) \quad (22)$$

The term $\hbar\omega \hat{a} \psi_n$ can be subtracted from both sides, allowing us to write the equations:

$$\hbar\omega \left(\hat{a}^\dagger \hat{a} + \frac{1}{2} \right) (\hat{a} \psi_n) = (E_n - \hbar\omega) (\hat{a} \psi_n) \quad (23)$$

$$\hbar\omega \left(\hat{a}^\dagger \hat{a} + \frac{1}{2} \right) \psi_{n-1} = E_{n-1} \psi_{n-1} \quad (24)$$

This last equation shows that $\psi_{n-1} = \hat{a} \psi_n$ is a new eigenfunction with energy eigenvalue $(E_n - \hbar\omega)$. In a similar way it may be proved that the operator \hat{a}^\dagger acting on eigenfunction ψ_n creates a new eigenfunction ψ_{n+1} with eigenenergy $(E_n + \hbar\omega)$. In bibliography it is quite common to refer to creation and annihilation operators as "raising" and "lowering" operators, since as it is obvious the harmonic oscillator eigenfunctions and eigenenergies could be visualised by a *ladder* in which those operators decide whether we should move higher or lower gaining the respective eigenfunctions and eigenenergies.

It must be clear up to this point that the lowering (annihilation) operator, \hat{a} can only be used to reduce the energy eigenvalue of any eigenstate. We assume

the existence of a "ground state" in which we have the lower possible energy. This obliges us to state that the *lowering operator* acting on this state gives

$$\hat{a}\psi_0 = 0 \quad (25)$$

At this point we know everything we need to calculate the wave-function for the ground state. Since

$$\hat{a} = \sqrt{\frac{m\omega}{2\hbar}} \left(\hat{x} + \frac{i\hat{p}_x}{m\omega} \right) = \sqrt{\frac{m\omega}{2\hbar}} \left(\hat{x} + \frac{\hbar}{m\omega} \frac{\partial}{\partial x} \right) \quad (26)$$

our definition of $\hat{a}\psi_0 = 0$ requires

$$\sqrt{\frac{m\omega}{2\hbar}} \left(\hat{x} + \frac{\hbar}{m\omega} \frac{\partial}{\partial x} \right) \psi_0 = 0 \quad (27)$$

The solution for the wave function is of Gaussian form

$$\psi_0 = A_0 e^{-\frac{x^2 m\omega}{2\hbar}} \quad (28)$$

where the normalization constant A_0 is found by the normalization requirement $\langle \psi_0 | \psi_0 \rangle = 1$ to be

$$A_0 = \sqrt[4]{\frac{m\omega}{\pi\hbar}} \quad (29)$$

In order to calculate the eigenenergy for the ground state wave function ψ_0 the only thing that remains to be done is inserting the equation 28 into the Schrödinger equation 18 for the 1-D harmonic oscillator. Schrödinger equation reads:

$$\left(-\frac{\hbar^2}{2m} \frac{d^2}{dx^2} + \frac{m\omega^2}{2} x^2 \right) \psi_0 = \left(\frac{-\hbar^2}{2m} \left(\frac{2m\omega}{\hbar} + 4x^2 \left(\frac{m\omega}{2\hbar} \right)^2 \right) + \frac{m\omega^2}{2} x^2 \right) \psi_0 \quad (30)$$

$$\left(\frac{\hbar\omega}{2} - \frac{m\omega^2}{2} x^2 + \frac{m\omega^2}{2} x^2 \right) \psi_0 = E_0 \psi_0 \quad (31)$$

so that the value of the ground state energy, E_0 is

$$E_0 = \frac{\hbar\omega}{2} \quad (32)$$

The non-ground states of the harmonic oscillator are called *excited states*. Starting from the ground state, we can construct the excited states by acting on the ground state the creation operator. For the first excited state we multiply the ground state of the harmonic oscillator by \hat{a}^\dagger in the Schrödinger equation:

$$\hat{a}^\dagger \hbar\omega \left(\hat{a}^\dagger \hat{a} + \frac{1}{2} \right) \psi_n = \hat{a}^\dagger E_n \psi_n = \hat{a}^\dagger \hat{H} \psi_n \quad (33)$$

$$\hbar\omega \left(\hat{a}^\dagger \hat{a}^\dagger \hat{a} + \frac{\hat{a}^\dagger}{2} \right) \psi_n = E_n \hat{a}^\dagger \psi_n = \hat{a}^\dagger \hat{H} \psi_n \quad (34)$$

With the use of the commutation relation $[\hat{a}, \hat{a}^\dagger] = 1$, and some algebra we show that:

$$\hbar\omega \left(\hat{a}^\dagger (\hat{a}\hat{a}^\dagger - 1) + \frac{\hat{a}^\dagger}{2} \right) \psi_n = \left(\hbar\omega (\hat{a}^\dagger \hat{a}\hat{a}^\dagger - \hat{a}^\dagger) + \frac{\hat{a}^\dagger}{2} \right) \psi_n = E_n \hat{a}^\dagger \psi_n \quad (35)$$

$$\hbar\omega \left((\hat{a}\hat{a}^\dagger - 1) \hat{a}^\dagger + \frac{\hat{a}^\dagger}{2} \right) \psi_n = \left(\hbar\omega (\hat{a}^\dagger \hat{a} - 1) + \frac{1}{2} \right) \hat{a}^\dagger \psi_n = E_n \hat{a}^\dagger \psi_n \quad (36)$$

$$\hbar\omega \left(\hat{a}^\dagger \hat{a} + \frac{1}{2} \right) (\hat{a}^\dagger \psi_n) = (E_n + \hbar\omega) (\hat{a}^\dagger \psi_n) \quad (37)$$

It is clear now that the eigenenergy of the n-th state of the 1-D harmonic oscillator is given by the equation

$$E_n = \hbar\omega \left(n + \frac{1}{2} \right) \quad (38)$$

where it is obvious that we have used the number operator in order to obtain the eigenvalues of the term $\hat{a}^\dagger \hat{a} = \hat{N}$ and therefore the eigenenergy of the n-th level. So far we have showed that the operators \hat{a} and \hat{a}^{dag} act upon the state ψ_n , in such a way that:

$$\hat{a}\psi_n = A_{n+1}\psi_{n+1} \quad (39)$$

$$\hat{a}^\dagger \psi_n = A_{n-1}\psi_{n-1} \quad (40)$$

The normalization constants are calculated by using the statements that $\langle n|n\rangle = \langle n-1|n-1\rangle = 1$ and $[\hat{a}, \hat{a}^{dag}] = 1$. Since the state $\hat{a}\psi_n = |n+1\rangle$ is also required to be normalized, we may write:

$$|A_{n+1}|^2 \langle \hat{a}^\dagger n | \hat{a}^\dagger n \rangle = 1 \quad (41)$$

Equation 41 may be written as:

$$|A_{n+1}|^2 \langle \hat{a} | \hat{a}^\dagger \rangle = |A_{n+1}|^2 \langle n | (\hat{a}^\dagger \hat{a} + 1) n \rangle = |A_{n+1}|^2 (n+1) \langle n | n \rangle = 1 \quad (42)$$

Therefore, since we require A_{n+1} to be a real number, the normalization gives us the result

$$A_{n+1} = \frac{1}{\sqrt{n+1}} \quad (43)$$

Therefore we may write that:

$$|n+1\rangle = \frac{1}{\sqrt{n+1}} |\hat{a}^\dagger n\rangle \leftrightarrow |\hat{a}^\dagger n\rangle = \sqrt{n+1} |n+1\rangle \quad (44)$$

In the same way we can prove that

$$|\hat{a}n\rangle = \sqrt{n} |n\rangle \quad (45)$$

It is quite useful to derive an expression such that we may obtain the n-th state $|n\rangle$ using the ground state $|0\rangle$:

$$|n\rangle = \frac{(\hat{a}^\dagger)^n}{\sqrt{(n!)}} |0\rangle \quad (46)$$

and

$$\hat{a}^\dagger |n\rangle = \frac{(\hat{a}^\dagger)^{n+1}}{\sqrt{n!}} |0\rangle = \frac{\sqrt{n+1} (\hat{a}^\dagger)^{n+1}}{\sqrt{(n+1)!}} |0\rangle = \sqrt{(n+1)} |n\rangle \quad (47)$$

Regarding the form of the wave functions of the n-th level of the harmonic oscillator, we will follow a similar treatment, acting the creation operator \hat{a} on the ψ_0 wave-function of the ground state that was obtained in 28. In order to simplify the notation, we will introduce a new spatial variable,

$$\xi = \sqrt[4]{\left(\frac{m\omega}{\pi\hbar}\right)} x \quad (48)$$

With the use of this new spatial variable we can rewrite the expression for the creation operator in terms of ξ as:

$$\hat{a}^\dagger = \frac{1}{\sqrt{2}} \left[\sqrt{\left(\frac{m\omega}{\hbar}\right)} x - \sqrt{\left(\frac{\hbar}{m\omega}\right)} \frac{\partial}{\partial x} \right] = \frac{1}{\sqrt{2}} \left(\xi - \frac{\partial}{\partial \xi} \right) \quad (49)$$

so, the expression of equation 28,becomes:

$$\psi_0(\xi) = A_0 e^{-\frac{\xi^2}{2}} \quad (50)$$

where the normalization constant now has become:

$$A_0 = \sqrt[4]{\left(\frac{1}{\pi}\right)} \quad (51)$$

Starting from the ground state and using the equation 46 to ensure that our result is normalized, we obtain a sequence of wave-functions:

$$\psi_0 \quad (52)$$

$$\psi_1 = \hat{a}^\dagger \psi_0 \quad (53)$$

$$\psi_2 = \frac{1}{\sqrt{2}} \hat{a}^\dagger \psi_1 = \frac{1}{\sqrt{2}} (\hat{a}^\dagger)^2 \psi_0 \quad (54)$$

$$\psi_3 = \frac{1}{\sqrt{2}} \hat{a}^\dagger \psi_2 = \frac{1}{\sqrt{2}\sqrt{3}} (\hat{a}^\dagger)^2 \psi_1 = \frac{1}{\sqrt{3!}} (\hat{a}^\dagger)^3 \psi_0 \quad (55)$$

$$\psi_n = \frac{1}{\sqrt{n!}} (\hat{a}^\dagger)^n \psi_0 \quad (56)$$

Now, using the expression of the ground state wave function using the spatial variable ξ 50, we will write the explicit expression of the first five states of the harmonic oscillator.

$$\psi_0 = A_0 e^{-\frac{\xi^2}{2}} \quad (57)$$

$$\psi_1 = \hat{a}^\dagger \psi_0 = \frac{1}{\sqrt{1!}} \frac{1}{\sqrt{2}} \left(\xi - \frac{\partial}{\partial \xi} \right) A_0 e^{-\frac{\xi^2}{2}} = \frac{1}{\sqrt{2}} 2\xi A_0 e^{-\frac{\xi^2}{2}} = \frac{1}{\sqrt{2}} 2\xi \psi_0 \quad (58)$$

$$\begin{aligned} \psi_2 = \hat{a}^\dagger \psi_1 &= \frac{1}{\sqrt{2!}} (\hat{a}^\dagger)^2 \psi_0 = \frac{1}{\sqrt{2!}} \frac{1}{\sqrt{2}} \left(\xi - \frac{\partial}{\partial \xi} \right) \frac{1}{\sqrt{2}} 2A_0 e^{-\frac{\xi^2}{2}} = \\ &= \frac{1}{\sqrt{2}} \frac{1}{\sqrt{4}} (4\xi^2 - 2) \psi_0 \end{aligned} \quad (59)$$

$$\begin{aligned} \psi_3 = \hat{a}^\dagger \psi_2 &= \frac{1}{\sqrt{3!}} (\hat{a}^\dagger)^3 \psi_0 = \frac{1}{\sqrt{3!}} \frac{1}{\sqrt{2}} \left(\xi - \frac{\partial}{\partial \xi} \right) \frac{1}{\sqrt{2}} (4\xi^2 - 2) \psi_0 = \\ &= \frac{1}{\sqrt{6}} \frac{1}{\sqrt{8}} (8\xi^3 - 12) \psi_0 \end{aligned} \quad (60)$$

$$\psi_4 = \hat{a}^\dagger \psi_3 = \frac{1}{\sqrt{4!}} (\hat{a}^\dagger)^4 \psi_0 = \frac{1}{\sqrt{24}} \frac{1}{\sqrt{16}} (16\xi^4 - 48\xi^2 + 12) \psi_0 \quad (61)$$

$$\psi_5 = \hat{a}^\dagger \psi_4 = \frac{1}{\sqrt{5!}} (\hat{a}^\dagger)^5 \psi_0 = \frac{1}{\sqrt{120}} \frac{1}{\sqrt{32}} (32\xi^5 - 160\xi^3 + 120\xi) \psi_0 \quad (62)$$

One may easily observe the fact that the functions are alternately even and odd functions, whereas the form of the wavefunctions can be expressed as a function of Hermite polynomials $H_n(\xi)$ so that

$$\psi_n(\xi) = \hat{a}^\dagger \psi_{n-1}(\xi) = \frac{1}{\sqrt{2^n n!}} H_n(\xi) \psi_0(\xi) \quad (63)$$

while the explicit expression for Hermite polynomials is

$$H_n(\xi) = \left(\frac{d^n}{dt^n} e^{-t^2+2t\xi} \right)_{t=0} = (-1)^n e^{\xi^2} \frac{d^n}{d\xi^n} e^{\xi^{-2}} \quad (64)$$

If we wish to write the expression for the wave function of the harmonic oscillator in the original coordinate system, we substitute ξ from equation 48 in equation 50 to obtain:

$$\psi_n(x) = \sqrt{\frac{1}{2^n n!} \sqrt{\frac{m\omega}{\pi\hbar}}} e^{-\frac{m\omega}{2\hbar}x^2} H_n \left(\sqrt{\frac{m\omega}{\hbar}} x \right) \quad (65)$$

Using *Mathematica* we obtain figure 1, in which we plot the first five wavefunctions of the 1D harmonic oscillator and the potential $V = \frac{\xi^2}{2}$

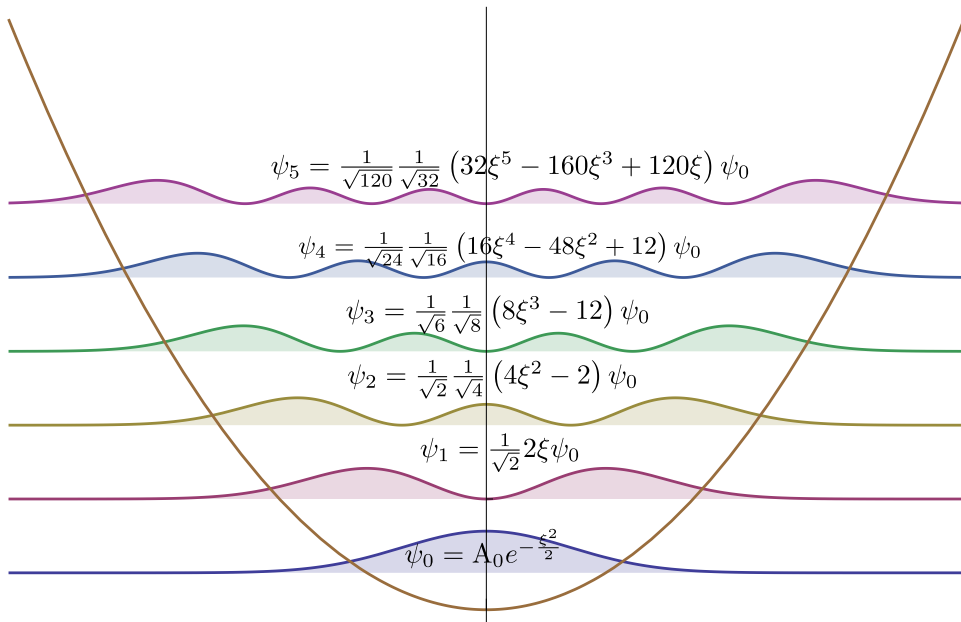


Figure 1: The ten first wave functions of the 1D harmonic oscillator and the potential $V = \frac{\xi^2}{2}$ in the dimensionless units.

2 Schrödinger picture

It is easy to prove that the mean values of an observable \hat{O} do not change under a unitary transformation \hat{U} which changes the basis of the system:

$$\hat{O} \rightarrow \hat{O}' = \hat{U}\hat{O}\hat{U}^\dagger \quad (66)$$

whereas state vectors change as:

$$\begin{aligned} |\psi\rangle &\rightarrow |\psi'\rangle = \hat{U}|\psi\rangle \\ \langle\psi| &\rightarrow \langle\psi'| = \hat{U}^\dagger\langle\psi| \end{aligned} \quad (67)$$

Moving to the basis of vector $|\psi\rangle$ to the basis of $|\psi'\rangle$, is done on the following way:

$$\langle\psi|\hat{O}|\psi\rangle = \langle\psi|\hat{U}^\dagger\hat{U}\hat{O}\hat{U}^\dagger\hat{U}|\psi\rangle = \langle\psi'|\hat{O}'|\psi'\rangle \quad (68)$$

Usually, when we evolve a state we don't follow this very same process. The time evolution of an initial state $|\psi(0)\rangle$ in time is written as:

$$|\psi(t)\rangle = e^{-i\frac{\hat{H}t}{\hbar}}|\psi(0)\rangle \quad (69)$$

This is a direct result of the Schrödinger equation and the observables do not change in time. This actually means, that if for the observable \hat{x} we want to compute the mean value at time t , we need to calculate the quantity:

$$\overline{\hat{x}(t)} = \langle\psi(t)|\hat{x}|\psi(t)\rangle \quad (70)$$

This means that we take \hat{x} as given and use the states at time t and this way of calculating the mean values of the observables is what is included in the *Schrödinger picture*.

We are not able to follow the same process to the unitary transformation $\hat{U}(t)$ that represents time evolution. If we follow the steps described in equations 66,67, we would have got the result

$$\overline{\hat{x}(t)} = \overline{\hat{x}(0)} \quad (71)$$

The above equation states that the mean value of the observable does not change in time, as if the system hasn't evolved at all in time. We usually denote quantities in the Schrödinger picture with the label S , eg $|\psi_S(t)\rangle$, meaning that this is a state in Schrödinger picture where the states, but not the observables evolve in time.

3 Heisenberg picture

Supposing now that there is time evolution not only in the state, but also in the observables, though, in such a way that we get the same result as the one we obtained in *Schrödinger picture* we need to make use of *Heisenberg picture*. Let's denote a state in the Heisenberg picture as $|\psi_H(t)\rangle$. In order to obtain them from a state initially described in Heisenberg picture, we transform it like:

$$|\psi_H(t)\rangle = \hat{S}^\dagger|\psi_S(t)\rangle \quad (72)$$

where

$$\hat{S}^\dagger = e^{i\frac{\hat{H}t}{\hbar}} \quad (73)$$

This expression looks similar to the time-evolution of a state in Schrödinger picture

$$|\psi_S(t)\rangle = e^{-i\frac{\hat{H}t}{\hbar}}|\psi_S(0)\rangle \quad (74)$$

Substituting in the expression for $|\psi_H(t)\rangle$ we obtain:

$$|\psi_H(t)\rangle = \hat{S}^\dagger|\psi_S(t)\rangle = e^{i\frac{\hat{H}t}{\hbar}}|\psi_S(t)\rangle = e^{i\frac{\hat{H}t}{\hbar}}e^{-i\frac{\hat{H}t}{\hbar}}|\psi_S(0)\rangle = |\psi_S(0)\rangle \quad (75)$$

Therefore, the states in the Heisenberg picture at any time t are equal to the states in the Schrödinger picture at initial time $t = 0$.

Supposing now we want to transform an observable \hat{O}_S from the Schrödinger picture to the same one \hat{O}_H in the Heisenberg picture, we would do it using the unitary operator \hat{S}^\dagger as follows:

$$\hat{O}_H = \hat{S}^\dagger\hat{O}_S\hat{S} = e^{i\frac{\hat{H}t}{\hbar}}\hat{O}_S e^{-i\frac{\hat{H}t}{\hbar}} \quad (76)$$

In this way, it is clear that now, even if \hat{O}_S doesn't depend explicitly on time, \hat{O}_H is time-dependent, thus we usually denote it as $\hat{O}_H(t)$.

In order to study the time evolution of $\hat{O}_H(t)$, we calculate its time derivative:

$$\begin{aligned} \frac{d\hat{O}_H(t)}{dt} &= \frac{d}{dt} \left[e^{i\hat{H}t/\hbar} \hat{O}_S e^{-i\hat{H}t/\hbar} \right] = \\ &= \frac{d}{dt} \left[e^{i\hat{H}t/\hbar} \right] \hat{O}_S e^{-i\hat{H}t/\hbar} + e^{i\hat{H}t/\hbar} \hat{O}_S \frac{d}{dt} \left[e^{-i\hat{H}t/\hbar} \right] = \\ &= \frac{i}{\hbar} \hat{H} e^{i\hat{H}t/\hbar} + e^{i\hat{H}t/\hbar} \hat{O}_S \left(-\frac{i}{\hbar} \hat{H} \right) e^{-i\hat{H}t/\hbar} = \\ &= \frac{i}{\hbar} \hat{O}_H(t) - e^{i\hat{H}t/\hbar} \hat{O}_S e^{-i\hat{H}t/\hbar} \left(-\frac{i}{\hbar} \hat{H} \right) = \\ &= \frac{i}{\hbar} \hat{H} \hat{O}_H(t) - \frac{i}{\hbar} \hat{O}_H(t) \hat{H} = \frac{i}{\hbar} [\hat{H}, \hat{O}_H(t)] \Leftrightarrow \\ \frac{d\hat{O}_H(t)}{dt} &= \frac{i}{\hbar} [\hat{H}, \hat{O}_H(t)] \end{aligned} \quad (77)$$

An outstanding exception of operators that are the same in both Heisenberg and Schrödinger pictures, is the Hamiltonian operator \hat{H} . To make this clear, we write:

$$\hat{H}_H(t) = e^{i\hat{H}t/\hbar} \hat{H}_S e^{-i\hat{H}t/\hbar} = e^{i\hat{H}t/\hbar} e^{-i\hat{H}t/\hbar} \hat{H}_S = \hat{H}_S \quad (78)$$

Regarding the expectation values of the observables in those two pictures, we may write:

$$\begin{aligned} \langle \psi_H(t) | \hat{O}_H(t) | \psi_H(t) \rangle &= \langle \psi_S(t) | e^{-i\hat{H}t/\hbar} e^{i\hat{H}t/\hbar} \hat{O}_S e^{-i\hat{H}t/\hbar} e^{i\hat{H}t/\hbar} | \psi_S(t) \rangle = \\ &= \langle \psi_S(t) | \hat{O}_S | \psi_S(t) \rangle \end{aligned} \quad (79)$$

The above expression shows that the expectation values of any observable, are the same in both pictures. A useful process when dealing with time dependent Hamiltonians, is the calculation of the time evolution of the expectation value of an observable.

Supposing we examine the observable \hat{O} and we need to calculate its expectation value, while working in the Schrödinger picture:

$$\overline{\hat{O}(t)} = \langle \psi(t) | \hat{O} | \psi(t) \rangle \quad (80)$$

Taking the time derivative we obtain:

$$\begin{aligned} \frac{d}{dt} \overline{\hat{O}(t)} &= \frac{d}{dt} \left[\langle \psi(t) | \hat{O} | \psi(t) \rangle \right] = \\ &= \frac{d\langle \psi(t) |}{dt} \hat{O} | \psi(t) \rangle + \langle \psi(t) | \hat{O} \frac{d|\psi(t)\rangle}{dt} \end{aligned} \quad (81)$$

Now, rewriting the time dependent Schrödinger equation as:

$$\frac{d|\psi(t)\rangle}{dt} = -\frac{i}{\hbar} \hat{H} |\psi(t)\rangle \Leftrightarrow \frac{d}{dt} \langle \psi(t) | = \langle \psi(t) | \hat{H} \frac{i}{\hbar} \quad (82)$$

Returning to the expression for the time derivative, 79, we may write:

$$\begin{aligned} \frac{d}{dt} \overline{\hat{O}(t)} &= \frac{i}{\hbar} \langle \psi(t) | \hat{H} \hat{O} | \psi(t) \rangle - \frac{i}{\hbar} \langle \psi(t) | \hat{O} \hat{H} | \psi(t) \rangle = \\ &= \frac{i}{\hbar} \langle \psi(t) | [\hat{H}, \hat{O}] | \psi(t) \rangle = \\ &= \frac{i}{\hbar} [\hat{H}, \hat{O}] \end{aligned} \quad (83)$$

4 Interaction Picture

Interaction picture is an "*intermediate*" picture, meaning that the time dependence of the states is only partially moved on the observables.

In general, in order to move to the interaction picture, we need to split the Hamiltonian under consideration into two parts: the free part $\hat{H}_S^{(0)}$ which is the exactly solvable part of the Hamiltonian and the interacting part \hat{V}_S , just like when dealing with a perturbation theory problem. Therefore, the Hamiltonian may be broken like:

$$\hat{H}_S = \hat{H}_S^{(0)} + \hat{V}_S \quad (84)$$

Next, we introduce the following unitary operator:

$$\hat{S}_0^\dagger = e^{i\hat{H}_S^{(0)} t/\hbar} \quad (85)$$

By acting with this operators, we define the interaction picture and we will use "I" as a label, following the rules:

$$|\psi_I(t)\rangle = \hat{S}_0^\dagger |\psi_S(t)\rangle = e^{i\hat{H}_S^{(0)}t/\hbar} |\psi_S(t)\rangle \quad (86)$$

$$\hat{O}_I(t) = \hat{S}_0^\dagger \hat{O}_S \hat{S}_0 = e^{i\hat{H}_S^{(0)}t/\hbar} \hat{O}_S e^{-i\hat{H}_S^{(0)}t/\hbar} \quad (87)$$

Starting from the definition of $\psi_I(t)$ and taking the time derivative, will lead us to an expression for its time evolution:

$$\begin{aligned} \frac{d}{dt} |\psi_I(t)\rangle &= \frac{i}{\hbar} \hat{H}_S^{(0)} |\psi_S(t)\rangle + e^{i\hat{H}_S^{(0)}t/\hbar} \frac{d}{dt} |\psi_S(t)\rangle = \\ &= \frac{i}{\hbar} \hat{H}_S^{(0)} |\psi_I(t)\rangle - \frac{i}{\hbar} e^{i\hat{H}_S^{(0)}t/\hbar} [\hat{H}_S^{(0)} + \hat{V}_S] |\psi_S(t)\rangle = -\frac{i}{\hbar} e^{i\hat{H}_S^{(0)}t/\hbar} \hat{V}_S |\psi_S(t)\rangle = \\ &= -\frac{i}{\hbar} e^{i\hat{H}_S^{(0)}t/\hbar} \hat{V}_S e^{-i\hat{H}_S^{(0)}t/\hbar} e^{i\hat{H}_S^{(0)}t/\hbar} |\psi_S(t)\rangle \Leftrightarrow \\ \frac{d}{dt} |\psi_I(t)\rangle &= -\frac{i}{\hbar} \hat{V}_I(t) |\psi_I(t)\rangle \Leftrightarrow \\ i\hbar \frac{d}{dt} |\psi_I(t)\rangle &= \hat{V}_I(t) |\psi_I(t)\rangle \end{aligned} \quad (88)$$

The last expression is analogous to the Schrödinger equation, but in the interaction picture, which allows us as we've seen throughout the text to tackle with time-dependent perturbation problems.

Regarding the time evolution of an operator in the interaction picture, we start from:

$$\hat{O}_I(t) = e^{i\hat{H}_S^{(0)}t/\hbar} \hat{O}_S e^{-i\hat{H}_S^{(0)}t/\hbar} \quad (89)$$

Taking the time derivative of both sides, we get

$$\begin{aligned} \frac{d}{dt} \hat{O}_I(t) &= \frac{i}{\hbar} \hat{H}_S^{(0)} e^{i\hat{H}_S^{(0)}t/\hbar} \hat{O}_S e^{-i\hat{H}_S^{(0)}t/\hbar} \hat{H}_S^{(0)} = \\ &= \frac{i}{\hbar} \hat{H}_S^{(0)} \hat{O}_I - \frac{i}{\hbar} \hat{O}_I \hat{H}_S^{(0)} \\ &= \frac{i}{\hbar} [\hat{H}_S^{(0)}, \hat{O}_I] \end{aligned} \quad (90)$$

In the interaction picture, $\hat{H}_S^{(0)}$ becomes:

$$\hat{H}_I^{(0)} = e^{i\hat{H}_S^{(0)}t/\hbar} \hat{H}_S^{(0)} e^{-i\hat{H}_S^{(0)}t/\hbar} = \hat{H}_S^{(0)} e^{i\hat{H}_S^{(0)}t/\hbar} e^{-i\hat{H}_S^{(0)}t/\hbar} = \hat{H}_S^{(0)} \quad (91)$$

Therefore $\hat{H}_I^{(0)}$ is the same as $\hat{H}_S^{(0)}$ and substitution in 90 yields:

$$\frac{d}{dt} \hat{O}_I = \frac{i}{\hbar} [\hat{H}_I^{(0)}, \hat{O}_I] \quad (92)$$

Summarizing we should point out that in the interaction picture the evolution of the states is controlled by \hat{V} , while the evolution of the observables is ruled by $\hat{H}^{(0)}$.

5 Dissipative processes in cavity QED

So far, we have analytically treated all of the systems under consideration making a silent but quite important hypothesis; that the cavity is perfectly isolated from the environment $\kappa = 0$, there are no thermal states in the cavity $\bar{n}_t h = 0$ and that there is no spontaneous emission inside the cavity ($\gamma = 0$).

Those limits of course are helpful in order to derive the physical processes that take place in such system, though Nature has laws that would never allow one to achieve these *ideal values* in an experiment.

Theoretical work on dissipative processes is formidably described in [27], [28] and [14]. It is not the purpose of the current thesis to extensively describe the derivation of the methods discussed in these works, instead we will use their results to briefly discuss the important role of environment interaction in our model.

The main reason for the foundation of this relatively new field described by the title "*Open Quantum Systems*" is the fact that when taking under consideration a system interacting with its environment, the Hilbert space that includes all the necessary information for the description of the model becomes so large, that analytical description of the differential equations involved is feasible for a very small subset of realistic situations, for example the *Resonant Fluorescence* [14]. Moreover, the description of the phenomena taking place cannot be expressed in terms of wavefunctions (which essentially describe pure states); instead, the **density matrix** evolution is what will allow us to keep track of the degradation of the open system. The reason is that, in contrast to what we have discussed so far, the evolution of the system is ruled by non-unitary (non-reversible) operations, which block us from using analytical methods.

The benefits of developing this sort of formalism are quite clear if we consider the fact that contemporary computational systems allow us to perform simulations making use of this formalism, which introduces the notion of *Super-operators* (operators that act on operators) and *collapse operators* that describe the dissipative influence of a closed system coupled to its environment.

In what follows, we will give a "compressed" description of the *Master Equation Approach* and the *Quantum Trajectory method* and include the numerical results derived using the Python open-source package *QuTip* [114]. In what follows, we will discuss the main steps of the derivation of the master equation following [27] and [28] and personal notes from the series of lectures Prof. Carmichael gave in

Singapore School of Physics on June 2012.

Lindblad Master Equation Approach

The density matrix of a system that contains all the necessary information regarding the statistical distribution of the system (either pure state, or mixed state) is defined by the relation:

$$\rho = \sum_n p_n |\psi_n\rangle\langle\psi_n| \quad (93)$$

where p_n is the classical probability that the system is in the quantum state $|\psi_n\rangle$. The standard approach for obtaining the equations of motion of a system S interacting with a heat reservoir (which is essentially the environment) R , is to extend the notion of the "System", so that it includes the closed system, the reservoir and their interaction. This combined quantum system can be then considered closed and its time evolution is then described by the equation:

$$\dot{\rho} = -\frac{i}{\hbar} [H, \rho] \quad (94)$$

where now the Hamiltonian H , contains the information for the initial closed system (the cavity), the heat reservoir (the environment) and their interaction, assuming that some of the infinite modes of the environment can be coupled to the cavity modes with the mediation of the cavity dissipation rate κ . Under those considerations, the Hamiltonian H may be written in the form:

$$H = H_S + H_R + H_{SR} \quad (95)$$

The terms H_S and H_R are the Hamiltonians of the system and the reservoir respectively, and H_{SR} carries the interaction between them. If the density matrix $\rho(t)$ describes the evolution of both the closed system and the reservoir in the Hilbert space $(S \oplus R)$, we can obtain the *reduced density matrix* of the system $\rho_S(t)$ by calculating the partial trace of the total system density matrix, over the reservoir states:

$$\rho_s(t) = Tr_R \rho(t) \quad (96)$$

If we transform the Schrödinger equation into the interaction picture in order to damp the fast oscillating terms, the modified density matrix becomes:

$$\tilde{\rho}(t) = e^{i/\hbar(H_S+H_R)t} \rho(t) e^{-i/\hbar(H_S+H_R)t} \quad (97)$$

In general, the interaction between the system and the reservoir is described by a time-dependent Hamiltonian $\tilde{H}_{SR}(t)$, which is given by the relation:

$$\tilde{H}_{SR}(t) = e^{i/\hbar(H_S+H_R)t} H_{SR} e^{-i/\hbar(H_S+H_R)t} \quad (98)$$

Therefore, we can write the Schrödinger equation as:

$$\dot{\tilde{\rho}}(t) = -\frac{i}{\hbar} \left[\tilde{H}_{SR}(T), \tilde{\rho}(t) \right] \quad (99)$$

Integration of this equation will provide us with an integral-differential equation, which can be iterated repeatedly, giving each time higher order approximations.

$$\tilde{\rho}(t) = \tilde{\rho}(0) - \frac{i}{\hbar} \int_0^t \left[\tilde{H}_{SR}(t'), \tilde{\rho}(t') \right] dt' \quad (100)$$

Substituting this expression of $\tilde{\rho}(t)$ in order to iterate once this equation, we obtain:

$$\tilde{\rho}(t) = -\frac{i}{\hbar} \left[\tilde{H}_{SR}(t), \tilde{\rho}(0) \right] - \frac{1}{\hbar^2} \int_0^t \left[\tilde{H}_{SR}(t), \left[\tilde{H}_{SR}(t'), \tilde{\rho}(t') \right] \right] dt' \quad (101)$$

This expression can provide us with a full expression that describes the system if it is iterated many times, since there is no approximation made. However, we can make certain approximations in order to simplify it. First of all, we must assume that at $t = 0$ (when the interaction is turned on), there is no correlation between the system and the reservoir. Therefore, the combined density matrix may be written as

$$\rho(0) = \rho_S(0)R_0 \quad (102)$$

where R_0 is the initial reservoir density operator. Tracing over the reservoir leads us to:

$$\begin{aligned} tr_R(\dot{\tilde{\rho}}(t)) &= -\frac{i}{\hbar} tr_R \left(\left[\tilde{H}_{SR}(t), \tilde{\rho}(0) \right] \right) - \\ &\quad - \frac{1}{\hbar^2} \int_0^t tr_R \left(\left[\tilde{H}_{SR}(t), \left[\tilde{H}_{SR}(t'), \tilde{\rho}(t') \right] \right] \right) dt' \end{aligned} \quad (103)$$

Setting the initial conditions so that we may discard the first term of this expression, we have:

$$\dot{\tilde{\rho}}_S(t) = -\frac{1}{\hbar^2} \int_0^t tr_R \left(\left[\tilde{H}_{SR}(t), \left[\tilde{H}_{SR}(t'), \tilde{\rho}(t') \right] \right] \right) dt' \quad (104)$$

Our first approximation regarding the problem, has been the fact that the system and the reservoir (ie. the cavity and its environment) are uncorrelated (not entangled) initially. In general, as time passes by they will start having entanglement, though in most cases, this correlation between the system and the reservoir, is very weak and the combined density matrix can be written as:

$$\rho(t) = \rho_S(t)R_0 + O(H_{SR}) \quad (105)$$

Now it is time to state the first "important" approximation in our problem, which is referred to as **Born approximation**. The reservoir can be considered much larger than the system, so that changes in system will not affect the reservoir, thus the reservoir will stay in the same, initial condition. The second assumption of Born approximation requires that the system and the environment remain separable throughout the evolution which is justified by the "weak-interaction" assumption. In summary, Born approximation declares that:

$$\rho(t) \simeq \rho(t) \otimes \rho_R \quad (106)$$

The next important approximation is referred to as **Markov approximation** and it assumes that the time-scale of the decay for the environment (let's say τ_R) is much shorter than the smallest time-scale of the system dynamics, which summarizes in:

$$\tau_S \gg \tau_R \quad (107)$$

Markov-approximation may seem crude with a first glance. Though, it states an important fact: *Despite the fact that the past history of the system is imprinted in the reservoir through the coupling, thus affecting future states of the system again, if we consider it very large, the changes in the reservoir caused by the system do not survive for very long, which deprives the reservoir from having "memory".* To understand how Markov approximation affects the treatment of our analysis, we will denote the interaction Hamiltonian as:

$$H_{SR} = \hbar \sum_i s_i R_i \quad (108)$$

where s_i and R_i are the operators in the Hilbert space of the system and the reservoir respectively. Moving to the interaction picture and performing Born approximation yields:

$$\dot{\tilde{\rho}}(t) = - \sum_{i,j} \int_0^t Tr_R \left(\left[\tilde{s}_i(t) \tilde{R}_i(t), \left[\tilde{s}_j(t') \tilde{R}_j(t'), \tilde{\rho}_S(t') R_0 \right] \right] \right) dt' \quad (109)$$

Hence, this equation can be written as:

$$\dot{\tilde{\rho}}_S(t) = - \sum_{i,j} \int_0^t \left(A \langle \tilde{R}_i(t) \tilde{R}_j(t') \rangle_R + B \langle \tilde{R}_j(t') \tilde{R}_i(t) \rangle_R \right) dt' \quad (110)$$

where A and B are given by the relations:

$$\begin{aligned} A &= \tilde{s}_i(t) \tilde{s}_j(t') \tilde{\rho}_S(t') - \tilde{s}_j(t') \tilde{\rho}_S(t') \tilde{s}_i(t) \\ B &= \tilde{\rho}_S(t') \tilde{s}_j(t') \tilde{s}_i(t) - \tilde{s}_i(t) \tilde{\rho}_S(t') \tilde{s}_j(t') \end{aligned} \quad (111)$$

The effect of the environment is evident in the terms:

$$\begin{aligned}\langle \tilde{R}_i(t)\tilde{R}_j(t') \rangle_R &= Tr_R \left(R_0 \tilde{R}_i(t) \tilde{R}_j(t') \right) \\ \langle \tilde{R}_j(t')\tilde{R}_i(t) \rangle_R &= Tr_R \left(R_0 \tilde{R}_j(t') \tilde{R}_i(t) \right)\end{aligned}\tag{112}$$

References - Bibliography

- [1] Cohen-Tannoudji, C., B. Diu, and F. Laloë: *Quantum mechanics. Quantum Mechanics*. Wiley, 1977, ISBN 9782705658342. <http://books.google.gr/books?id=CnkfAQAAQAAJ>.
- [2] Harris, E.G.: *Introduction to Modern Theoretical Physics: Quantum theory and statistical physics*. Number τ. 2 in *Introduction to Modern Theoretical Physics: Quantum Theory and Statistical Physics*. Wiley, 1975, ISBN 9780471353263. <http://books.google.gr/books?id=Qf8oAQAAQAAJ>.
- [3] Levi, A.F.J.: *Applied Quantum Mechanics*. Cambridge University Press, 2006, ISBN 9780521860963. <http://books.google.gr/books?id=40rRzNbuhpAC>.
- [4] Miller, David A. B.: *Quantum Mechanics for Scientists and Engineers*. Cambridge University Press, New York, NY, USA, 2008, ISBN 0521897831, 9780521897839. <http://books.google.gr/books?id=pwrBp3ZGaUYC>.
- [5] Trachanas, Stephanos: *Quantum Mechanics II*. Crete University Press, Heraklio, Crete, Grece, 2008, ISBN 978-960-524-267-1. <http://www.cup.gr/ViewShopProduct.aspx?ProductId=273160&LangId=1>.
- [6] Raimond, J. M., M. Brune, and S. Haroche: *Manipulating quantum entanglement with atoms and photons in a cavity*. Rev. Mod. Phys., 73:565–582, Aug 2001. <http://link.aps.org/doi/10.1103/RevModPhys.73.565>.
- [7] Haroche, S. and J.M. Raimond: *Exploring the Quantum: Atoms, Cavities, and Photons: Atoms, Cavities, and Photons*. Oxford graduate texts in mathematics. OUP Oxford, 2006, ISBN 9780198509141. <http://books.google.gr/books?id=QY6YuU-Qi-AC>.

- [8] E. M. Purcell, H. C. Torrey and R. V. Pound: *Proceedings of the american physical society*. Phys. Rev., 69:674–674, Jun 1946. <http://link.aps.org/doi/10.1103/PhysRev.69.674.2>.
- [9] Goy, P., J. M. Raimond, M. Gross, and S. Haroche: *Observation of cavity-enhanced single-atom spontaneous emission*. Phys. Rev. Lett., 50:1903–1906, Jun 1983. <http://link.aps.org/doi/10.1103/PhysRevLett.50.1903>.
- [10] Boi, L.: *The Quantum Vacuum: A Scientific and Philosophical Concept, from Electrodynamics to String Theory and the Geometry of the Microscopic World*. The Quantum Vacuum. Johns Hopkins University Press, 2011, ISBN 9781421402475. http://books.google.gr/books?id=rAEVOLae_FoC.
- [11] Gerry, C. and P. Knight: *Introductory Quantum Optics*. Cambridge University Press, 2004, ISBN 9780521527354. <http://books.google.gr/books?id=CgByyoBJJwgC>.
- [12] Lambropoulos, P. and D. Petrosyan: *Fundamentals of Quantum Optics and Quantum Information*. Springer, 2006, ISBN 9783540345718. <http://books.google.gr/books?id=53bpU-41U8gC>.
- [13] Milonni, P.W.: *The quantum vacuum: an introduction to quantum electrodynamics*. Academic Press, 1994, ISBN 9780124980808. <http://books.google.gr/books?id=P83vAAAAMAAJ>.
- [14] Scully, M.O. and S. Zubairy: *Quantum Optics*. Cambridge University Press, 1997, ISBN 9780521435956. <http://books.google.gr/books?id=20ISSQCKKmQC>.
- [15] Walls, D.F. and G.J. Milburn: *Quantum Optics*. Springer, 2008, ISBN 9783540285731. <http://books.google.gr/books?id=LiWsc3Nlf0kC>.
- [16] Nielsen, M.A. and I.L. Chuang: *Quantum Computation and Quantum Information: 10th Anniversary Edition*. Cambridge University Press, 2010, ISBN 9781107002173. <http://books.google.gr/books?id=-s4DEy7o-a0C>.
- [17] Mermin, N.D.: *Quantum Computer Science: An Introduction*. Cambridge University Press, 2007, ISBN 9780521876582. <http://books.google.gr/books?id=q2S9APxFdUQC>.

- [18] Williams, C.P.: *Explorations in Quantum Computing*. Texts in Computer Science. Springer, 2011, ISBN 9781846288869. <http://books.google.gr/books?id=QE8S--WjIFwC>.
- [19] McMahon, D.: *Quantum Computing Explained*. Wiley, 2007, ISBN 9780470181362. <http://books.google.gr/books?id=bDXwFHJNKFAC>.
- [20] Benioff, Paul: *The computer as a physical system: A microscopic quantum mechanical hamiltonian model of computers as represented by turing machines*. Journal of Statistical Physics, 22:563–591, 1980, ISSN 0022-4715. <http://dx.doi.org/10.1007/BF01011339>, 10.1007/BF01011339.
- [21] Feynman, R. P.: *Simulating physics with computers*. International Journal of Theoretical Physics, 21:467–488, June 1982. <http://www.cs.berkeley.edu/~christos/classics/Feynman.pdf>.
- [22] Deutsch, D.: *Quantum theory, the church-turing principle and the universal quantum computer*. Proceedings of the Royal Society of London. A. Mathematical and Physical Sciences, 400(1818):97–117, July 1985. <http://dx.doi.org/10.1098/rspa.1985.0070>.
- [23] Cleve, R., A. Ekert, C. Macchiavello, and M. Mosca: *Quantum algorithms revisited*. Phil.Trans.Roy.Soc.Lond.A, 1997. <http://arxiv.org/pdf/quant-ph/9708016>.
- [24] Brown, J. and D. Deutsch: *Quest for the Quantum Computer*. Touchstone Book. Simon & Schuster, 2001, ISBN 9780684870045. <http://books.google.gr/books?id=ECWm59h2pLAC>.
- [25] Jaynes E.T., Cummings F.W.: *Comparison of quantum and semiclassical radiation theories with application to the beam maser*. Proceedings of the IEEE, 51:89–109, Jan 1963. <http://ieeexplore.ieee.org/xpl/articleDetails.jsp?arnumber=1443594>.
- [26] Shore, Bruce W. and Peter L. Knight: *The jaynes-cummings model*. Journal of Modern Optics, 40(7):1195–1238, 1993. <http://www.tandfonline.com/doi/abs/10.1080/09500349314551321>.
- [27] Carmichael, H.J.: *Statistical Methods in Quantum Optics 1: Master Equations and Fokker-Planck Equations*. Texts & Monographs in Physics. Springer, 2003, ISBN 9783540548829. <http://books.google.gr/books?id=oCGRgM-yJacC>.

- [28] Carmichael, H.J.: *Statistical Methods in Quantum Optics 2: Non-Classical Fields.* Theoretical and Mathematical Physics. Springer, 2007, ISBN 9783540713197. <http://books.google.gr/books?id=xgxOYkxW8JoC>.
- [29] Carmichael, H.: *An Open Systems Approach to Quantum Optics: Lectures Presented at the Université Libre de Bruxelles, October 28 to November 4, 1991.* Lecture notes in physics: Monographs. Springer-Verlag, 1993, ISBN 9783540566342. <http://books.google.gr/books?id=E15gxgxWhpgC>.
- [30] Deutsch, D. and R. Jozsa: *Rapid solution of problems by quantum computation.* Royal Society of London Proceedings Series A, 439:553–558, December 1992. <http://www.qudev.ethz.ch/phys4/studentspresentations/djalgo/DeutschJozsa.pdf>.
- [31] Grover, Lov K.: *Quantum mechanics helps in searching for a needle in a haystack.* Phys. Rev. Lett., 79:325–328, Jul 1997. <http://link.aps.org/doi/10.1103/PhysRevLett.79.325>.
- [32] Grover, Lov K.: *Complex quantum queries.* 1997. <http://arxiv.org/abs/quant-ph/9706005>.
- [33] Grover, Lov K.: *Quantum computers can search rapidly by using almost any transformation.* Phys. Rev. Lett., 80:4329–4332, May 1998. <http://link.aps.org/doi/10.1103/PhysRevLett.80.4329>.
- [34] Jozsa, Richard: *Searching in grover's algorithm.* 1999. <http://arxiv.org/abs/quant-ph/9901021>.
- [35] Shor, P. W.: *Polynomial-Time Algorithms for Prime Factorization and Discrete Logarithms on a Quantum Computer.* eprint arXiv:quant-ph/9508027, August 1995. <http://arxiv.org/abs/quant-ph/9508027v2>.
- [36] Scully, M. O. and M. S. Zubairy: *Cavity qed implementation of the discrete quantum fourier transform.* Physical Review A, 65(5):052324, May 2002. <http://pra.aps.org/abstract/PRA/v65/i5/e052324>.
- [37] Yamaguchi, F., P. Milman, M. Brune, J. M. Raimond, and S. Haroche: *Quantum search with two-atom collisions in cavity qed.* Physical Review A, 66(1):010302, July 2002. <http://pra.aps.org/abstract/PRA/v66/i1/e010302>.

- [38] Lloyd, S.: *Universal quantum simulators*. *Science*, **273**:1073–1078, August 1996. <http://research.physics.illinois.edu/demarco/lloyd%2096%20paper.pdf>.
- [39] Angelakis, Dimitris G., Marcelo Franca Santos, and Sougato Bose: *Photon-blockade-induced mott transitions and xy spin models in coupled cavity arrays*. *Phys. Rev. A*, **76**:031805, Sep 2007. <http://link.aps.org/doi/10.1103/PhysRevA.76.031805>.
- [40] Hood, C. J., M. S. Chapman, T. W. Lynn, and H. J. Kimble: *Real-time cavity qed with single atoms*. *Phys. Rev. Lett.*, **80**:4157–4160, May 1998. <http://link.aps.org/doi/10.1103/PhysRevLett.80.4157>.
- [41] Boca, A., R. Miller, K. M. Birnbaum, A. D. Boozer, J. McKeever, and H. J. Kimble: *Observation of the vacuum rabi spectrum for one trapped atom*. *Phys. Rev. Lett.*, **93**:233603, Dec 2004. <http://link.aps.org/doi/10.1103/PhysRevLett.93.233603>.
- [42] Duan, L. M., B. Wang, and H. J. Kimble: *Robust quantum gates on neutral atoms with cavity-assisted photon scattering*. *Phys. Rev. A*, **72**:032333, Sep 2005. <http://link.aps.org/doi/10.1103/PhysRevA.72.032333>.
- [43] Boozer, A. D., A. Boca, R. Miller, T. E. Northup, and H. J. Kimble: *Reversible state transfer between light and a single trapped atom*. *Phys. Rev. Lett.*, **98**:193601, May 2007. <http://link.aps.org/doi/10.1103/PhysRevLett.98.193601>.
- [44] Khudaverdyan, M., W. Alt, I. Dotsenko, L. FG?rster, S. Kuhr, D. Meschede, Y. Miroshnychenko, D. Schrader, and A. Rauschenbeutel: *Adiabatic quantum state manipulation of single trapped atoms*. *Phys. Rev. A*, **71**:031404, 2005. <http://arxiv.org/pdf/quant-ph/0411120>.
- [45] Miroshnychenko, Y., W. Alt, I. Dotsenko, L. FG?rster, M. Khudaverdyan, D. Meschede, D. Schrader, and A. Rauschenbeutel: *An atom-sorting machine*. *Nature*, **442**:151, 2006. <http://www.nature.com/nature/journal/v442/n7099/full/442151a.html>.
- [46] Brakhane, S., W. Alt, T. Kampschulte, M. Martinez-Dorantes, R. Reimann, S. Yoon, A. Widera, and D. Meschede: *Bayesian feedback control of a two-atom spin-state in an atom-cavity system*. *Phys. Rev. Lett.*, **109**:173601, 2012. <http://arxiv.org/abs/1206.3184>.

- [47] Cirac, J. I. and P. Zoller: *Quantum computations with cold trapped ions*. Phys. Rev. Lett., 74:4091–4094, May 1995. <http://link.aps.org/doi/10.1103/PhysRevLett.74.4091>.
- [48] Leibfried, D., R. Blatt, C. Monroe, and D. Wineland: *Quantum dynamics of single trapped ions*. Rev. Mod. Phys., 75:281–324, Mar 2003. <http://link.aps.org/doi/10.1103/RevModPhys.75.281>.
- [49] Monroe, C., D. M. Meekhof, B. E. King, W. M. Itano, and D. J. Wineland: *Demonstration of a fundamental quantum logic gate*. Phys. Rev. Lett., 75:4714–4717, Dec 1995. <http://link.aps.org/doi/10.1103/PhysRevLett.75.4714>.
- [50] L.M.K., Vandersypen, Steffen M., G. Breyta, C. S. Yannoni, M. H. Sherwood, and I. L. Chuang: *Experimental realization of shor's quantum factoring algorithm using nuclear magnetic resonance*. Nature, 414:883–887, December 2001. <http://arxiv.org/abs/quant-ph/0112176>.
- [51] Blais, Alexandre, Ren Shou Huang, Andreas Wallraff, S. M. Girvin, and R. J. Schoelkopf: *Cavity quantum electrodynamics for superconducting electrical circuits: An architecture for quantum computation*. Phys. Rev. A, 69:062320, Jun 2004. <http://link.aps.org/doi/10.1103/PhysRevA.69.062320>.
- [52] Devoret, M. H., A. Wallraff, and J. M. Martinis: *Superconducting qubits: A short review*. eprint arXiv:cond-mat/0411174, November 2004. <http://arxiv.org/abs/cond-mat/0411174>.
- [53] Dicarlo, L., J. M. Chow, J. M. Gambetta, L. S. Bishop, B. R. Johnson, D. I. Schuster, J. Majer, A. Blais, L. Frunzio, S. M. Girvin, and R. J. Schoelkopf: *Demonstration of two-qubit algorithms with a superconducting quantum processor*. Nature, 460:240–244, July 2009. <http://www.nature.com/nature/journal/v460/n7252/full/nature08121.html>.
- [54] Glauber, Roy J.: *Coherent and incoherent states of the radiation field*. Phys. Rev., 131:2766–2788, Sep 1963. <http://link.aps.org/doi/10.1103/PhysRev.131.2766>.
- [55] Sudarshan, E. C. G.: *Equivalence of semiclassical and quantum mechanical descriptions of statistical light beams*. Phys. Rev. Lett., 10:277–279, Apr 1963. <http://link.aps.org/doi/10.1103/PhysRevLett.10.277>.

- [56] Walther, H., B. T. H. Varcoe, B. G. Englert, and T. Becker: *Cavity quantum electrodynamics*. Reports on Progress in Physics, 69:1325–1382, May 2006. <http://iopscience.iop.org/0034-4885/69/5/R02>.
- [57] Heinichs, Todd: *Cavity qed approaches to quantum information and quantum computing*. A Quantum Information Science and Technology Roadmap, 2004. http://qist.lanl.gov/qcomp_map.shtml.
- [58] Heinzen, D. J., J. J. Childs, J. E. Thomas, and M. S. Feld: *Enhanced and inhibited visible spontaneous emission by atoms in a confocal resonator*. Phys. Rev. Lett., 58:1320–1323, Mar 1987. <http://link.aps.org/doi/10.1103/PhysRevLett.58.1320>.
- [59] Heinzen, D. J. and M. S. Feld: *Vacuum radiative level shift and spontaneous-emission linewidth of an atom in an optical resonator*. Phys. Rev. Lett., 59:2623–2626, Dec 1987. <http://link.aps.org/doi/10.1103/PhysRevLett.59.2623>.
- [60] Casimir, H. B. G. and D. Polder: *The influence of retardation on the london-van der waals forces*. Phys. Rev., 73:360–372, Feb 1948. <http://link.aps.org/doi/10.1103/PhysRev.73.360>.
- [61] Kuhr, S., S. Gleyzes, C. Guerlin, J. Bernu, U. B. Hoff, S. Deléglise, S. Osnaghi, M. Brune, J. M. Raimond, S. Haroche, E. Jacques, P. Bosland, and B. Visentin: *Ultrahigh finesse fabry-p[le-acute]rot superconducting resonator*. Applied Physics Letters, 90(16):164101, 2007. <http://link.aip.org/link/?APL/90/164101/1>.
- [62] Brune, M., F. Schmidt-Kaler, A. Maali, J. Dreyer, E. Hagley, J. M. Raimond, and S. Haroche: *Quantum rabi oscillation: A direct test of field quantization in a cavity*. Phys. Rev. Lett., 76:1800–1803, Mar 1996. <http://link.aps.org/doi/10.1103/PhysRevLett.76.1800>.
- [63] Wiseman, H. M. and G. J. Milburn: *Quantum theory of field-quadrature measurements*. Phys. Rev. A, 47:642–662, Jan 1993. <http://link.aps.org/doi/10.1103/PhysRevA.47.642>.
- [64] Barenco, Adriano, Charles H. Bennett, Richard Cleve, David P. DiVincenzo, Norman Margolus, *et al.*: *Elementary gates for quantum computation*. Phys. Rev., A52:3457, 1995. <http://arxiv.org/abs/quant-ph/9503016>.

- [65] Cormen, T.H., C.E. Leiserson, R.L. Rivest, and C. Stein: *Introduction to Algorithms, Third Edition*. MIT Press, 2009, ISBN 9780262533058. <http://books.google.gr/books?id=h2xRPgAACAAJ>.
- [66] Ettinger, M., P. Hoyer, and E. Knill: *The quantum query complexity of the hidden subgroup problem is polynomial*. arXiv:quant-ph/0401083, January 2004. <http://arxiv.org/abs/quant-ph/0401083>.
- [67] Regev, O.: *Quantum computation and lattice problems*. eprint arXiv:cs/0304005, April 2003. <http://arxiv.org/abs/cs/0304005>.
- [68] Paul, W.: *Electromagnetic traps for charged and neutral particles*. Reviews of Modern Physics, 62:531–540, July 1990. <http://www.quddev.phys.ethz.ch/content/courses/phys4/studentspresentations/iontraps/RMP.pdf>.
- [69] Lu, C. Y., D. E. Browne, T. Yang, and J. W. Pan: *Demonstration of a compiled version of shor’s quantum factoring algorithm using photonic qubits*. Physical Review Letters, 99(25):250504, December 2007. <http://prl.aps.org/abstract/PRL/v99/i25/e250504>.
- [70] Lanyon, B. P., T. J. Weinhold, N. K. Langford, M. Barbieri, D. F. V. James, A. Gilchrist, and A. G. White: *Experimental demonstration of a compiled version of shor’s algorithm with quantum entanglement*. Physical Review Letters, 99(25):250505, December 2007. <http://arxiv.org/abs/0705.1684>.
- [71] Rauschenbeutel, A., P. Bertet, S. Osnaghi, G. Nogues, M. Brune, J. M. Raimond, and S. Haroche: *Controlled entanglement of two field modes in a cavity quantum electrodynamics experiment*. Physical Review A, 64(5):050301, November 2001. <http://pra.aps.org/abstract/PRA/v64/i5/e050301>.
- [72] Brune, M., S. Haroche, V. Lefevre, J. M. Raimond, and N. Zagury: *Quantum nondemolition measurement of small photon numbers by rydberg-atom phase-sensitive detection*. Phys. Rev. Lett., 65:976–979, Aug 1990. <http://link.aps.org/doi/10.1103/PhysRevLett.65.976>.
- [73] Nogues, G., A. Rauschenbeutel, S. Osnaghi, M. Brune, J. M. Raimond, and S. Haroche: *Seeing a single photon without destroying it*. Nature, 400(6741):239–242, July 1999, ISSN 0028-0836. <http://dx.doi.org/10.1038/22275>.

- [74] Osnaghi, S., P. Bertet, A. Auffeves, P. Maioli, M. Brune, J. M. Raimond, and S. Haroche: *Coherent control of an atomic collision in a cavity*. Phys. Rev. Lett., 87:037902, Jun 2001. <http://link.aps.org/doi/10.1103/PhysRevLett.87.037902>.
- [75] Zheng, Shi Biao and Guang Can Guo: *Efficient scheme for two-atom entanglement and quantum information processing in cavity qed*. Phys. Rev. Lett., 85:2392–2395, Sep 2000. <http://link.aps.org/doi/10.1103/PhysRevLett.85.2392>.
- [76] Brune, M., F. Schmidt-Kaler, A. Maali, J. Dreyer, E. Hagley, J. M. Raimond, and S. Haroche: *Quantum rabi oscillation: A direct test of field quantization in a cavity*. Phys. Rev. Lett., 76:1800–1803, Mar 1996. <http://link.aps.org/doi/10.1103/PhysRevLett.76.1800>.
- [77] Zubairy, M. Suhail, Moochan Kim, and Marlan O. Scully: *Cavity-qed-based quantum phase gate*. Phys. Rev. A, 68:033820, Sep 2003. <http://link.aps.org/doi/10.1103/PhysRevA.68.033820>.
- [78] Zoller, P., Th. Beth, D. Binosi, R. Blatt, H. Briegel, D. Bruss, T. Calarco, J. I. Cirac, D. Deutsch, J. Eisert, A. Ekert, C. Fabre, N. Gisin, P. Grangiere, M. Grassl, S. Haroche, A. Imamoglu, A. Karlson, J. Kempe, L. Kouwenhoven, S. Kr?ll, G. Leuchs, M. Lewenstein, D. Loss, N. L?tkenhaus, S. Massar, J. E. Mooij, M. B. Plenio, E. Polzik, S. Popescu, G. Rempe, A. Sergienko, D. Suter, J. Twamley, G. Wendum, R. Werner, A. Winter, J. Wrachtrup, and A. Zeilinger: *Quantum information processing and communication*. The European Physical Journal D - Atomic, Molecular, Optical and Plasma Physics, 36:203–228, 2005, ISSN 1434-6060. <http://dx.doi.org/10.1140/epjd/e2005-00251-1>.
- [79] Hauke, Philipp, Fernando M Cucchietti, Luca Tagliacozzo, Ivan Deutsch, and Maciej Lewenstein: *Can one trust quantum simulators?* Reports on Progress in Physics, 75(8):082401, 2012. <http://stacks.iop.org/0034-4885/75/i=8/a=082401>.
- [80] Brown, Katherine L., William J. Munro, and Vivien M. Kendon: *Using quantum computers for quantum simulation*. Entropy, 12(11):2268–2307, 2010, ISSN 1099-4300. <http://www.mdpi.com/1099-4300/12/11/2268>.
- [81] Cirac, J. Ignacio, Paolo Maraner, and Jiannis K. Pachos: *Cold atom simulation of interacting relativistic quantum field theories*. Phys. Rev.

- Lett., 105:190403, Nov 2010. <http://link.aps.org/doi/10.1103/PhysRevLett.105.190403>.
- [82] Angelakis, D. G., M. Huo, D. Chang, L. C. Kwek, and V. Korepin: *Mimicking interacting relativistic theories with stationary pulses of light*. ArXiv e-prints, July 2012.
- [83] Jaksch, D., C. Bruder, J. I. Cirac, C. W. Gardiner, and P. Zoller: *Cold Bosonic Atoms in Optical Lattices*. Physical Review Letters, 81:3108–3111, October 1998. <http://arxiv.org/abs/cond-mat/9805329>.
- [84] Lewenstein, M., A. Sanpera, V. Ahufinger, B. Damski, A. Sen, and U. Sen: *Ultracold atomic gases in optical lattices: mimicking condensed matter physics and beyond*. Advances in Physics, 56:243–379, March 2007. <http://arxiv.org/abs/cond-mat/0606771>.
- [85] Jaksch, D. and P. Zoller: *The cold atom hubbard toolbox*. Annals of Physics, 315(1):52 – 79, 2005, ISSN 0003-4916. <http://www.sciencedirect.com/science/article/pii/S0003491604001782>, <ce:title>Special Issue</ce:title>.
- [86] Bloch, I., J. Dalibard, and S. Nascimbène: *Quantum simulations with ultracold quantum gases*. Nature Physics, 8:267–276, April 2012. <http://www.nature.com/nphys/journal/v8/n4/full/nphys2259.html>.
- [87] Lanyon, B. P., C. Hempel, D. Nigg, M. Müller, R. Gerritsma, F. Zähringer, P. Schindler, J. T. Barreiro, M. Rambach, G. Kirchmair, M. Hennrich, P. Zoller, R. Blatt, and C. F. Roos: *Universal digital quantum simulation with trapped ions*. Science, 334:57–, October 2011. <http://www.sciencemag.org/content/334/6052/57.abstract>.
- [88] Deng, X. L., D. Porras, and J. I. Cirac: *Effective spin quantum phases in systems of trapped ions*. Phys. Rev. A, 72:063407, Dec 2005. <http://link.aps.org/doi/10.1103/PhysRevA.72.063407>.
- [89] Hennessy, K., A. Badolato, M. Winger, D. Gerace, M. Atatüre, S. Gulde, S. Fält, E. L. Hu, and A. Imamoglu: *Quantum nature of a strongly coupled single quantum dot-cavity system*. Nature, 445:896–899, February 2007. <http://www.nature.com/nature/journal/v445/n7130/full/nature05586.html>.
- [90] Blatt, R. and C. F. Roos: *Quantum simulations with trapped ions*. Nature Physics, 8:277–284, April 2012. <http://www.nature.com/nphys/journal/v8/n4/full/nphys2252.html>.

- [91] Somaroo, S., C. H. Tseng, T. F. Havel, R. Laflamme, and D. G. Cory: *Quantum simulations on a quantum computer*. Phys. Rev. Lett., 82:5381–5384, Jun 1999. <http://link.aps.org/doi/10.1103/PhysRevLett.82.5381>.
- [92] Britton, J. W., B. C. Sawyer, A. C. Keith, C. C. J. Wang, J. K. Freericks, H. Uys, M. J. Biercuk, and J. J. Bollinger: *Engineered two-dimensional ising interactions in a trapped-ion quantum simulator with hundreds of spins*. "Nature", 484:489–492, April 2012. <http://www.nature.com/nature/journal/v484/n7395/full/nature10981.html>.
- [93] Hartmann, M. J., F. G. S. L. Brandao, and M. B. Plenio: *Quantum many-body phenomena in coupled cavity arrays*. ArXiv e-prints, August 2008. <http://arxiv.org/abs/0808.2557>.
- [94] Greentree, A. D., C. Tahan, J. H. Cole, and L. C. L. Hollenberg: *Quantum phase transitions of light*. Nature Physics, 2:856–861, December 2006. <http://www.nature.com/nphys/journal/v2/n12/abs/nphys466.html>.
- [95] Kay, A. and D. G. Angelakis: *Reproducing spin lattice models in strongly coupled atom-cavity systems*. EPL (Europhysics Letters), 84:20001, October 2008. <http://arxiv.org/abs/0802.0488>.
- [96] Cho, Jaeyoon, Dimitris G. Angelakis, and Sougato Bose: *Simulation of high-spin heisenberg models in coupled cavities*. Phys. Rev. A, 78:062338, Dec 2008. <http://link.aps.org/doi/10.1103/PhysRevA.78.062338>.
- [97] Carusotto, I., D. Gerace, H. E. Tureci, S. De Liberato, C. Ciuti, and A. Imamoglu: *Fermionized photons in an array of driven dissipative nonlinear cavities*. Phys. Rev. Lett., 103:033601, Jul 2009. <http://link.aps.org/doi/10.1103/PhysRevLett.103.033601>.
- [98] Tomadin, A., V. Giovannetti, R. Fazio, D. Gerace, I. Carusotto, H. E. Türeci, and A. Imamoglu: *Signatures of the superfluid-insulator phase transition in laser-driven dissipative nonlinear cavity arrays*. Phys. Rev. A, 81:061801, Jun 2010. <http://link.aps.org/doi/10.1103/PhysRevA.81.061801>.
- [99] Angelakis, D. G., S. Bose, and S. Mancini: *Steady-state entanglement between hybrid light-matter qubits*. EPL (Europhysics Letters), 85:20007, January 2009. <http://arxiv.org/abs/0711.1830>.

- [100] Angelakis, D. G., L. Dai, and L. C. Kwek: *Coherent control of long-distance steady-state entanglement in lossy resonator arrays*. EPL (Europhysics Letters), 91:10003, July 2010. <http://arxiv.org/abs/0906.2168>.
- [101] Knap, Michael, Enrico Arrigoni, Wolfgang von der Linden, and Jared H. Cole: *Emission characteristics of laser-driven dissipative coupled-cavity systems*. Phys. Rev. A, 83:023821, Feb 2011. <http://link.aps.org/doi/10.1103/PhysRevA.83.023821>.
- [102] Nissen, Felix, Sebastian Schmidt, Matteo Biondi, Gianni Blatter, Hakan E. Türeci, and Jonathan Keeling: *Nonequilibrium dynamics of coupled qubit-cavity arrays*. Phys. Rev. Lett., 108:233603, Jun 2012. <http://link.aps.org/doi/10.1103/PhysRevLett.108.233603>.
- [103] Nunnenkamp, A., J. Koch, and S. M. Girvin: *Synthetic gauge fields and homodyne transmission in Jaynes-Cummings lattices*. New Journal of Physics, 13(9):095008, September 2011. <http://arxiv.org/abs/1105.1817>.
- [104] Umucalilar, R. O. and I. Carusotto: *Artificial gauge field for photons in coupled cavity arrays*. Phys. Rev. A, 84:043804, Oct 2011. <http://link.aps.org/doi/10.1103/PhysRevA.84.043804>.
- [105] Grujic, T, S R Clark, D Jaksch, and D G Angelakis: *Non-equilibrium many-body effects in driven nonlinear resonator arrays*. New Journal of Physics, 14(10):103025, 2012. <http://stacks.iop.org/1367-2630/14/i=10/a=103025>.
- [106] Houck, A. A., H. E. Türeci, and J. Koch: *On-chip quantum simulation with superconducting circuits*. Nature Physics, 8:292–299, April 2012. <http://www.nature.com/nphys/journal/v8/n4/full/nphys2251.html>.
- [107] Zoubi, Hashem, Meir Orenstien, and Amiram Ron: *Coupled microcavities with dissipation*. Phys. Rev. A, 62:033801, Aug 2000. <http://link.aps.org/doi/10.1103/PhysRevA.62.033801>.
- [108] Haus, H. A., W. P. Huang, and A. W. Snyder: *Coupled-mode formulations*. Opt. Lett., 14(21):1222–1224, Nov 1989. <http://ol.osa.org/abstract.cfm?URI=ol-14-21-1222>.
- [109] Ogden, C. D., E. K. Irish, and M. S. Kim: *Dynamics in a coupled-cavity array*. Phys. Rev. A, 78:063805, Dec 2008. <http://link.aps.org/doi/10.1103/PhysRevA.78.063805>.

- [110] James, D F and J Jerke: *Effective hamiltonian theory and its applications in quantum information.* Canadian Journal of Physics, 85(6):625–632, 2007. <http://www.nrcresearchpress.com/doi/abs/10.1139/p07-060>.
- [111] Bamba, Motoaki, Atac Imamoğlu, Iacopo Carusotto, and Cristiano Ciuti: *Origin of strong photon antibunching in weakly nonlinear photonic molecules.* Phys. Rev. A, 83:021802, Feb 2011. <http://link.aps.org/doi/10.1103/PhysRevA.83.021802>.
- [112] Loss, Daniel and David P. DiVincenzo: *Quantum computation with quantum dots.* Phys. Rev. A, 57:120–126, Jan 1998. <http://link.aps.org/doi/10.1103/PhysRevA.57.120>.
- [113] Wineland, D.J., C. Monroe, W.M. Itano, D. Leibfried, B.E. King, et al.: *Experimental issues in coherent quantum state manipulation of trapped atomic ions.* J.Res.Natl.Inst.Stand.Tech., 103:259, 1998. <http://arxiv.org/abs/quant-ph/9710025>.
- [114] Johansson, J.R., P.D. Nation, and Franco Nori: *Qutip: An open-source python framework for the dynamics of open quantum systems.* Computer Physics Communications, 183(8):1760 – 1772, 2012, ISSN 0010-4655. <http://www.sciencedirect.com/science/article/pii/S0010465512000835>.
- [115] Mangano, S.: *Mathematica Cookbook.* O'Reilly Cookbooks. O'Reilly Media, Incorporated, 2010, ISBN 9780596520991. http://books.google.gr/books?id=BkDxC_01WisC.

Acknowledgements

During our lives we get to know many people. Personally, I consider two large classifications: there are people that encourage us to do "one more step" and others that try to stop any progress under way. Since my enrolment in the Master of T.U.C, I had the opportunity to meet people that belong to both those categories, though I would like to thank especially those who urged me to go one step further in anything I was achieving, rather than putting obstacles. Especially, I would like to thank my supervisor *Dr. D. Angelakis* for the composure he managed to inspire during some admittedly difficult situations as well as for giving to a Master's student the opportunity to see the "Big Picture" and skip local "perturbations" in his academic course.

Getting involved with the field of Quantum Optics and Quantum Computation was something I didn't expect when I was enrolling to the Master of the Science Department of T.U.C. and especially being hosted by *Centre of Quantum Technologies, Singapore* was beyond my greatest expectations. The three months spent there, undistracted from the tough situations in Greece were probably the reason for successfully finishing this thesis on schedule, as well as the chance for me to meet wonderful people, like: *Dr. Changsuk Noh, Dr. Su-Yong Lee, Dr. Amit Rai, Dr. Priyam Das* and my room-mates Adriana Marais, Felix Binder and Tom Grujic who did their best to make those three months productive and unforgettable. I also need to thank my fellow colleagues in T.U.C., *N. Schetakis, A. Blazaki and K. Koukoutsakis* for all the great moments we had during our classes in those two years, as well as *Dr. S. Mousaizis* for the support he supplied to all of us when it was required.

The decision of enrolling to the Master of T.U.C. in the first place, wouldn't have been made without the incitement from my parents and especially my mother, during a very difficult period for our family. It was very hard to stay on the course and they were patient with me when my patience ran out, especially during writing the thesis. I also want to thank my father, for the inspiration he provided regarding how to explain Physics to students and eventually to other physicists.

Finally, I need to thank my companion, Aneta, for all the unconditional

affection she keeps providing after so many years and the positive mood she keeps sustaining even when things turn out bad, helping me to go over them. Without her support, understanding and encouragement, I am afraid this thesis wouldn't have been even started.

List of Figures

1.1	Optical phase space representation for a Fock state.	6
1.2	Optical phase space representation for a coherent state.	9
1.3	Atom energy levels after setting the zero energy level in the middle of the two levels E_g and E_e . The atomic transition frequency is denoted with ω_0	12
1.4	Atomic inversion for number states with different number of n	15
1.5	Atomic inversion for $\bar{n} = 10$	17
1.6	Atomic inversion for $\bar{n} = 5$	17
1.7	Split of the energy levels of the bare states (left) due to the interaction with a quantized field and the dressed states energy levels (right) . .	21
1.8	Dressed states energies versus detuning for the dressed states $ 1, \pm\rangle$, $ 2, \pm\rangle$ and $ 3, \pm\rangle$	21
1.9	Photograph of the cavity assembly used in [61] with the top mirror removed. The atomic beam path is visualized by the arrow. The four posts are used to mount the upper mirror.	25
1.10	Representation of a the main characteristics of cavity QED configu- ration	26
1.11	Decay of the Fock state $ 15\rangle$ in a leaky cavity with $\kappa = 10$, using the master equation approach (green line) and quantum trajectories (blue line).	29
1.12	Jaynes Cummings model in a leaky cavity using the master equation. The parameters used here, are: $\omega_0 = \omega = 10000$, $g = 10^{-4}\omega_0$, $\kappa = 0.2g$	32
2.1	Bloch-sphere representation of the operation performed by Pauli X gate. A ket $ 0\rangle$ (green line) is rotated by π over the x axis without modification of its length.	37
2.2	Deutsch-Jozsa algorithm	41
2.3	Improved version of Deutsch-Jozsa algorithm [23]	43
2.4	Geometric Proof of the function of Grover's algorithm	45
2.5	Probability amplitudes of the four states in the superposition	47
2.6	Probability amplitudes after applying the inversion operator	47

2.7	Probability amplitudes after applying the diffusion operator.	47
2.8	Quantum circuit representing the Quantum Fourier Transform for n qubits. Image rebuilt using Qcircuit from Wikipedia	51
3.1	Qubit definition for Grover's algorithm.	54
3.2	Experimental setup for the realization of Grover algorithm in cavity QED. Atoms 1 and 2 cross the cavity with the same velocities but on different positions and undergo pulses S,H,P from external microwave sources and interact together twice inside the cavity via assisted van der Waals interactions.	57
3.3	Three level system	59
3.4	Quantum circuit realizing the quantum Fourier transform for q=3. $A_i \equiv U_{\pi/4,\pi/2}$ represent the one bit gates and $B_{jk} \equiv Q_{\pi/2^{k-j}}$ represent the two-qubit quantum phase gates.	62
3.5	Atom in V configuration. Transition $ b\rangle \rightarrow a\rangle$ is completely off resonant with the cavity field, while $ b\rangle \rightarrow c\rangle$ is dispersively coupled to the cavity.	63
3.6	Atomic levels under the influence of the magnetic field. For each atom the ground state $ b\rangle$ corresponds to $ 1\rangle$ and $ a_i\rangle$ to $ 0\rangle$	64
3.7	Experimental setup for the realization of QFT for 3 qubits.	64
4.1	Two coupled cavities interacting with fixed atoms.	71
4.2	Probability amplitudes corresponding to exciting a specific cavity mode or a specific atom as a function of time, for the case of large hopping assuming the system started from the state $ eg00\rangle$. Here, $J = 10g$, $\Delta = 0.1g$ and $\omega = 1000g$,while the time is scaled by period $T = \frac{2\pi}{GJ}$	74
4.3	Probability amplitudes corresponding to exciting a specific cavity mode or a specific atom as a function of time, for the case of large detuning, assuming the system started from the state $ eg00\rangle$. Here we chose $\Delta = 10g$, $g = 5 \times 10^{-3}\omega_0$, $J = 2g/5$,while the time is scaled by period $T = \frac{\pi\Delta^2}{g^2J}$	76
4.4	Probability amplitudes corresponding to exciting a specific cavity mode or a specific atom as a function of time, for the resonant case, assuming the system started from the state $ eg00\rangle$. In this case, $\Delta = 10g$, $g = 10^{-3}\omega_0$, $J = 10g$,while the time is scaled by period $T = \frac{2\pi}{g}$	78
4.5	Resonant case with $\kappa = 0.1g$	81
4.6	Resonant case with $\kappa = g$	81
4.7	Resonant case with $\kappa = 10g$	81
4.8	Large hopping case with $\kappa = 0.1g$	81

4.9 Large hopping case with $\kappa = 1g$	81
4.10 Large hopping case with $\kappa = 10g$	81
4.11 Dispersive case with $\kappa = 0.1g$	81
4.12 Dispersive case with $\kappa = 1g$	81
4.13 Dispersive case with $\kappa = 10g$	81
4.14 Quantum circuit representing the operations required in order to obtain the $CNOT$ gate using \sqrt{SWAP} gate.	83
4.15 Representation of the quantum circuit for the Deutsch-Jozsa algorithm.	83
4.16 Fidelity of \sqrt{SWAP} gate versus κ , with κ expressed using coupling rate g of the cavities for the dispersive case (blue line $g = 5 \cdot 10^{-3} \omega_0$, $J = 2/5g$, $\Delta = 10g$, $T_{disp}/4 = \pi\Delta^2/2g^2J$), resonant case (red line, $g = 5 \cdot 10^{-3} \omega_0$, $J = 10g$, $\Delta = 10g$, $T_R/4 = \pi/2g$) and large hopping case (green line $g = 5 \times 10^{-3} \omega_0$, $J = 10g$, $\Delta = 0.1g$, $T_{LH}/4 = \pi J/2(g^2)$).	84
1 The ten first wave functions of the 1D harmonic oscillator and the potential $V = \frac{\xi^2}{2}$ in the dimensionless units.	103

List of Tables

2.1 One qubit gates	38
2.2 Two qubit gates	40
2.3 Three qubit gates	41
3.1 Definition of the angle of rotation for the realization of the oracles.	55